

Winter 12-27-2018

Characterization and Functional Rescue of Congenital Muscular Dystrophy with Megaconial Myopathy in a Mouse Model of the Disease

Ambreen A. Sayed

University of Maine, ambreen.sayed@maine.edu

Follow this and additional works at: <https://digitalcommons.library.umaine.edu/etd>

 Part of the [Animal Experimentation and Research Commons](#), [Congenital, Hereditary, and Neonatal Diseases and Abnormalities Commons](#), and the [Disease Modeling Commons](#)

Recommended Citation

Sayed, Ambreen A., "Characterization and Functional Rescue of Congenital Muscular Dystrophy with Megaconial Myopathy in a Mouse Model of the Disease" (2018). *Electronic Theses and Dissertations*. 3014.
<https://digitalcommons.library.umaine.edu/etd/3014>

This Open-Access Thesis is brought to you for free and open access by DigitalCommons@UMaine. It has been accepted for inclusion in Electronic Theses and Dissertations by an authorized administrator of DigitalCommons@UMaine. For more information, please contact um.library.technical.services@maine.edu.

**CHARACTERIZATION AND FUNCTIONAL RESCUE OF CONGENITAL
MUSCULAR DYSTROPHY WITH MEGACONIAL MYOPATHY IN A MOUSE
MODEL OF THE DISEASE**

By

Ambreen A. Sayed

B.Sc. Jai Hind College, Mumbai, India, 2010

M.Sc. Guru Nanak Khalsa College, Mumbai, India, 2012

A DISSERTATION

Submitted in Partial Fulfillment of the

Requirements for the Degree of

Doctor of Philosophy

(in Biomedical Sciences)

The Graduate School

The University of Maine

December 2018

Advisory Committee:

Gregory A. Cox, Associate Professor, The Jackson Laboratory, Advisor

Robert W. Burgess, Professor, The Jackson Laboratory

Gareth R. Howell, Associate Professor, The Jackson Laboratory

Roger B. Sher, Research Associate Professor, Stony Brook University

Samuel T. Hess, Professor, University of Maine

Calvin P. Vary, Professor, Maine Medical Center Research Institute

**CHARACTERIZATION AND FUNCTIONAL RESCUE OF CONGENITAL
MUSCULAR DYSTROPHY WITH MEGAONIAL MYOPATHY IN A MOUSE
MODEL OF THE DISEASE**

By: Ambreen A. Sayed

Dissertation Advisor: Dr. Gregory Cox

An Abstract of the Thesis/Dissertation Presented
in Partial Fulfillment of the Requirements for the
Degree of Doctor of Philosophy
(in Biomedical Sciences)
December 2018

Congenital muscular dystrophy with megaconial myopathy (MDCMC) is an autosomal recessive disorder characterized by progressive muscle weakness and wasting. Megamitochondria in skeletal muscle biopsies and cognitive impairments in MDCMC patients are observations exclusive to this type of muscular dystrophy. The disease is caused by loss of function mutations in the choline kinase beta (*CHKB*) gene which results in dysfunction of the Kennedy pathway for the synthesis of phosphatidylcholine (PC). A rostro-caudal muscular dystrophy (*rmd*) mouse with a deletion in the *Chkb* gene resulting in MDCMC-like symptoms has been reported by our lab. In order to test if the *rmd* mice show signs of cognitive impairments as observed in MDCMC patients, I engineered a transgenic *rmd* mouse model (Tg-*rmd*) which I used for MS/MS^{ALL} mass spectrometry analysis of brain tissue and to test for working memory and learning impairments. These tests show us that even though Tg-*rmd* mice

showed significantly different lipid profiles in brain, these changes were not translated in the behavioral assays conducted.

I have worked on the development of and tested gene therapy strategies for the rescue and alleviation of dystrophy symptoms using the *rmd* mouse model. I have observed that introduction of a muscle-specific *Chkb* transgene completely rescues motor and behavioral function in the *rmd* mouse model, confirming the cell-autonomous nature of the disease. Intramuscular gene therapy, post-disease onset, using an AAV6 vector carrying a functional copy of *Chkb* gene is capable of rescuing the dystrophy phenotype in *rmd* mice. In addition, upregulating choline kinase alpha (*Chka*), a gene paralog of *Chkb*, via a similar AAV6 viral vector showed increased muscle regeneration and alleviation of muscular dystrophy symptoms as was observed with *Chkb* AAV injections.

Together, my results suggest *rmd* mice do not model the cognitive impairments observed in MDCMC patients and that replacement of the *Chkb* gene or upregulation of endogenous *Chka* could serve as potential lines of therapy for MDCMC patients.

© 2018 Ambreen A. Sayed

All Rights Reserved

DEDICATION

My work is dedicated to those burdened by Congenital Muscular Dystrophy with Megaconial Myopathy.

ACKNOWLEDGEMENTS

It's the people you meet on your way who turn your walk into a journey...

A number of people have influenced my life turning it into a wonderful journey and to them, I express my gratitude...

My PhD journey would not have been possible without the guidance and support of my mentor Dr. Gregory Cox, probably the only mentor who likes building cars, Superman and Power Puff girls alike. Learning and experimenting would not have been fun without my lab mates David Schroeder (DNA Dave), Dr. Amy Hicks, Paige Martin and Jennifer Stauffer. Research is about new ideas and taking different directions when things don't go as planned and that would not have been possible without the invigorating discussions with my committee members Dr. Robert Burgess, Dr. Gareth Howell, Dr. Roger Sher, Dr. Samuel Hess and Dr. Calvin Vary.

I am sincerely thankful to the Graduate School of Biomedical Sciences (GSBSE) for having me in this wonderful program and to our Director of program, Dr. David Neivandt for his excellent leadership in making this program collaborative, expansive and providing us with many career opportunities. I extend this gratitude to our current Director, Dr. Clarissa Henry. To Tammy Crosby, for always being available and able to sort out complicated administrative procedures and making everything seem so simple. To Carrie Cowan, Director of pre and post-doc education at the Jackson lab, for providing us with opportunities for all-round development and for all the career advice. To the Jackson Laboratory; President and CEO Dr. Ed Liu and all my colleagues here who provided me with a supportive and collaborative environment to pursue my scientific goals.

My transition to the USA would not have been easy if it weren't for friends like Elisabeth Adkins, Megan and Kyle Beauchemin, Christy Flizpatrick, Shannon Bean, Eraj Khokar, Navjeet Lotey, and the entire Bar Harbor Association of South Asians. You made me feel at home and you are now my family. To all GSBSE current students and alumni for making this an exceptional learning process filled with such good memories. A huge thank you to Muneer Hasham and Jane Branca for all their help and support during my rotation and after.

I am very thankful for my supportive aunts, uncles and cousins who were always present to celebrate every milestone, however small, with me. To my in-laws, Tabassum Zahra, Sarosh Zahra and Hasnain Ali, for their constant encouragement towards my goals. I'm truly fortunate to have you'll in my life. I am very thankful for my grandparents, Fizza and Hatim Bharmal and Khadija and Abdurrehman Sayed for always believing in me. Your blind faith in me has always pushed me to achieve higher.

To my loving husband, Hasan Zahid, thank you for being in my life. Your encouragement and support these past years have been invaluable. Thank you for being patient and raking up miles on your car by driving all the way up here just to listen to my nerdy banter. Thank you for being my best friend, and partner in crime!

Most of all, I would like to thank my parents Hasina and Ahmed Sayed. I am what I am because of you'll. You'll have taught me the true meaning of hard work and perseverance. You'll have always believed in my dreams and helped me turn them into reality. Thank you for making me the independent woman I am today. It wasn't always easy for you'll but you'll are, truly, my North star.

TABLE OF CONTENTS

DEDICATION.....	iii
ACKNOWLEDGEMENTS.....	iv
LIST OF TABLES.....	xi
LIST OF FIGURES.....	xii
LIST OF ABBREVIATIONS.....	xiv
Chapter	
1. A REVIEW OF CONGENITAL MUSCULAR DYSTROPHY WITH MEGAONIAL MYOPATHY (MDCMC).....	1
An introduction to Congenital Muscular Dystrophy (CMD).....	1
Congenital Muscular Dystrophy with Megaconial Myopathy (MDCMC).....	2
The Kennedy pathway and its implications in MDCMC.....	7
2. FUNCTIONAL RESCUE OF CONGENITAL MUSCULAR DYSTROPHY WITH MEGAONIAL MYOPATHY IN A MOUSE MODEL OF THE DISEASE.....	10
Abstract.....	10
Introduction.....	11
Results.....	13
Muscle-specific expression of Chkb transgene prevents muscular dystrophy.....	13
Dietary circumvention of defects in Kennedy pathway fail to rescue rmd phenotype.....	23

Introduction of Chkb post-disease onset improves dystrophy phenotype in rmd mice.....	24
Chka can compensate for lack of Chkb in rmd mutant mice.....	28
Discussion.....	31
Materials and methods.....	35
Mouse colonies.....	35
Generation of transgenic (rescue) mouse.....	35
Mitochondrial area.....	36
Specimen preparation.....	36
Mitochondrial area calculations.....	36
Behavioral and motor assays.....	37
Open field test.....	37
Rotarod test.....	37
Grip Strength test.....	37
Erasmus Ladder.....	38
CDP-choline diet supplementation.....	38
Adeno-Associated Viral vector design.....	39
Transduction of muscle fibers and tissue processing.....	40
Muscle fiber staining.....	40
Gordon and Sweets stain for reticular fibers.....	40
Hematoxylin and Eosin staining.....	40
Statistical analysis.....	41

3. SIGNIFICANT DIFFERENCES IN BRAIN LIPID PROFILES DO NOT TRANSLATE TO BEHAVIORAL DIFFERENCES IN TRANSGENIC RMD MICE.....	42
Abstract.....	42
Introduction.....	43
Choline and phosphocholine in normal brain development.....	44
Differences in brain lipid profile in normal and cognitively impaired humans and rodents.....	45
Results.....	46
rmd mutant mice have lower muscle strength than WT littermates.....	46
rmd mutant mice show significant changes in lipid profile.....	49
Tg-rmd mice as test models for cognitive impairments in rmd mutant mice.....	55
Tg-rmd mice show significantly different lipid profile when compared to controls.....	56
Absence of cognitive defects in Tg-rmd mice.....	60
Aging does not lead to memory deficits in Tg-rmd mice.....	65
Expression of Chkb transgene does not influence spatial awareness and memory in mice	68
Young <i>rmd</i> mice do not show impairments in spatial awareness and memory.....	70
Discussion.....	73
Materials and Methods.....	76
Lipidomic analysis.....	76
Behavioral analysis for cognition.....	76
Spontaneous alternation.....	76

	Novel spatial recognition/Spontaneous alternation with delay.....	77
	Paired associates learning (dPAL).....	77
	Statistical analysis.....	78
4.	GENETIC AND THERAPEUTIC MECHANISMS TARGETED TOWARDS THE RESCUE OF RMD MUTANT PHENOTYPE.....	79
1.	Mitofusin as a modifier gene for the rescue of rmd muscular dystrophy.....	79
	Results.....	83
	Partial rescue of mitochondrial dimensions in <i>Mfn1^{-/-}HSA.CreTg^{+/-}rmd/rmd</i> and <i>Mfn2^{-/-}HSA.CreTg^{+/-}rmd/rmd</i> mice.....	83
	Changes in mitochondrial dimensions do not rescue body weights and grip strength.....	87
2.	S107 compound for the treatment of muscular dystrophy.....	92
	Results.....	93
	S107 administration did not improve body weight and growth curve of rmd mutant mice.....	93
	Discussion.....	95
	Materials and Methods.....	96
	Growth curve.....	96
	Wire hang.....	96
	Mitochondrial area analysis.....	96
5.	CONCLUSION AND FUTURE DIRECTIONS.....	97
	Medical management of muscular dystrophy.....	97
	AAV mediated gene therapy for MDCMC.....	98

Therapeutic rescue of dystrophy in <i>rmd</i> mice.....	99
Therapeutic intervention using CDP-choline and S107 as oral supplements.....	100
Use of Mitofusin 1 and Mitofusin 2 as genetic modifiers in <i>rmd</i>	101
Gene therapy by up-regulation of <i>Chkb</i>	101
Gene therapy by up-regulation of <i>CHKA</i>	102
Implication of choline kinase alpha in cancer.....	103
Differential function of Chka and Chkb.....	104
Expression patterns of Chka and Chkb in different tissues.....	105
Absence of cognitive impairments in <i>rmd</i> mice.....	106
Summary of contributions to the field.....	107
APPENDIX A: Chapter 2 Supplemental data.....	109
APPENDIX B: Chapter 3 Supplemental data.....	113
APPENDIX C : Chapter 5 Supplemental data.....	115
REFERENCES.....	117
BIOGRAPHY OF THE AUTHOR.....	126

LIST OF TABLES

Table 1.	Top 10 significantly altered TAG (1-3) and SM (4-6) lipid species in the cerebellum, cortex and Mid-Hind brain region of <i>rmd</i> mice.....	54
Table 2.	Top10 significantly altered DAG, MDAG (1-3) and GPL (4-6) lipid species in the cerebellum, cortex and Mid-Hind brain region of <i>rmd</i> mice.....	55
Table 3.	Top 10 significantly altered lipid species in the cortex and Mid-Hind brain region of test (<i>rmd</i>) and control (<i>rmd</i> ^{+/-}) mice, demonstrating changes in branch length, side chains and saturation.....	60
Table 4.	Tukey's multiple comparisons test for weights on different <i>Mfn1</i> genotypes.....	88
Table 5.	Tukey's multiple comparisons test for weights on different <i>Mfn2</i> genotypes.....	89
Table 6.	Tukey's mutltiple comparisons test for <i>Mfn1</i> ^{-/-} HAS.Cre.Tg ^{+/-} <i>rmd/rmd</i> mice on wire hang assay.....	90
Table 7.	Tukey's mutltiple comparisons test for <i>Mfn2</i> ^{-/-} HAS.Cre.Tg ^{+/-} <i>rmd/rmd</i> mice on wire hang assay.....	91

LIST OF FIGURES

Figure 1.	The CDP-choline branch of the Kennedy pathway.....	9
Figure 2.	Chkb-transgene construct, related phenotype and expression levels in mice.....	14
Figure 3.	Test of muscle strength in Tg-rmd mice.....	17
Figure 4.	Mitochondrial phenotype in Tg-rmd mice.....	20
Figure 5.	Effects of <i>Chkb</i> transgene expression in a WT mouse.....	22
Figure 6.	Effects of AAV-Chkb injection on <i>rmd</i> muscle phenotype.....	26
Figure 7.	Effects of AAV-Chkb injections on <i>rmd</i> muscle weights, centralized nuclei and fiber size.....	27
Figure 8.	Effects of AAV-Chka injections on <i>rmd</i> muscle, centralized nuclei and fiber size.....	30
Figure 9.	Measurement of open field activity in <i>rmd</i> mice.....	47
Figure 10.	Measurement of grip strength in <i>rmd</i> mice.....	48
Figure 11.	Measurement of rotarod activity in <i>rmd</i> mice.....	49
Figure 12.	PCA of TAGs in brain.....	50
Figure 13.	PCA of SMs in brain.....	51
Figure 14.	PCA of DAGs in brain.....	52
Figure 15.	PCA of glycerophospholipids in the brain.....	53
Figure 16.	Lipid differences in the cortex region across genotypes.....	57
Figure 17.	Lipid differences in the Mid and Hind brain region across genotypes.....	59

Figure 18.	Testing working memory in Tg-rmd mice.....	61
Figure 19.	Testing for short-term memory in Tg-rmd mice.....	62
Figure 20.	Learning curves of Tg-rmd mice in the PI and dPAL tasks.....	63
Figure 21.	Testing for learning impairments in Tg-rmd mice.....	64
Figure 22.	Testing working memory in aged Tg-rmd mice.....	66
Figure 23.	Testing short-term memory in aged Tg-rmd mice.....	67
Figure 24.	Testing of spatial awareness in Tg-WT mice.....	69
Figure 25.	Testing for short-term memory in Tg-WT mice.....	70
Figure 26.	Testing working memory in young <i>rmd</i> mice.....	71
Figure 27.	Testing short-term memory in young <i>rmd</i> mice.....	72
Figure 28.	TEM images of muscle triad structure.....	80
Figure 29.	Representational image of WT and <i>rmd</i> muscle structure.....	80
Figure 30.	TEM images of gastrocnemius muscle from WT and <i>rmd</i> mice.....	81
Figure 31.	Breeding scheme to obtain <i>Mfn1</i> ^{2^{-/-}} -HSA.Cre.Tg ^{+/+} - <i>rmd/rmd</i> mice.....	83
Figure 32.	Mitochondrial dimensions across <i>Mfn1</i> genotypes.....	84
Figure 33.	Mitochondrial dimensions across <i>Mfn2</i> genotypes.....	85
Figure 34.	Mitochondrial areas across <i>Mfn1</i> and <i>Mfn2</i> genotypes.....	86
Figure 35.	Growth curve across <i>Mfn1</i> genotypes.....	87
Figure 36.	Growth curve across <i>Mfn2</i> genotypes.....	88
Figure 37.	Wire hang assay on <i>Mfn1</i> ^{1^{-/-}} -HSA.Cre.Tg ^{+/+} - <i>rmd/rmd</i> mice.....	89
Figure 38.	Wire hang assay on <i>Mfn2</i> ^{2^{-/-}} -HSA.Cre.Tg ^{+/+} - <i>rmd/rmd</i> mice.....	91
Figure 39.	Growth curve of <i>rmd</i> mice on S107 supplement.....	94

LIST OF ABBREVIATIONS

MD	Muscular Dystrophy
CMD	Congenital Muscular DYstrophy
MDCMC	Congenital Muscular Dystrophy with Megaconial Myopathy
CK	Creatinine Kinase
DGC	Dystrophin-Glycoprotein Complex
<i>rmd</i>	rostro caudal muscular dystrophy
<i>Chka</i>	Choline kinase alpha
<i>Chkb</i>	Choline kinase beta
WT	Wild Type
PC	Phosphatidylcholine
PE	Phosphatidylethanolamine
CT	CTP: phosphocholine cytidyltransferase
CK	Choline Kinase
dPAL	different Paired Associates Learning
<i>Mfn</i>	Mitofusin
SR	Sarcoplasmic reticulum
EC	excitation-contraction
mtDNA	mitochondrial DNA
B6	C57BL/6J

PCA	Principal component analysis
SM	Sphingomyelin
DAG	Diacylglycerols
TEM	Transmission Electron microscope

CHAPTER 1
A REVIEW OF CONGENITAL MUSCULAR DYSTROPHY WITH MEGACONIAL
MYOPATHY (MDCMC)

*“Sometimes my body wakes me up and says
‘Hey, you haven’t had pain in a while. HOW ABOUT PAIN?’
And sometimes
I can’t breathe,
And that’s hard to live with.
But I still celebrate life and
DON’T GIVE UP”*

- *Mattie Stepanek, poet, philosopher, victim of muscular dystrophy.*

An Introduction To Congenital Muscular Dystrophy (CMD)

The Muscular Dystrophy Association (MDA) defines muscular dystrophy (MD) as a group of diseases characterized by progressive muscle weakness or hypotonia and loss of muscle mass (www.mda.org). Muscular dystrophy is caused by inherited and occasionally spontaneous genetic mutations, the symptoms of which, are identified at a different time points in individuals depending on the gene involved and type of mutation. Muscular dystrophies can be classified into 55 different genetic forms which can affect both males and females, leading to skeletal muscle degeneration and loss of motor strength that affecting walking, breathing, swallowing and may also include cardiomyopathy (www.mda.org, www.ninds.nih.gov). Many of these dystrophies present themselves at birth with rapidly progressing symptoms. These early-onset

muscular dystrophies, more specifically defined as a heterogeneous group of disorders characterized by disease onset at birth with rapidly progressing symptoms are termed as Congenital Muscular Dystrophies (CMD) (S. E. Sparks & Escolar, 2011) . To date, there are approximately 30 different types of CMD reported, each based on the gene or protein affected. Most CMD's reported so far arise as a result of an autosomal recessive mutation in the gene that codes for a member of the group of extracellular matrix proteins like collagen, laminin, dystroglycan and integrin. According to statistics provided by the National Organization of Rare Disorders, the exact incidence and prevalence of CMD in the world is not known. A study of the population of Italy reported an incidence of 1 in 125,000 whereas another study based on the population in western Sweden based the prevalence of CMD at 1 in 16,000. CMD is estimated to affect about 250,000 Americans with the Italian population in particular shows an incidence and prevalence of 1 in 4.65×10^5 and 8×10^6 in the North East (Mercuri, Sewry, Brown, & Muntoni, 2002). Some forms of CMD are highly prevalent in certain parts of the world with Laminin alpha-2 deficiency and collagen VI-deficient CMDs being the most common subtypes in many countries with populations of European origin. However, due to failure in diagnosis of primary muscle disease in individuals with mild muscles weakness, with or without intellectual disability may continue to result in underestimation of the prevalence of CMD (S. Sparks et al., 2012).

Congenital Muscular Dystrophy with Megaconial Myopathy (MDCMC)

In the year 1998, a group of Japanese doctors reported 4 patients suffering from an unusual form of muscular dystrophy that displayed the presence of giant mitochondria or megamitochondria in muscle biopsies (Nishino et al., 1998). These patients had unaffected parents and siblings,

indicating that this was an autosomal recessive genetic disorder. Since the phenotype of megamitochondria had not been observed in the spectrum of MD diseases, these patients were not classified into any MD subtype and the genetic cause was unknown. Histologic examination of muscle biopsies showed that the megamitochondria were situated at the periphery of muscle fibers just under the sarcolemma and mitochondria were absent from the central regions of the sarcoplasm. A second biopsy from one of the 4 patients taken at 13 years (after a 12 year interval from the first biopsy) showed that the peripheral location of the megamitochondria did not change with time. All patients showed elevated serum creatinine kinase (CK) levels and an increased proportion of necrotic and regenerating fibers with age, indicating an increase in the progression of dystrophy. Since megamitochondria was a prominent phenotype, patient mitochondrial DNA was analyzed for the presence of mutations. None of the patients showed deletion or duplication mutations in mitochondrial DNA, indicating that the mitochondrial phenotype was likely caused by mutation of a nuclear gene. In addition to this, serum lactate levels and respiratory chain enzyme activities were normal, providing further indication that the dystrophic phenotype was not due to alterations in mitochondrial DNA (mtDNA) sequence. Together, this suggested that the disease was unlike any of the previously reported merosin positive or dystrophin-glycoprotein complex dystrophies.

In 2006, a spontaneous recessive mouse mutation leading to a progressive muscular dystrophy with a rostral-to-caudal gradient of severity and a neonatal bone deformity was identified by the Cox lab at The Jackson Laboratory. This mouse was termed as *rmd*, to indicate the increasing gradient of severity of the muscular dystrophy in a rostral to caudal fashion (Sher et al., 2006). Positional cloning identified a 1663 bp genomic deletion encompassing exon 3 to intron 9 in mouse choline kinase beta (*Chkb*) gene on chromosome 15. Transcription of the gene

would encode a truncated CHKB protein in which the choline binding and active sites were removed. Choline kinase beta is an important enzyme in the Kennedy pathway of skeletal muscles, playing an important role in the first-step conversion of choline to phosphocholine and subsequently into phosphatidylcholine (PC) (Gibellini & Smith, 2010). The *rmd* mutant mice lost significant control of hindlimb motor activity as indicated by dragging of hindlimbs at 2-3 months of age. Histological examination of quadriceps muscles from mice aged 6, 14, 26 and 59 days, revealed presence of megamitochondria and significantly increased number of centralized nuclei in the hindlimb muscles of *rmd* mice. Interestingly, forelimb muscles showed sparse but not significant numbers of megamitochondria and no significant number of centralized nuclei on comparison with unaffected C57BL/6J littermates (WT mice). Membrane integrity testing using Evans Blue Dye, suggested that the muscular dystrophy was not likely the result of impaired sarcolemmal integrity. Testing for amounts of phosphatidylcholine and phosphatidylethanolamine (PE) levels in muscle tissue from fore and hindlimbs showed no significant changes in PE levels but a 38% decrease in PC levels in the forelimbs and 31% in the hindlimbs, suggesting that absolute levels of PC, alteration in the distribution of PC species or changes in PC:PE ratio are crucial to the progression of dystrophy symptoms in *rmd* mice. The gradient in the severity of dystrophy symptoms was thought to result from a differential ability of tissues to compensate for a loss of choline kinase beta protein. This observation was further corroborated by Wu. et. al. in 2009 and 2010 where they showed that there exists a tissue-specific distribution of enzymes like citidyltransferase (CT), the rate limiting enzyme in the Kennedy pathway. When CT activity is significantly reduced in hindlimbs of *rmd* mice it impairs PC synthesis resulting in a decrease in PC levels in hindlimbs of *rmd* mice. This decrease can also be explained by a >2 fold increase in PC catabolism and turnover in the hindlimb skeletal

muscles. There is a greater percent contribution of mitochondrial PC to total muscle PC in the hindlimb skeletal muscles, which may result in the mitochondria diverting PC from the sarcolemma and contributing it to the muscular dystrophy, thus also adding to the increased mitochondrial dimensions (Wu, Sher, Cox, & Vance, 2009). This adds to impaired mitochondrial function in *rmd* mice where a 40% lower mitochondrial inner membrane potential is observed indicating compromised mitochondrial function. Together, these results indicate that a deficiency in PC results in muscular dystrophy phenotype in *rmd* mice. In WT mice, megamitochondria may form in response to an increase in intracellular reactive oxygen species (ROS), where the mitochondria try to decrease this increase in ROS levels by decreasing consumption of oxygen by formation of megamitochondria. Megamitochondria can also lead to apoptotic signals in unfavorable cellular environments, thus protecting the organism (Wakabayashi, 2002). Thus, in short-term, megamitochondria are considered protective to the organism. However, in the longer-term megamitochondria formation compromises mitochondrial function (Wu et al., 2009). These studies accelerated MDCMC research by characterizing the biochemical influences that lead to muscular dystrophy symptoms and phenotype in *rmd* mice.

Muscles of the forelimbs of the *rmd* mice did not show as many megamitochondria and had relatively normal fiber structure and architecture compared to hindlimb skeletal muscles. The mechanism by which the severity of muscular dystrophy phenotype was greater in the skeletal muscles of the hindlimbs of *rmd* mice whereas the forelimbs remained relatively less affected remained unclear until 2010, when it was reported that *Chkb* deficiency did not impair PC synthesis in the forelimb of *rmd* mice (Sher et al., 2006)(Wu, Sher, Cox, & Vance, 2010). This is because choline kinase alpha (*Chka*), a gene paralog of choline kinase beta gene, can

compensate for lack of choline kinase beta. *Chka* and *Chkb* have evolved from a process of duplication and divergence from a common ancestral gene (Aoyama, Liao, & Ishidate, 2004). Western and northern blot analysis showed that both *Chka* and *Chkb* mRNA's and proteins are expressed ubiquitously and concurrently in most mouse tissues. Subsequent immunoprecipitation showed that CHKA and CHKB proteins may function as homodimers or heterodimers but the predominant part of choline kinase (CK) activity is as a α - β heterodimer. *In vitro* studies with COS-7 cells co-transfected with HA-tagged CHKA or CHKB along with a Myc-tagged counterpart suggested that the activity of CK in each cell type is regulated by the level of each isoform along with the combination of each isoform subunit to generate the active dimer complexes (Aoyama et al., 2004). Approximately 70% of the total CK activity in the skeletal muscles of forelimb of mice is governed by *CHKA* whereas 80% of the total CK activity in the hindlimb skeletal muscles is governed by *Chkb* (Wu et al., 2010b). This explains why in the absence of *Chkb*, the forelimbs of *rmd* mice are less affected and why there is a gradient of severity of muscular dystrophy phenotype in these mice. Immunoblots of muscles from fore and hindlimbs of WT mice at 1, 3 and 8 weeks of age suggests that with an increase in age of the mouse, *Chka* expression increases in the forelimbs and decreases in the hindlimbs. In contrast, *Chkb* expression increases significantly in the hindlimb skeletal muscles of WT mice (Wu et al., 2010). The residual expression of CHKA could explain why the muscular dystrophy is less evident in forelimbs of *rmd* mutant mice. Together, these results indicate that there is a rostrocaudally defined developmental heterogeneity in a number of factors responsible for the development of vertebrate skeletal muscle and that these factors also play an important role in defining the pattern and severity of muscular dystrophy symptoms in *rmd* mice.

Post identification of the *rmd* mouse, the patients identified by Nishino et al. in 1998 were sequenced and it was found that all of them showed mutation in the *CHKB* gene that lead to muscular dystrophy, megamitochondria and severe cognitive impairments. These patients were classified as congenital muscular dystrophy with megaconial myopathy (MDCMC) (Mitsuhashi, Ohkuma, et al., 2011). Following this, many more cases of MDCMC were reported. These results suggest that the *rmd* mouse is a good model for the study of MDCMC in humans, providing an excellent starting point for my experiments towards further characterization of the disease and towards designing strategies of functional rescue.

The Kennedy pathway and its implications in MDCMC

The Kennedy pathway elucidated in 1956 by Kennedy Weiss describes the pathway for the *de novo* synthesis of PE and PC. There are two branches of the Kennedy pathway based upon the formation of characteristic high-energy intermediates-CDP-ethanolamine, for the synthesis of PE and CDP-choline, for the synthesis of PC. Hence, the two branches of the Kennedy pathway are often referred to as CDP-ethanolamine and CDP-choline pathway (Gibellini & Smith, 2010).

In the CDP-ethanolamine Pathway, the first step is initiated by the ATP-dependent phosphorylation of ethanolamine to phosphoethanolamine. The second step, also the rate-limiting step, involves CTP:phosphoethanolamine cytidyltransferase (ECT) using phosphoethanolamine and CTP to form high-energy donor CDP-ethanolamine with the release of pyrophosphate. The third and final steps involves CDP-ethanolamine:1,2-diacylglycerol ethanolaminephosphotransferase using CDP-ethanolamine and a lipid anchor like Diacylglycerol (DAG) to form PE and CMP as byproducts. Analogous CDP-choline pathway is also a 3 step pathway, using a series of similar reactions to form PC. In the CDP-choline pathway, choline

kinase instead of ethanolamine kinase catalyzes the first step phosphorylation of choline to phosphocholine. Similarly, cytidine-diphosphate and CDP-choline cholinephosphotransferase are the enzymes that catalyze the second and third step of the CDP-choline pathway (Gibellini & Smith, 2010). In mammals, there are three isoforms of choline kinase-choline kinase alpha 1 and choline kinase alpha 2 synthesized by the same gene and choline kinase beta synthesized by a gene paralog. Ethanolamine kinase has two isoforms- ethanolamine kinase 1 and ethanolamine kinase 2 (Hong et al., 2010)(Gibellini & Smith, 2010).

The enzymes of the Kennedy pathway can overlap in substrate usage. In mammals, choline kinase isoforms that are able to phosphorylate ethanolamine have been identified (Gibellini & Smith, 2010). In mammals, CDP-choline pathway is predominant for the synthesis of PC in all tissues except the liver where significant amount of PC is made by methylation of PE. It has been reported that phospholipid methyltransferase activity in non-hepatic tissues is extremely low relative to CDP-choline pathway activity (Kent, 1995). This in-turn indicates that synthesis of PC in skeletal muscles is predominantly dependent on the CDP-choline branch of the Kennedy pathway.

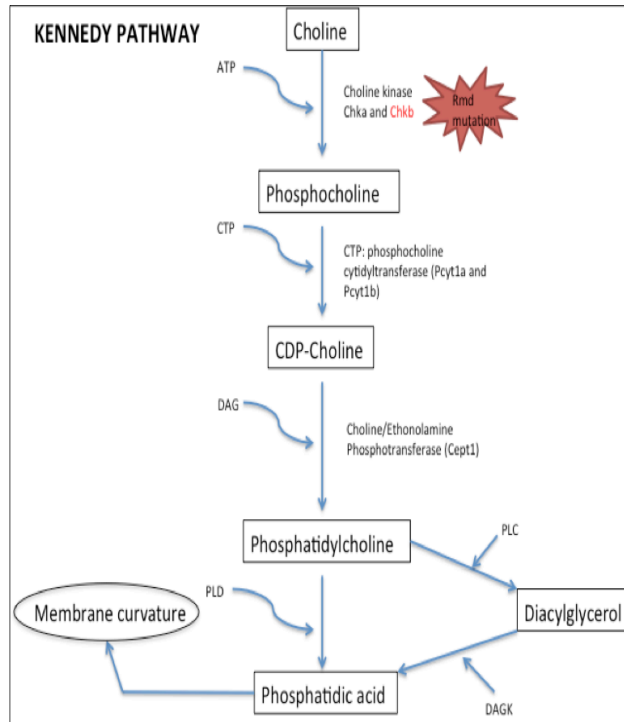


FIG 1: The CDP-choline branch of the Kennedy pathway.

CHAPTER 2

FUNCTIONAL RESCUE OF CONGENITAL MUSCULAR DYSTROPHY WITH MEGACONIAL MYOPATHY IN A MOUSE MODEL OF THE DISEASE.

Abstract:

Congenital muscular dystrophy with megaconial myopathy (MDCMC) is an autosomal recessive disorder characterized by progressive muscle weakness and wasting. The observation of megamitochondria in skeletal muscle biopsies is exclusive to this type of muscular dystrophy. The disease is caused by loss of function mutations in the choline kinase beta (*CHKB*) gene which results in dysfunction of the Kennedy pathway for the synthesis of phosphatidylcholine (PC). We have previously reported a rostro-caudal muscular dystrophy (*rmd*) mouse with a deletion in the *Chkb* gene resulting in MDCMC-like symptoms, and we used this mouse to test gene therapy strategies for the rescue and alleviation of dystrophic symptoms. Introduction of a muscle-specific *Chkb* transgene completely rescues motor and behavioral function in the *rmd* mouse model, confirming the cell-autonomous nature of the disease. Intramuscular gene therapy post-disease onset using an AAV6 vector carrying a functional copy of *Chkb* is also capable of rescuing the dystrophy phenotype. In addition, we examined the ability of choline kinase alpha (*Chka*), a gene paralog of *Chkb*, to improve dystrophic symptoms when upregulated in skeletal muscles of *rmd* mutant mice using a similar AAV6 vector. The sum of our results in a preclinical model of disease suggest that replacement of the *Chkb* gene or upregulation of endogenous *Chka* could serve as potential lines of therapy for MDCMC patients.

Introduction:

Congenital muscular dystrophies (CMDs) are a group of autosomal recessive disorders exhibiting muscle weakness, wasting and hypotonia at or soon after birth with progressively increasing symptoms (Mercuri et al., 2002). There are currently at least 30 different types of CMD. In 2006, we reported a spontaneous mouse mutation displaying muscular dystrophy in a rostral to caudal gradient, with its hindlimbs being more affected than its forelimbs coupled with the presence of giant/mega mitochondria, leading us to name it rostrocaudal muscular dystrophy (*rmd*)(Sher et al., 2006b). The *rmd* mouse carries a 1.6kb deletion in the choline kinase beta (*Chkb*) gene, resulting in complete loss of CHKB activity. Choline kinase beta is an important enzyme in the Kennedy pathway, required for *de-novo* synthesis of phosphatidylcholine. In mammals, choline kinase is the enzyme in the first step conversion of choline to phospho-choline which is ultimately converted to phosphatidylcholine (PC), one of the four major biolipids in all cellular membranes (Gibellini & Smith, 2010). In mammals, choline kinase activity is encoded by two separate paralogous genes, choline kinase alpha (*Chka*) and choline kinase beta (*Chkb*), which function either as homo- or hetero-dimers. Both of these genes have wide tissue expression profiles and both encoded enzymes phosphorylate choline to phosphocholine.

Following the publication of the *rmd* mouse model, a group of 15 patients with congenital muscular dystrophy and mega mitochondria were sequenced and found to contain loss of function mutations in the *CHKB* gene. The disease was classified as Congenital Muscular Dystrophy with Megaconial Myopathy (MDCMC), OMIM: 602541 (Mitsuhashi, Hatakeyama, et al., 2011). Both MDCMC patients and mice have loss of function mutations in the *CHKB* or *Chkb* gene and develop progressive muscular dystrophy indicates that the *rmd* mice have good face and construct validity as models of MDCMC. To date, there are at least 48 reported cases of MDCMC worldwide. These were children born of unaffected parents and having none or one

affected sibling, indicating an autosomal recessive inheritance. In all reported cases, patients showed generalized muscle weakness starting at about 5 years of age. Some patients were reported as early as 22 months of age. These patients missed all major motor milestones and showed speech defects, with initial speech occurring at about 5 years of age and pronounced cognitive impairments at about 12 years of age. Many of these patients were first reported due to floppiness and increased tendencies to fall while walking or running and /or due to the presence of diffuse skin disorders like mild ichthyosis (Nishino et al., 1998)(Mitsuhashi, Ohkuma, et al., 2011)(Quinlivan et al., 2013)(Castro-Gago et al., 2014)(Oliveira et al., 2015)(Castro-Gago et al., 2016)(Brady, Giri, Provias, Hoffman, & Tarnopolsky, 2016)(Gutiérrez Ríos et al., 2012)(Cabrera-Serrano et al., 2015)(Haliloglu, Talim, Sel, & Topaloglu, 2015).

Here we test several methods of functional rescue of dystrophy using the *rmd* mouse model. These tests included examining the effects of dietary intervention with CDP-choline, a downstream compound of the Kennedy pathway, in an effort to circumvent the defects in the pathway. We also tested pre- and post-disease onset upregulation of CHKB in the rescue of muscular dystrophy phenotype in the *rmd* mutant mice. Pre-disease onset rescue of *rmd* was tested by overexpression of the *Chkb* gene in an engineered muscle-specific transgenic mouse where *Chkb* expression was driven by the *Titin (Ttn)* gene promoter in the skeletal and cardiac muscles. These Tg-*rmd* mice also allowed us to examine the cell-type specificity required for rescue of muscular dystrophy. Post-disease onset rescue was tested by intramuscular injections of adeno-associated viral (AAV) vectors expressing either the *Chka* or *Chkb* genes in *rmd* mutant mice. Expression of the *Chka* gene normally shuts down during postnatal muscle differentiation (Wu, Sher, Cox, & Vance, 2010a) and our previous work suggested that residual CHKA activity in anterior muscle groups of the *rmd* mouse correlated with reduced severity of dystrophic

symptoms (Wu et al., 2010a). Thus, we sought to determine if CHKA could compensate for the lack of choline kinase beta as an alternative rescue mechanism in *rmd* mice. We found that viral delivery of *Chka* was also efficacious with comparable potency to rescue with the *Chkb* gene.

Results

Muscle-specific expression of *Chkb* transgene prevents muscular dystrophy: We engineered a full-length cDNA of the mouse *Chkb* gene under the control of the muscle-specific titin promoter and created a line of transgenic *rmd* (Tg-*rmd*) mice (Fig 2A) (Maddatu et al., 2005a). The Ttn-*Chkb* transgene was also carried on a wild-type background. The Tg-*rmd* and Tg-WT mice were physically indistinguishable from their wild-type littermates at birth and through adulthood (Fig 2B and 2E). Real-time PCR assays on tissue from gastrocnemius muscle of Tg-*rmd*, Tg-WT, *rmd* and *+/rmd* mice was performed to assess the levels of *Chkb* cDNA expression. We observed 18-fold higher expression of *Chkb* mRNA levels in the Tg-*rmd* muscles, compared to C57BL/6J controls, with no detectable levels in mutant *rmd* muscle, a 0.21 fold expression in heterozygous *+/rmd* muscles and 14-fold higher expression of *Chkb* in the Tg-WT mice (Fig 2C). Body weights of Tg-*+/rmd* mice were not significantly different from Tg-*rmd* and *+/rmd*, indicating absence of a detrimental effect of *Chkb* overexpression (Fig 2D). It was also observed that Tg-*rmd* and Tg-WT mice were physically indistinguishable from each other (Fig 2E).

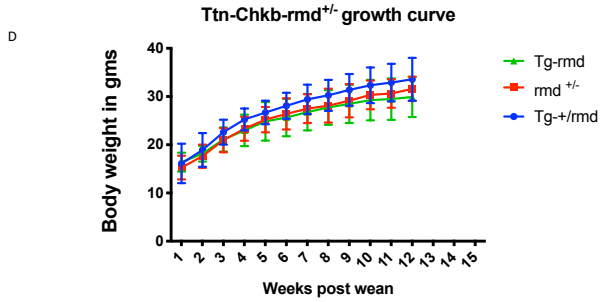
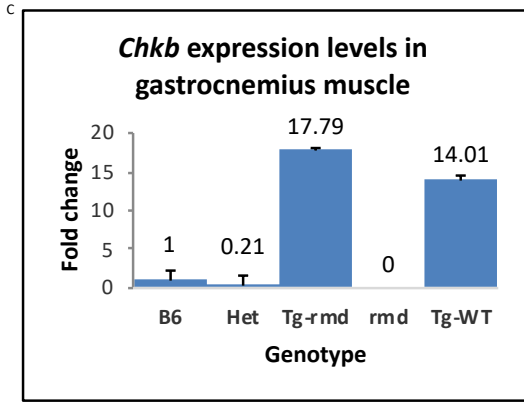
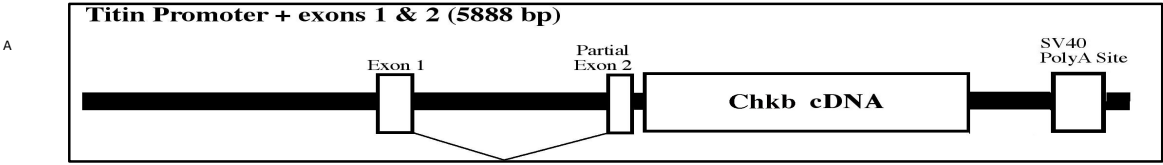


FIG 2. *Chkb*-transgene construct, related phenotype and expression levels in mice.

(A) demonstrates the *Chkb* transgene construct with a functional copy of *Chkb* cDNA inserted downstream of a complete exon 1 and partial exon 2 structure followed by a SV40Poly A site downstream of the *Chkb* cDNA. (B) shows a WT (+/+), Tg-*rmd* and *rmd* (*rmd/rmd*) mouse from top to bottom with the Tg-*rmd* mouse being physically comparable to the WT. *Chkb* gene expression in muscle is 18-fold higher in Tg-*rmd* and 14-fold higher in Tg-WT mice as seen from real time PCR analysis, whereas expression in *rmd* mice was not detectable and that in +/-*rmd* mice was 0.21 times higher than in *rmd* mice (C). Tg-*rmd*, +/-*rmd* (unaffected littermates) and Tg+/-*rmd* mice do not show significant differences in their body weights when measured starting at 3 weeks of age (post wean) (D). The Tg-*rmd* and Tg-WT mice are physically indistinguishable from each other (E). N=4 mice/sex/genotype.

To determine if our transgene functionally rescued motor performance, we tested for rescue of motor performance in 8-10 week old Tg-*rmd* mice (n=10 mice/sex/genotype) using behavioral assays including open field, rotarod, grip strength and the Erasmus ladder tests. Mutant *rmd* mice showed megamitochondria with decreased mitochondrial numbers and increased mitochondrial areas at 2 weeks of age (Supplementary Fig 3 A-D) accompanied by significant motor deficits at 4-5 weeks of age, rendering them unsuitable for testing at 8-10 weeks as with the Tg-*rmd* mice. (Supplementary Fig 3 E-K).

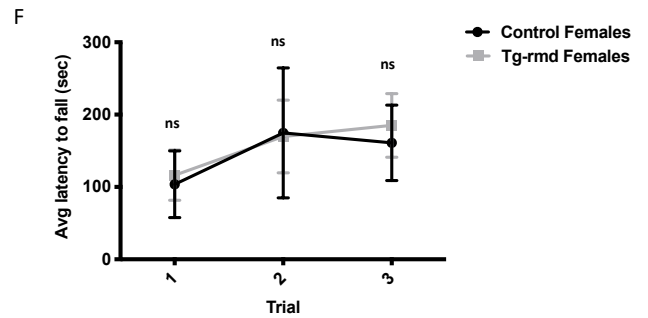
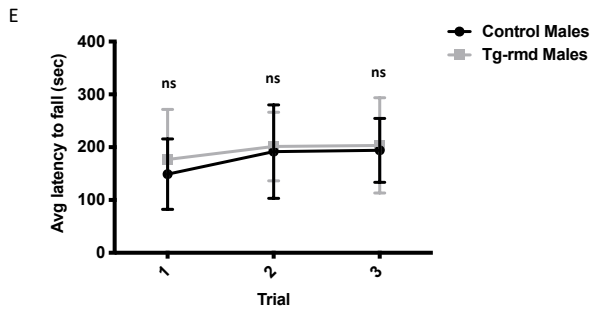
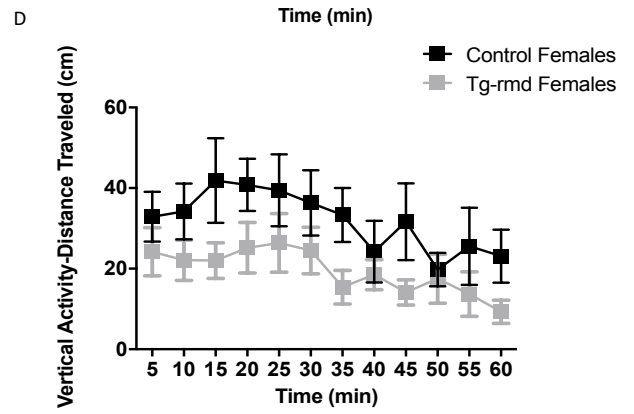
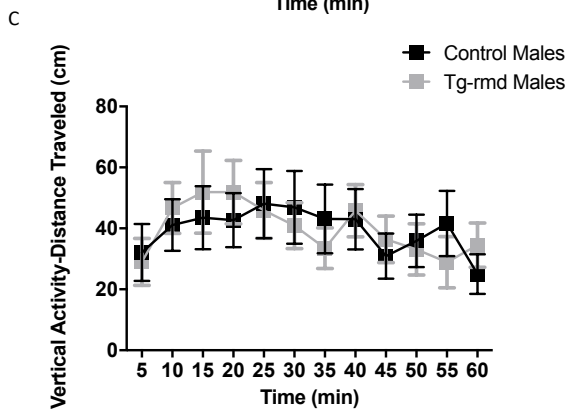
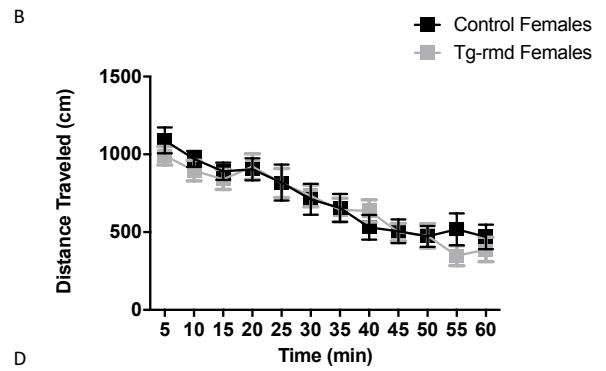
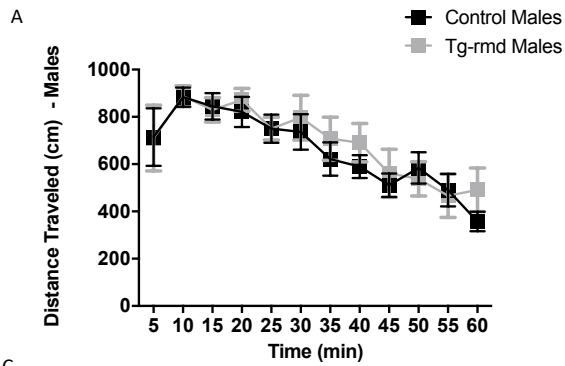
The open field test was used to assess basic locomotor function (ambulation) (Paumier, Rizzo, 2013, Bailey, Crawley, 2009). Tg-*rmd* male and female mice travelled an equal distance (Fig 3 A-B) and showed similar vertical activity (Fig 3 C-D) as the control male and female

mice, suggesting normal ambulation and rearing ability.

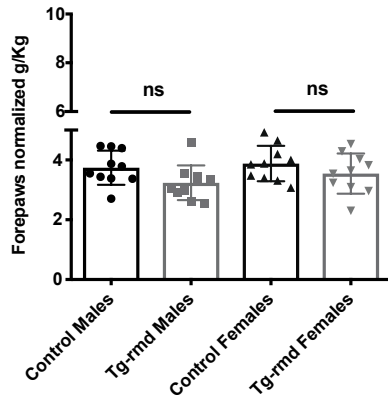
The accelerating rotarod is a forced performance test used to examine motor impairments (Paumier et al., 2013)(van der Vaart, van Woerden, Elgersma, de Zeeuw, & Schonewille, 2011). When tested for their ability to perform on the rotarod, our *Tg-rmd* mice were not different from their control littermates, indicating normal motor endurance and performance levels (Fig 3 E-F).

We tested muscle function using a grip strength assay (Brooks, Simon, 2009). Grip strength of fore paws and all paws were tested and normalized to body weight in order to gauge the severity of the dystrophy phenotype. The *Tg-rmd* males and females showed a grip strength similar to their control littermates indicating normal fore paw and all paw grip strength (Fig 3 G-H).

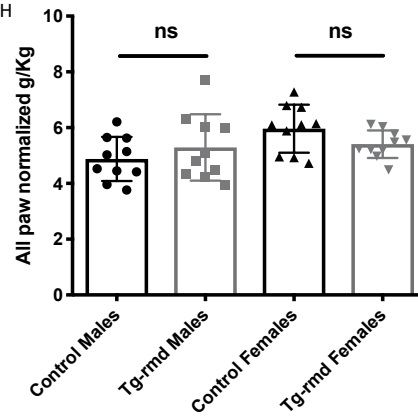
Fine motor coordination and balance were tested using the Erasmus ladder, which specifically tests cerebellar motor coordination related to the precision and accurate timing of movement. The Erasmus ladder assay is sensitive to perturbations or disorders in fine movement, equilibrium, posture and fine learning and can distinguish between motor learning and motor coordination problems more accurately than other tests, making it a suitable device to test for subtle motor coordination disabilities in rodents (van der Vaart et al., 2011)(M. F. Vinueza Veloz et al., 2012)(Mara Fernanda Vinueza Veloz et al., 2014). A greater percentage of missteps and back steps on the ladder rungs indicate motor balance and coordination deficiencies. Our *Tg-rmd* males and females were not significantly different from the controls in percent backsteps and percent missteps during the assay. Both, control and *Tg-rmd* mice had a similar reaction to the addition of a sound cue on day 5 and showed similar increases (but not significantly different from each other) in the percent back steps in both male and female mice (Fig 3 I-L).



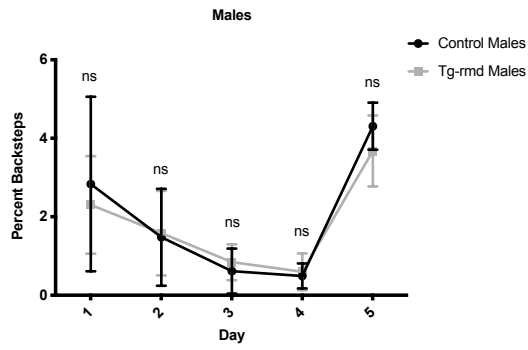
G



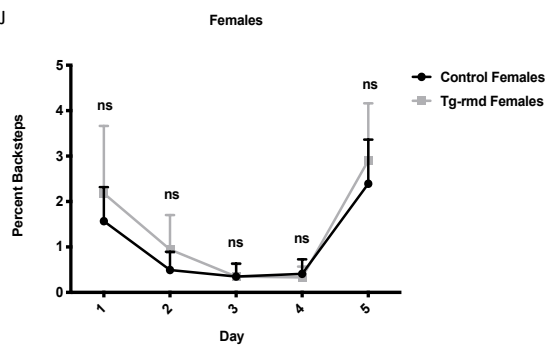
H



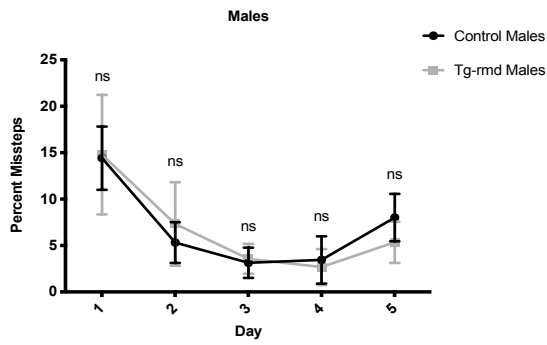
I



J



K



L

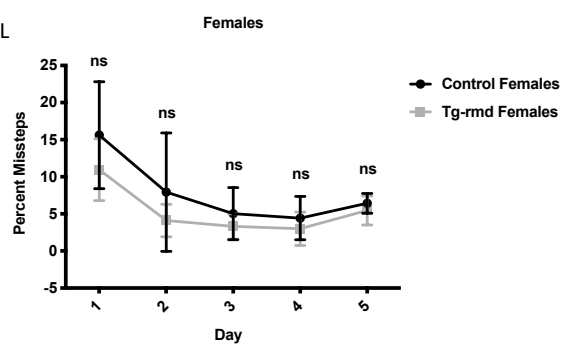


FIG 3. Test of muscle strength in *Tg-rmd* mice. Open field results for spontaneous locomotion, suggests normal ambulation in the *Tg-rmd* mice, with distance travelled not significantly different from that of the controls tested in males ($p=0.96$) and females ($p=0.66$) (A)(B). *Tg-rmd* male ($p=0.31$) and female ($p=0.67$) mice show no significant differences in their vertical activity (C)(D). Latency to fall from 3 individual trials on the rotarod assay show normal motor strength in the *Tg-rmd* male ($p=0.41$) and female ($p=0.74$) mice (E)(F). Grip strength assay results suggests normal forepaw and all paw normalized grip strength, respectively, in the *Tg-rmd* mice compared to the unaffected controls tested. Where males showed a $p=0.07$ and females showed $p=0.25$ in forepaw grip strength (G), whereas males showed a $p=0.37$ and females, a $p=0.09$ in all paw grip strength (H). Erasmus assay for fine motor balance and co-ordination in *Tg-rmd* mice shows no significant difference in percent backsteps (males, $p=0.59$ and females, $p=0.54$) (I)(J) and percent missteps (males, $p=0.14$ and females, $p=0.56$) (K)(L), suggesting no perturbation in motor coordination when compared to controls. N=10 mice/sex/genotype, aged 8-10 weeks. Error bars represent mean with SD.

Mitochondrial area measurements ($n=4$ mice/sex/genotype) from sections of the gastrocnemius muscle analyzed by transmission electron microscopy showed that while *rmd* mutant mice had mitochondria that averaged 5 times larger than those of wild type mice ($p < 10^{-4}$), mitochondrial size was restored to normal in *Tg-rmd* mice ($p = 0.1355$; Fig 4 A-D). This can also be seen in the frequency distribution of mitochondrial areas where *Tg-rmd* mice restore the percentage of small mitochondria while reducing the frequency of mitochondria exceeding 1 nm^2 , whereas the *rmd* mice showed few mitochondria as large as 6 nm^2 (Fig 4E). Mitochondrial

numbers are reduced by half in the affected *rmd* mice whereas, *Tg-rmd* mice show similar mitochondrial numbers to their wild type littermates (Fig 4F). Therefore, restoration of *Chkb* gene expression in skeletal muscle provides a cell-type specific rescue of *Chkb* expression and rescues the mutant *rmd* phenotype.

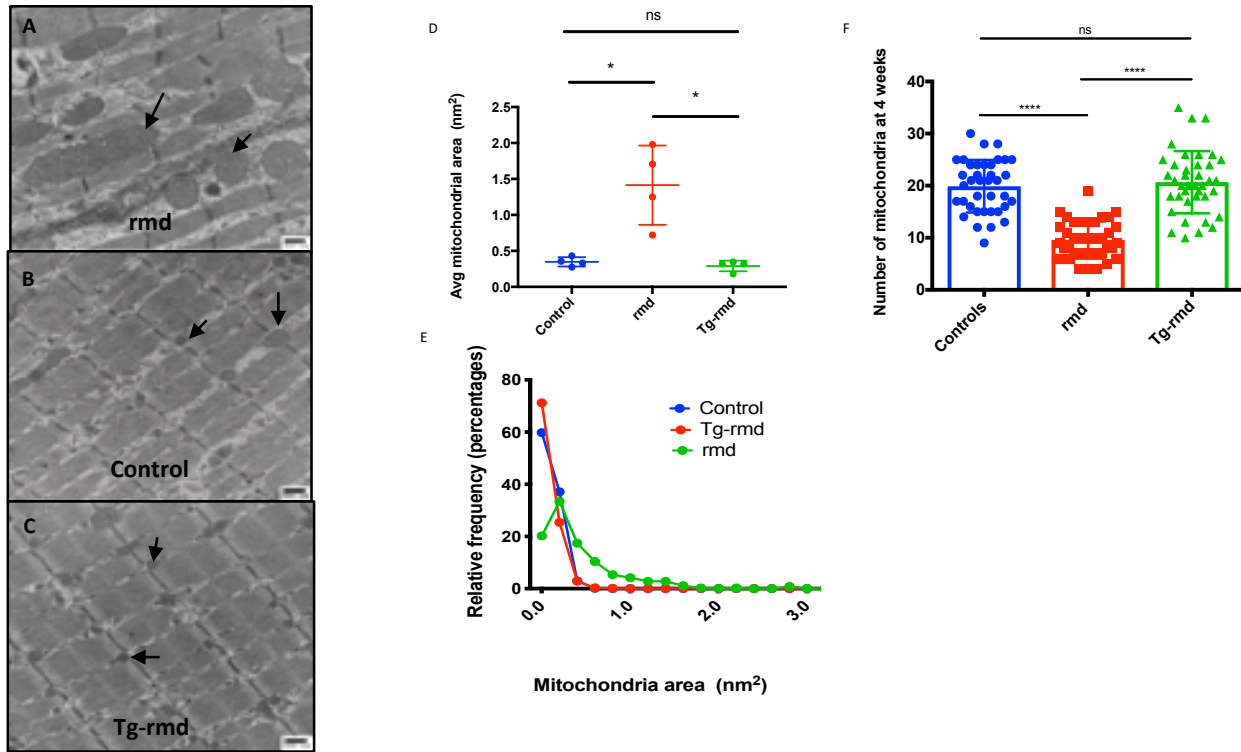


FIG 4. Mitochondrial phenotype in *Tg-rmd* mice. Demonstration of megamitochondria in *rmd* mice (A) normal sized mitochondria in WT littermates (B) and rescued, normal sized mitochondria in *Tg-rmd* mice (C). Mitochondrial areas are rescued in *Tg-rmd* (rescue) mice as compared to WT (control) and *rmd* (affected) littermates with *Tg-rmd* mice having mitochondrial areas closer in value to control mice (D). *Tg-rmd* mice show a higher percent of larger fibers (area of fibers) when compared to *rmd* mice (E). Mitochondrial numbers are restored in *Tg-rmd* mice compared to the decreased numbers in *rmd* mice, $p < 0.0001$ (D). $N = 4$ mice/sex/genotype aged 4 weeks. Error bars represent mean with SD.

Together, these results indicate restoration of muscle strength and coordination in Tg-*rmd* mice and hence a prevention of the *rmd* disease phenotype. No aberrant mouse behavior or deaths were observed in any transgenic mice indicating an absence of toxic effects from overexpression of the *Chkb* transgene. However, in order to test this in a more thorough manner, we examined wild-type C57BL/6J mice carrying the Ttn-*Chkb* transgene (Tg-WT) and assessed levels of *Chkb* expression and motor strength.

The Tg-WT mice were tested on the open field, rotarod and grip strength assays to confirm absence of any detrimental effects of transgene overexpression on motor performance.

Open field tests performed on n=10 mice/sex/genotype, showed distance travelled by Tg-WT is similar to that of WT mice (Fig 5 A-B). The Tg-WT male and female mice showed a similar latency to fall compared to the WT controls on the rotarod assay (Fig 5 C-D). In the grip strength assay, the Tg-WT males are not significantly different from WT male controls in their fore paw and all paw grip strength normalized to body weight. While the Tg-WT females did not show any difference in their fore paw grip strength, they showed a slightly significant increase in their all paw grip strength compared to WT controls ($p=0.01$) (Fig 5 E-F). These results confirm that overexpression of *Chkb* gene does not result in any immediate detrimental effects in mice.

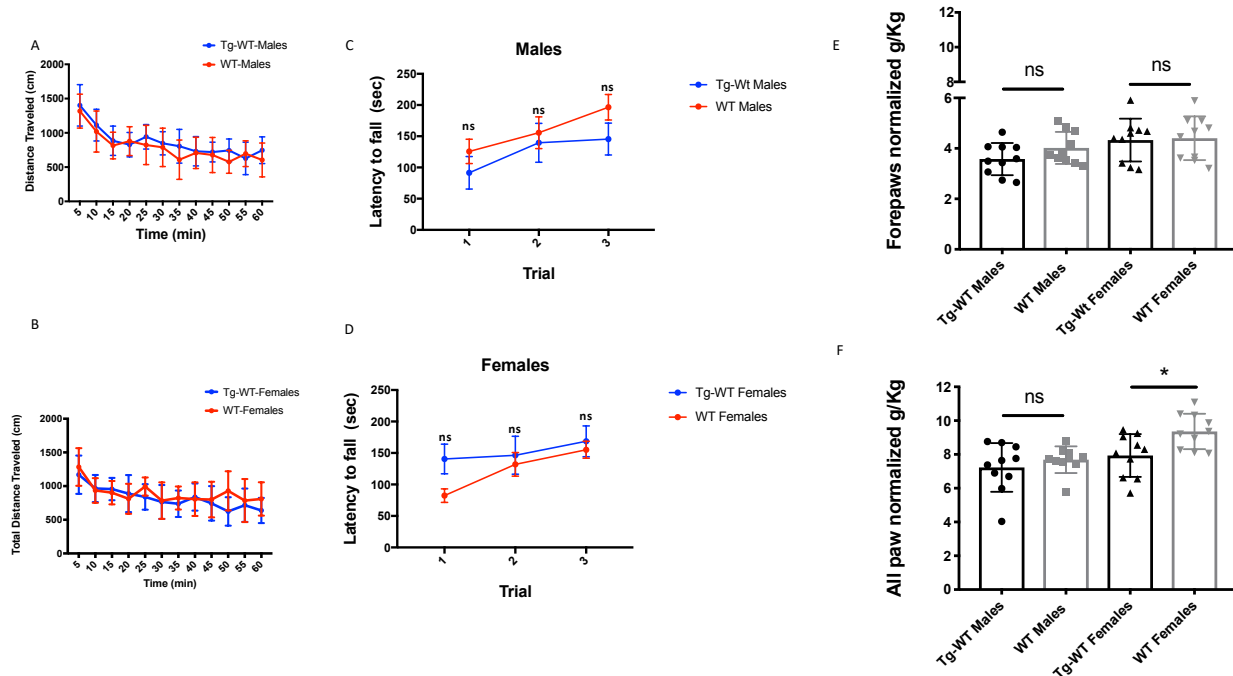


FIG 5. Effects of *Chkb* transgene expression in a WT mouse. When tested for detrimental effects of over-expression of *Chkb* transgene in a WT mouse, it was observed that Tg-WT mice did not show significant differences in locomotor activity in both male ($p=0.45$) and female ($p=0.10$) groups when compared to WT mice on the open field assay (A)(B). Latency to fall on the rotarod assay in males, $p=0.25$, (C) and females, $p=0.25$ (D) and fore paw and all paw grip strength in male ($p=0.13$ and $p=0.39$) (E) Tg-WT mice were not significantly different compared to WT controls. The female Tg-WT mice did not show difference in fore paw grip strength ($p=0.86$) but showed slight difference in all paw grip strength ($p=0.01$), when compared to WT controls. These tests indicate lack of immediate toxic effects in transgene expression. $N=10$ mice/sex/genotype aged 8-10 weeks. Error bars represent mean and SD.

Dietary circumvention of defects in Kennedy pathway fail to rescue *rmd* phenotype:

While the restoration of *Chkb* gene expression with a muscle-specific transgene was capable of preventing the onset and progression of dystrophic symptoms, we also sought to test whether we could bypass the biochemical defect by providing a downstream metabolic product of the Kennedy pathway via dietary supplementation. Previous studies have shown that intravenous injections of CDP-choline, a metabolite in the Kennedy pathway that is downstream of the action of CHKB, can help to prevent acute muscle damage in *rmd* mutant mice (Wu et al., 2009). We tested whether dietary supplementation with CDP-choline could also decrease dystrophy in the absence of *Chkb*. For the study, 500mg/kg/day of CDP-choline was provided in the diet for a period of 3 months beginning at 3 weeks of age (Secades JJ, 1995)(Agut J., 1983)(Bachmanov, Reed, Beauchamp, & Tordoff, 2002). Mutant *rmd* mice (n=8 mice/sex) on dietary supplementation were weighed daily for changes in growth rate and effects of supplementation of the overt dystrophic symptoms compared to their non-supplemented controls (n=4 mice/sex) and supplemented WT mice (n=4 mice/sex). However, no improvements were observed in the growth rate or behavior of treated mice over the study duration (Supplemental Fig 1 A-B). At the end of this study, 2 mice/sex/genotype were randomly selected to perform mass spectrometry analysis for components of the Kennedy pathway in muscle tissues of the treated mice and body weights were analyzed. Mass spectrometry analyses showed no significant differences in the levels of CDP-choline in the gastrocnemius muscle between the control and test groups (Supplemental Fig1C). These results indicate that a dietary supplementation of CDP-choline does not lead to improvement of muscular dystrophy in adult *rmd* mice.

Introduction of *Chkb* post-disease onset improves dystrophy phenotype in *rmd* mice:

The mutant *rmd* disease phenotype is observed as early as 2 weeks of age, with the mice showing giant mitochondria with decreased mitochondrial numbers and decreased muscle strength (Supplemental fig 2 A-D). Hence, in order to test the effects of up-regulation of *Chkb* expression in post-disease onset adult skeletal muscle, we performed intramuscular injections of *rmd* mutant mice at 3 weeks of age with an adeno-associated viral vector-6 carrying a 3X Flag-Tagged functional copy of the mouse *Chkb* cDNA and a self-cleaving p2A peptide-EGFP reporter gene into the gastrocnemius muscle. Each *rmd* mouse served as its own control with the left leg being injected with the AAV vector and the right leg being sham injected with an equal volume of saline. Seven weeks post-injection, their gastrocnemius muscles were analyzed for changes in muscle weight, fiber area and percent of centralized nuclei. Gross observation showed an increase in muscle size in the AAV-injected muscle (Fig 6A). *In vivo* fluorescence images of injected *rmd* and unaffected WT mice showed that EGFP fluorescence was localized to the site of injection indicating localized muscle transduction. No EGFP fluorescence was detected in the saline injected leg (Fig 6B). Gross H&E-stained histological sections (Supplemental Fig 3 A-B) revealed a significant improvement in muscle fiber morphology in the AAV-*Chkb* injected muscles compared with the saline injected muscles. Montage images of the medial and lateral gastrocnemius muscle show a rescue of muscle fiber morphology in AAV-*Chkb* injected muscles (Fig 6C) when compared to the saline injected muscle (Fig 6D). We describe this as a partial rescue with the majority of muscle fibers in the injected *rmd* leg having cross-sectional fiber areas comparable to that of unaffected muscle fibers and show no centralized nuclei. However, there remain a percentage of muscle fibers with significantly smaller cross-sectional areas comparable to those of *rmd* mutant muscle and that show centralized nuclei. The partial nature of

rescue can be attributed to the fact that not all fibers may have been transduced when injected at 3 weeks of age. The AAV-injected muscles of *rmd* mice showed a significant increase in muscle weight in both males ($p=0.004$) and females ($p=0.006$) compared to the saline injected muscles, whereas, the AAV-injected muscles of the unaffected WT mice showed no difference in muscle weight ($p>0.99$ in males and $p=0.65$ in females) suggesting that overexpression of CHKB rescues muscle in dystrophic mice but does not induce muscle hypertrophy in control mice (Fig 7 A-B). AAV-injected *rmd* muscles showed a reduced percent of centralized nuclei compared to saline injected muscles ($p=0.001$ in males and $p=0.06$ in females), while those from AAV-injected WT muscles did not show any significant differences when compared to the saline injected contralateral muscles ($p=0.35$ and 0.29 in males and females respectively) (Fig 7 C-D), reflective of the specificity of rescue of the disease phenotype without alteration of normal muscle. Analysis of cross-sectional myofiber areas showed a significant increase ($p=0.0001$) in the average fiber areas of AAV-*Chkb* injected *rmd* muscles. Classifying fiber areas in 4 quartiles into small (S=0-307 nm^2), medium 1 (M1=307.01-795 nm^2), medium (M2= 795.01-1391 nm^2) and large (L=1391.01-14093 nm^2) showed a significant increase in the percent of M1, M2 and L fiber sizes and a significant decrease in the percent of S fiber sizes in the AAV-injected *rmd* muscle compared with the saline injected muscle (Fig 7 E-F).

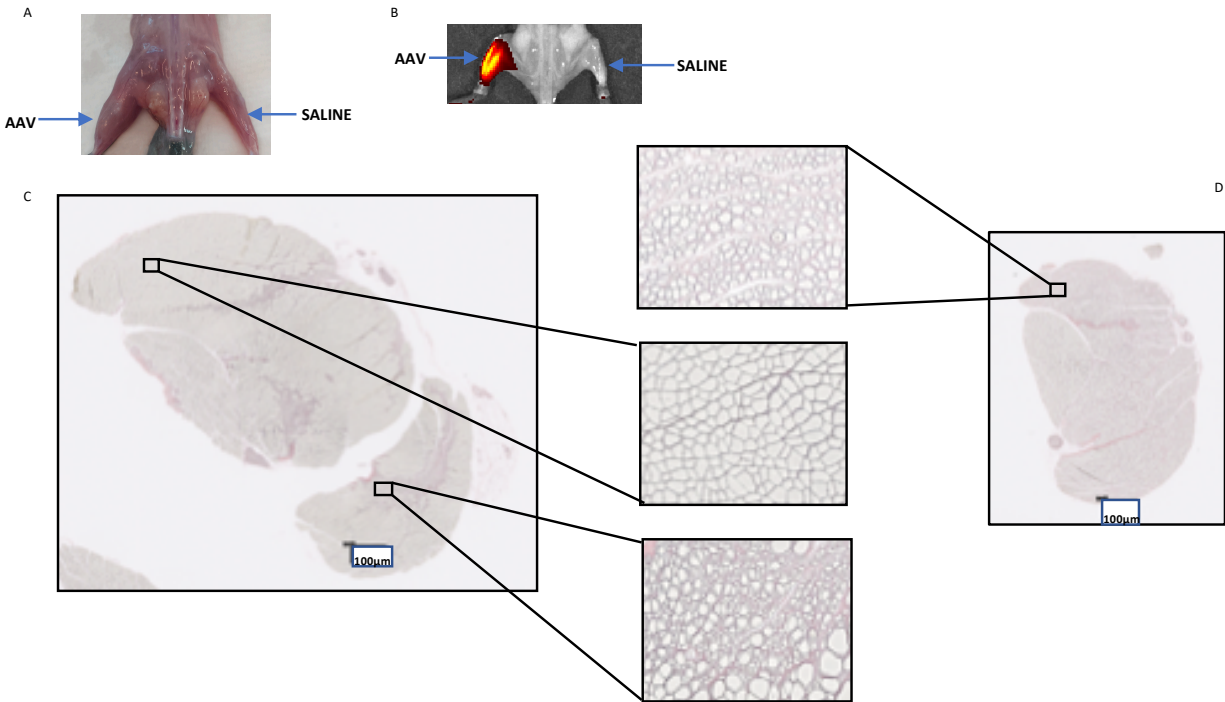


FIG 6. *Effects of AAV-Chkb injection on rmd muscle phenotype.* Gross anatomical observations show comparatively larger size of the injected muscle compared to saline injected muscle (A). In vitro fluorescence imaging show fluorescence localized to the injected muscle and no fluorescence in the saline injected muscle (B). Cross sections of whole gastrocnemius muscle at 1.25X on the nanozoomer show comparatively larger size of the injected muscle (C) compared to the saline injected muscle (D). Inset figures at 20X magnification represent partial restoration of muscle fiber in AAV-injected muscles as opposed to saline injected muscle.

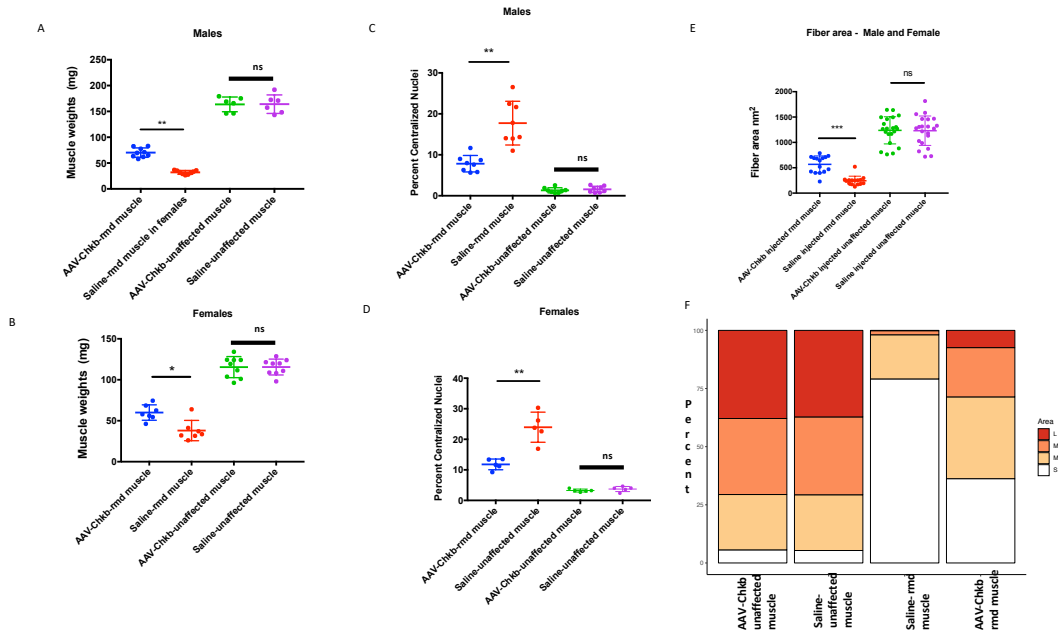


FIG 7. Effects of AAV-Chkb injections on rmd muscle weights, centralized nuclei and fiber size. AAV-Chkb injected gastrocnemius muscles in males (A) and females (B) show significantly higher and restored muscle weights compared to sham injected muscles, whereas there is no difference in the AAV-Chkb and sham injected gastrocnemius muscles of unaffected mice. Percent of centralized nuclei, an indicator of poor muscle health, was observed to be significantly reduced in AAV-Chkb injected rmd muscles compared to the sham injected muscles in both males (C) and females (D). Injected unaffected muscles did not show any significant differences when compared to sham injected unaffected muscles in both males and females (C-D). Injected rmd muscles show a significant ($p=0.0001$) increase in average fiber areas, in males and females, compared to sham injected rmd muscle with a significant increase in percentage of large (L) and medium (M1, M2) fibers and a decrease in the percent of small (S) muscle fibers (E-F). $N= 8$ mice/sex/genotype. Mice were injected at 3 weeks of age and their gastrocnemius muscles harvested at 7 weeks of age. Error bars represent mean and SD.

***Chka* can compensate for lack of *Chkb* in *rmd* mutant mice.** The normal developmental loss of *Chka* gene expression in mouse caudal muscles during postnatal muscle differentiation makes skeletal muscles of the hindlimb particularly susceptible to disease in the case of *Chkb* gene mutations in mice. In order to test the hypothesis that the paralogous CHKA protein can functionally compensate for CHKB deficiency in *rmd* mice, we injected *rmd* muscles with an AAV vector expressing a human *CHKA* cDNA. The AAV-injected muscles were observed to be larger than the saline injected muscles seven weeks post-injection (Supplemental Fig 3 C). *In vivo* fluorescence imaging of *rmd* mice showed that EGFP fluorescence was localized to the site of injection whereas the saline injected site did not display any fluorescence (Supplemental Fig 3 D). Like the *Chkb* gene therapy experiment, H&E staining of AAV injected muscles showed major regions of restored muscle structure (Supplemental Fig 3 E-F). Montage images stained with Gordon and Sweet's to highlight the circumference of each myofiber showed significant regions with normal morphology and regions of partial rescue in the AAV-*CHKA* injected *rmd* muscles (Supplemental Fig 4 E-F). The AAV-injected muscles of *rmd* mice weighed significantly more than the saline-injected contralateral muscles with a $p=0.008$ and $p=0.006$ in males and females respectively. The difference in muscle weights between the AAV and sham injected WT control mice was not significant ($p=0.31$ in both males and females) (Fig 8 A-B). AAV-injected *rmd* muscles showed a decrease in the percent of centralized nuclei in comparison to saline injected *rmd* muscle ($p=0.16$ and $p=0.008$ in males and females respectively), while the AAV-injected control muscles were not significantly different from the saline-injected control muscles ($p=0.06$ and $p=0.16$ in males and females respectively) (Fig 8 C-D). Similar to our AAV-*Chkb* injections, treatment with the AAV-*CHKA* virus rescues the disease phenotype in dystrophic muscles without inducing hypertrophy of normal muscle in WT mice. AAV-injected

muscles showed a significant increase ($p < 0.0001$) in average muscle fiber area in males and females. Fiber areas were classified into 4 quartiles, as in case of *Chkb* injections, into small (S=0-209 nm^2), medium (M1=209.01-630 nm^2), medium (M2=630.01-1159 nm^2) and large (L=1159.01-8387 nm^2). AAV-injected *rmd* muscles showed a significant increase in the percent of M1, M2 and L fiber sizes and a significant decrease in the percent of S fiber sizes (Fig 8 E-F).

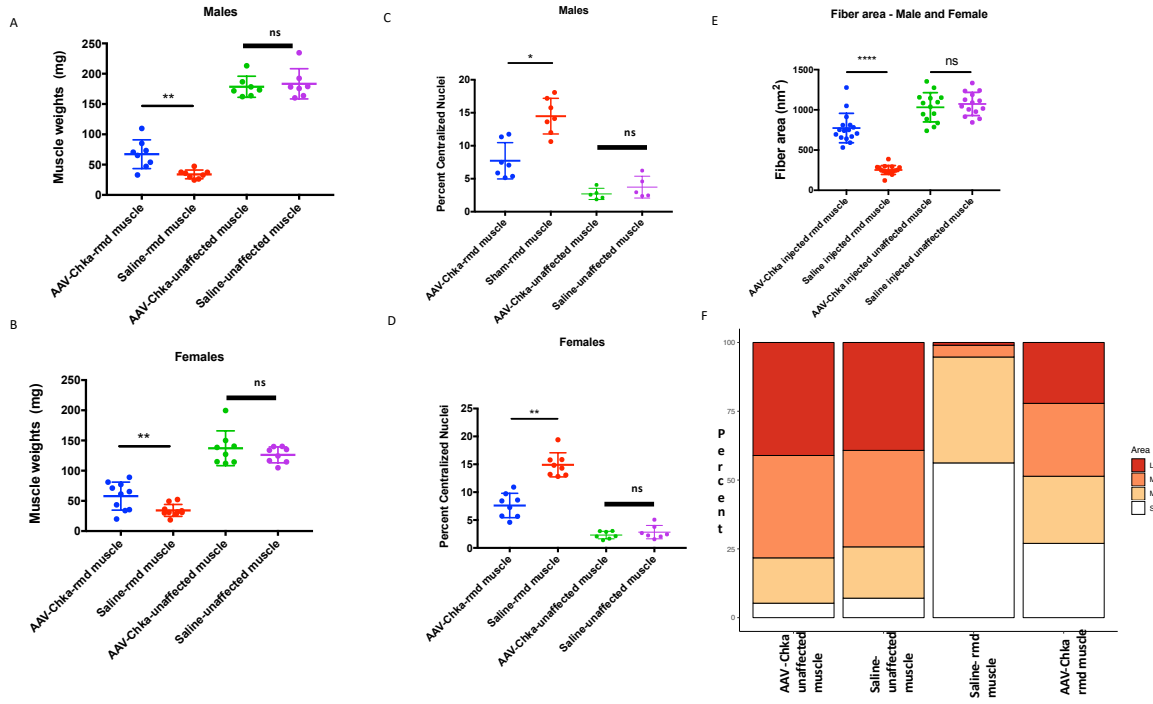


FIG 8. Effects of AAV-Chka injections on rmd muscle weights, centralized nuclei and fiber size. AAV-Chka injected gastrocnemius muscles in males (A) and females (B) show significantly higher and restored muscle weights compared to sham injected muscles, whereas there is no difference in the AAV-Chkb and sham injected gastrocnemius muscles of unaffected mice. Percent of centralized nuclei was observed to be significantly reduced in AAV-Chka injected rmd muscles compared to the sham injected muscles in both males (C) and females (D). Injected unaffected muscles did not show any significant differences when compared to sham injected unaffected muscles in both males and females (C-D). Injected rmd muscles show a significant ($p < 0.0001$) increase in average fiber areas, in males and females, compared to sham injected rmd muscle with a significant increase in percentage of large (L) and medium (M1, M2) fibers and a decrease in the percent of small (S) muscle fibers (E-F). N= 8 mice/sex/genotype. Mice were injected at 3 weeks of age and their gastrocnemius muscles harvested at 7 weeks of age. Error bars represent mean and SD.

Discussion:

The discovery and characterization of the spontaneous *rmd* mutant mouse led to the discovery of *CHKB* as the gene underlying MDCMC (Sher et al., 2006b)(Mitsuhashi, Hatakeyama, et al., 2011), establishing the validity of the *rmd* mouse as a model of the human disease and opening up avenues for mechanistic and preclinical studies. MDCMC is caused by recessive loss of function mutations in the choline kinase beta gene. We have shown that the ubiquitous loss of *Chkb* in *rmd* mutant mice leads to a cell and tissue-specific disease which can be restored by upregulating expression of *Chkb* in skeletal muscle tissues only, indicating that regeneration of skeletal muscles in a *Chkb*-deficient environment is cell-autonomous. Intramuscular AAV injections of *Chkb* and *Chka* gene also help restore muscle morphology in *rmd* mutant mice, while dietary supplementation of Kennedy pathway intermediates does not have a regenerative or rescue effect.

Gene replacement of *Chkb* by transgenesis or by AAV6 delivery rescues the muscular dystrophy phenotype of the *rmd* mouse. Introduction of a functional copy of the *Chkb* transgene under a muscle-specific promoter prevented disease onset, with the Tg-*rmd* mice showing normal mitochondrial dimensions and muscle strength. This indicates that although the *Chkb* gene is ubiquitously expressed, the enzyme deficiency results in a muscle-specific defect in phosphatidylcholine biosynthesis that can only be rescued by a cell-autonomous increase of *CHKB* activity within muscle cells themselves. Overexpression of the *Chkb* gene up to a 14-fold magnitude does not cause a negative impact on the Tg-WT animals, with mice showing behavioral and muscle strength phenotypes comparable to their non-transgenic littermates. Further, introduction of the *Chkb* gene using AAV6 post-disease onset in young adult *rmd* mice can help reverse the degenerative muscle disease. Intramuscular AAV6 vector injections

containing a functional copy of *Chkb* gene in adult skeletal muscle resulted in improved muscle regeneration capacity and subsequent increased muscle weights and fiber areas with a decreased number of centralized nuclei compared to untreated *rmd* muscles (Hollinger & Chamberlain, 2015)(Zincarelli, Soltys, Rengo, & Rabinowitz, 2008)(Ramos, Chamberlain, & Muscular, 2015). A detailed analysis of fiber areas shows an increase in the percent of large and medium sized fibers in AAV injected muscles with a significant decrease in the percent of small sized fibers. The presence of different fiber sizes pre and post AAV-*Chkb* injections illustrate the partial nature of fiber rescue. It can be inferred that the transduced *rmd* muscle fibers regenerated to a healthier phenotype whereas, the *rmd* muscle fibers that were already atrophied and wasted or that were not transduced remained unhealthy, showing a dystrophic phenotype. These results suggest that replacing *Chkb* gene, post disease-onset and in adult mice helps reverse muscular dystrophy by increasing muscle regeneration in a cell-autonomous manner in dystrophic *rmd* mice. Injecting and thus upregulating *Chkb* expression in unaffected muscles did not have any detrimental effects as indicated by lack of hypertrophy in AAV-*Chkb* injected skeletal muscles, indicating that upregulation of the *CHKB* gene in MDCMC patients via AAV mediated gene therapy can be a possible therapeutic measure. We have also shown that up-regulation of *CHKA* by localized AAV-*CHKA* injections helps to restore muscle regeneration and alleviate the dystrophic phenotype in *rmd* muscles, similar to AAV-*Chkb* injections, making this another potential therapy for MDCMC.

Biochemical studies suggest that choline kinase alpha and beta can function either as homodimers or heterodimers in the phosphorylation of choline to phosphocholine for the production of phosphatidylcholine (Aoyama et al., 2004). In *rmd* mice, total choline kinase activity in the hindlimbs is absent whereas in the forelimbs, choline kinase activity is attenuated

by only 50% (Wu et al., 2010a). These results led to the hypothesis that there must be an age-dependent reliance on the activity of CHKB in WT hindlimb skeletal muscles of mice as *Chka* gene expression decreases. The partial retention of choline kinase activity in the forelimbs of adult *rmd* mice (due to residual *Chka* expression) provides a possible explanation for the decreased severity of disease in forelimb muscles versus the much more severe and progressive dystrophy in hindlimb muscles. This led us to test the possibility that CHKA can functionally compensate for CHKB deficiency in the severely affected hindlimb muscles of the *rmd* mutant mouse. The mechanism by which the expression of *Chka* shuts down in adult mouse skeletal muscles is still unclear. A study of CHKA expression in human skeletal muscle over time has not been tested, however, GTEx expression data across 53 adult tissues shows that *CHKA* transcript levels are the lowest in adult skeletal muscles (GETx Portal Version V7). Our data indicated that increasing the expression of CHKA in post-disease onset, adult skeletal muscles results in improved muscle regeneration, increased muscle weights and fiber areas and a decrease in the percent of centralized nuclei with no immediate observable toxic effects. This suggests that even though CHKA expression is normally shut down in adult skeletal muscles, upregulation of its expression can compensate for lack of CHKB activity.

Increase expression of choline kinase alpha, but not beta, has been implicated in tumorigenesis, with *CHKA* overexpression detected in 40-60% of human tumors (Chang, Few, Konrad, & See Too, 2016). Transfecting human (Hek293T) cells with *Chka* resulted in anchorage independent growth activity similar to that demonstrated by Rho-A activation (Ramírez De Molina et al., 2005). It can be inferred that, *CHKA* upregulation via AAV injections can potentially cause non-cancer cells to take on a cancerous phenotype, while siRNA downregulation can lead to death of cancer cells. Immediate evidence (7 weeks post-injection)

for this was not found in our experiments of localized intramuscular injections of CHKA in *rmd* skeletal muscles. CHKA injected mice will need to be aged and studied for potential tumorigenic effects of gene upregulation in order to determine whether the association between CHKA and cancer is directly causative of disease or whether it is instead a biomarker of the cancerous state.

Chkb deficiency causes muscular dystrophy in a rostral to caudal gradient in mice as *Chka* expression is shut down in caudal adult skeletal muscles. One might expect that there is a functional reason for the observed decrease in normal *Chka* gene expression in adult skeletal muscles, however our data suggests that overexpression of CHKA via an AAV gene therapy approach is not deleterious in skeletal muscles. In the CHKB-deficient condition, CHKA can compensate for the lack of choline kinase beta to form functional α - α homodimers for the phosphorylation of choline to phosphocholine in skeletal muscles. Our results support that both the upregulation of either CHKB or CHKA can be used as a potential therapy for the rescue of MDCMC symptoms. As gene therapy may not be appropriate for all patients, strategies to upregulate the endogenous *CHKA* locus might also prove effective for the alleviation of MDCMC symptoms. Interestingly, the upregulation of CHKB or CHKA also reduces the presence of megamitochondria, indicating that the two phenotypes are related and cannot be rescued independent of each other. Megamitochondria are thought to result in a disruption of normal myofiber structure, with altered cellular architecture including disordered sarcomeric and muscle triad structures that are necessary for the orderly distribution of energy-producing mitochondria. Whether the generation of megamitochondria in skeletal muscle directly causes the muscular dystrophy or is just a biomarker of the disease remains to be tested.

Materials and Methods

Mouse colonies: All mice were bred and maintained at the Jackson Laboratory following procedures and protocols approved by our institutional animal care and use committee (IACUC). For breeding, mice were kept in humidity and temperature controlled rooms with a 12:12 dark:light cycle. They were given an NIH-mouse diet with 6% fat (PMI Feeds, Inc., St. Louis, MO) ad libitum with free access to water (HCl-acidified, pH 2.8–3.2). For all motor and behavioral tests, the mice were moved to a separate room and singly housed where they were maintained under IACUC approved conditions until completion of the test procedures. In this facility, the mice were kept on a 4% extruded grain diet and were provided with clean acid water unless mentioned otherwise.

Generation of transgenic (rescue) mouse: Expression of Chkb transgene in transgenic mice, for the generation of rescues was achieved by using the titin (Ttn) promoter to express the Chkb cDNA transgene specifically in skeletal and cardiac muscles (Maddatu et al., 2005a). This promoter reproduces the endogenous pattern of titin expression in muscles prior to the onset of the rmd disease symptoms. The Ttn promoter includes 3.5 kb of sequence upstream of the non-coding Ttn exon 1, the entire 2.1 kb of intron 1 and exon 2 is truncated just before the start codon. The inclusion of an intron in the construct is beneficial for proper long term expression in transgenic mice and to take advantage of any possible control elements that might be located in the first intron. The polyadenylation signal is a 200 bp fragment derived from the SV40 viral genome that we have successfully used in numerous transgenic lines. A 1589bp Chkb cDNA fragment, including 234bp upstream from the exon 1 ATG start codon (Ch15 reverse strand, 89,429,834bp, Ensembl GRCm38) to 145 bp downstream from the exon 11 TGA stop codon (89,426,584bp) was PCR cloned and blunt-ligated into the Ttn plasmid backbone immediately

after the truncated exon 2. The completed pTtn-Chkb constructs were injected into fertilized C57BL/6J eggs by the microinjection. Transgenic founders were bred to C57BL/6J mice to generate a stable colony and maintain the transgene on an inbred background. Transgenic mice were identified through PCR of tail DNA with a forward primer in the 3' end of the TTN promoter sequences, TTN100F (5'-TCTCCACCAAGAAGACGCTG-3') together with a reverse primer in the 3rd exon of Chkb, Chkb-e3R (5'-CTTTCTAATACCAAGGAGTCTACACC-3').

Mitochondrial area

Specimen preparation: For Transmission Electron (TE) microscopy, 4 mice per genotype (*rmd*, WT and Tg-*rmd*) were used to analyze mitochondrial structure. The medial and lateral gastrocnemius muscle were isolated and fixed in a solution of 2% paraformaldehyde, 2% glutaraldehyde, in 0.1 M cacodylate buffer (pH 7.2) at 4°C overnight. Tissues were then washed, dehydrated in graded series of ethanol and processed for 812 resin embedding. Samples were then cured at 70°C for 48 hours followed by thin sectioning (90nm) with a Leica EM UC6 ultramicrotome (Leica Microsystems, Buffalo Grove, IL) on a diamond knife. The sections were then placed on 300 mesh copper grids and stained using 2% uranyl acetate and Reynolds lead citrate. Samples were evaluated at 80 kV using a JEOL JM-1230 transmission electron microscope (JEOL, Tokyo, Japan) and images collected with an AMT 2K digital camera (Advanced Microscopy Techniques, Woburn, MA).

Mitochondrial area calculations: 10 pictures per sample (n=4) were taken using the TE microscope. Mitochondrial areas were measured using FiJi and analysis of variance calculations were performed on Prism software (version 7.0c for Mac OS X).

Behavioral and motor assays: Adult mice (n=10 per sex, per genotype) were put through a battery of behavioral tests for motor function. The tester was blinded for the duration of the entire battery of assays. The time of the day at which each test was performed was kept constant for each assay performed. The mice were allowed a minimum resting period of 2 days between every test. All equipment was sprayed down and wiped with 70% ethanol before and in between testing mice. The test animals were habituated for 60 mins in the testing room before each test. The order of testing was as follows; open field, rotarod, grip strength and Erasmus ladder.

Open field test: Post habituation in testing room, mice were individually placed in standard Verasamax chambers, under standard lighting conditions of ~500 lux and with standard background noise levels of about 62 -65 dB. The mice were tested for 60 mins with data collection in 5 min bins. Analysis was performed for total distance travelled (cm), (Paumier et al., 2013)(Seibenhener & Wooten, 2015)(Asinof et al., 2015)(Crawley, 2000)(Tatem et al., 2014)(Sukoff Rizzo et al., 2018).

Rotarod test: The Ugo Basile rotarod was used to analyze motor co-ordination and balance in mice. The rotarod drum was steadily accelerated from 4 to 40 rpm over a 300 sec duration. Each animal was put through 3 consecutive trials and the average latency to fall was recorded. Mean of combined latency to fall of the entire group was also calculated (Paumier et al., 2013)(van der Vaart et al., 2011).

Grip strength test: Animals were individually tested using the force gauge by BIOSEB. Each animal was tested for three forepaw trials and three all paw trials (6 total trials). A force transducer is used to measure maximum force generated which is then normalized to body weight and analyzed using the BIO-CIS software (Brooks & Dunnett, 2009)(van der Vaart et al., 2011).

Erasmus Ladder: Fully automated Erasmus ladder was used to study locomotion and motor coordination in mice. Noldus equipment with software Version 1.1 as described by R Van Der Giessen, et al, 2008 and Vinueza et al, 2012, were used for the testing procedure. Each animal was run through 42 trials per day for 5 consecutive days. For all the trials there was perturbation but no tone cue used. Tone cue was added to the trials on day 5 of the testing. (Van Der Giessen et al., 2008)(M. F. Vinueza Veloz et al., 2012). During data acquisition, the mice were kept in the pexiglass chamber of the goal box. Data for percent missed steps and percent backsteps, were recorded and later analyzed (Mara Fernanda Vinueza Veloz et al., 2014).

CDP-choline diet supplementation: For this study, 4 WT mice/sex and 8 rmd mice/sex were provided with CDP-choline supplemented 76A lab diet gel from Clear H₂O and 4 rmd mice/sex were used as controls and were fed plain diet gel. Same sex mice were housed in doublets in each side of a duplex mouse cage. 87.5mg of CDP-choline was mixed in 56gms of standard 76A lab diet gel cups. On an average a mouse eats 8gms of diet gel per day giving them a dose of 500mg/Kg/day. Diet gel cups were changed 3 times a week (Bachmanov et al., 2002). The WT mice were administered diet gel cups spiked with CDP-choline to assess to possibility of toxic effects due to increased consumption of CDP-choline. 8 rmd mice/sex were administered CDP-choline spiked diet gel cups, these are referred to as Test mice and the remaining 4 rmd mice/sex were administered standard diet gel cups with no CDP-choline added, these are referred to as control mice. The total length of this study was 3 months. Mice were weighed and assessed for general health every week (Wu et al., 2012)(Secades JJ, 1995)(Wurtman, Regan, Ulus, & Yu, 2000).

Adeno-Associated Viral vector design: Adeno-Associated Viral vector design: An AAV subtype 6 was selected as it shows higher gene expression and tropism in skeletal muscles (Zincarelli et al., 2008)(Hollinger & Chamberlain, 2015). AAV vector plasmid AAV-Chkb was derived from AAV-CAG-GFP plasmid (Addgene #28014). This plasmid contains mouse Chkb cDNA tagged by a 3X Flag Tag (5'-GACTACAAAGACCATGACGGTGATTATAAAGATCATGACATCGACTACAAGGATGACGATGACAAG-3') at the 5' end in order to distinguish transduced Chkb expression from endogenous expression, all under the control of a CAG (CMV early enhancer/chicken beta actin) promoter. The plasmid also contains EGFP as a gene expression reporter protein, the expression of which is driven by the CAG promoter through P2A ribosomal skipping sequence downstream of the Chkb coding sequence (Y. Wang, Wang, Wang, Zhao, & Xia, 2015). Recombinant AAV6 vectors were produced by triple transfection of HEK293T/17 cells with Chkb plasmid DNA, pAAV2/6 packaging plasmid, and pAd delta F6 helper plasmid (Penn Vector Core) using linear polyethylenimine (PEI). Transfected cells were incubated at 37°C, 5% CO₂ in DMEM supplemented with 2.5% fetal bovine serum. Three days after transfection, the crude vector fraction was obtained by combining the precipitated products from culture medium with final 8% polyethylene glycol and the cell extracts lysed by repeated freeze–thaw cycles. The crude vectors were then purified by iodixanol density-gradient ultracentrifugation. Purified AAV6 vector was dialyzed against 1× PBS with 5% sorbitol. Viral titer was measured using real time PCR with primers for the ITR region (5'-GGAACCCCTAGTGATGGAGTT-3' and 5'-CGGCCTCAGTGAGCGA-3'). A final volume of 300µl with a concentration of 1.84 X 10¹³ vg/ml was obtained for AAV-Chkb injections and 150µl of 2 X 10¹⁴ vg/ml of AAV-Chka.

Transduction of muscle fibers and tissue processing: The left gastrocnemius muscle of 3 week old rmd mice and unaffected controls were injected locally with 2×10^{10} vg of AAV vector solution in 25 μ l PBS. The right gastrocnemius muscle was treated as control and injected with 25 μ l of sterile PBS solution only (Lu et al., 2003)(Liu, Yue, Harper, Grange, & Jeffrey, 2008). The injected animals were aged on shelf for 7 weeks post-injection and the gastrocnemius muscles were harvested at 10 weeks of age and fixed in 10% neutral buffered formalin for 24hrs before embedding in paraffin.

Muscle fiber staining:

Gordon and Sweets stain for reticular fibers: Injected gastrocnemius muscles were harvested 7 weeks post injection and fixed in 10% Neutral buffered Formalin (NBF). Samples were then oxidized in 1% potassium permanganate solution, bleached in oxalic acid, sensitized in 2.5% ferric ammonium sulfate and impregnated with ammoniacal silver solution. Following a rinse and a 2 min fix in formalin, the samples are toned in 0.2% gold chloride solution and washed with 5% sodium thiosulphate. Samples are rinsed, dehydrated and clear mounted for microscopy analysis.

Hematoxylin and Eosin staining: Injected muscle fibers were fixed in 10% NBF and embedded. Post embedding, the samples were processed in a Leica automated stainer by Histology core services at the Jackson Laboratory.

Statistical analysis: All the experiments were performed at the Jackson Laboratory, Bar Harbor. All mouse handling, testing, and analysis were performed blinded for mouse genotype. Where appropriate, statistical significance was calculated using Student's t-test or 2-way ANOVA with post-hoc Bonferroni corrections unless otherwise noted. Calculations were performed using Prism 7.0c software for Mac OS X and any significant differences ($p < 0.05$) between test and control strains are denoted by an asterisk symbol.

CHAPTER 3

SIGNIFICANT DIFFERENCES IN BRAIN LIPID PROFILES DO NOT TRANSLATE TO BEHAVIORAL DIFFERENCES IN TRANSGENIC *RMD* MICE.

Abstract:

Congenital muscular dystrophy with megaconial myopathy (MDCMC) is characterized by an early onset of muscle degeneration and wasting, megamitochondria and severe cognitive impairments. As reported earlier, we have identified a spontaneous mutant mouse- *rmd*, with a 1.5kb deletion in choline kinase beta gene (*Chkb*) that shows muscular dystrophy in a rostral to caudal gradient and megamitochondria. The *rmd* mouse has been characterized for muscle strength, function and enzyme biochemistry, all of which match the phenotype seen in MDCMC patients. Here we tested whether the *rmd* mice can also be used to model the cognitive impairments seen in MDCMC patients. We have used a muscle-specific *Chkb* transgene to rescue the muscular dystrophy in *rmd* mutant mice in order to conduct behavioral assays for the determination of working memory and learning in *Chkb* deficient conditions. Along with this, we have also conducted a detailed MS/MS^{ALL} mass spectrometry analysis on *rmd* and Tg-*rmd* mice in comparison to WT mice to test for differences in brain lipid profiles as has been observed in cases of cognitive impairment. We observed that even though there are significant differences in the lipid profiles of brain tissue from *rmd* and Tg-*rmd* mice compared to WT mice, these changes do not translate to significant differences in behavioral analysis of the same mouse models. Our data contributes to the characterization of cognitive impairments in a mouse model of MDCMC and defines lipidomic changes in the brain of *Chkb*-deficient mice.

Introduction:

Congenital muscular dystrophy with megaconial myopathy (MDCMC) is a rare form of muscular dystrophy in which patients suffer from muscle wasting and have giant mitochondria. In addition, in all reported cases of MDCMC, patients were found to have cognitive impairments, demonstrated by an IQ lower than the general average of 90 on the Stanford-Binet scale, speech defects and slow learning (Nishino et al., 1998)(Mitsuhashi, Ohkuma, et al., 2011). As reported in chapter 1, we have discovered a mutant mouse (*rmd*) carrying a spontaneous deletion in the *Chkb* gene and display an early onset progressive muscular dystrophy with prominent megamitochondria. Mutant *rmd* mice show two out of three phenotypes observed in MDCMC patients and here we determined whether *rmd* mice could also model the cognitive impairments observed in the MDCMC patients, thus making it a model for all of the major aspects in MDCMC phenotype.

Cognitive impairment in a mouse can be tested by running a battery of behavioral assays that include tests for working and short-term memory and learning potential in the mice. These assays require the mice to perform tasks that require a certain level of physical activity. The *rmd* mice start dragging their hindlimbs at about 8 weeks of age, making this level of physical activity near impossible for some of the tests that continue even after the mice are about 6 months of age. As a result, the *rmd* mice could not be used to assess cognitive impairments. As reported in chapter 2, the Tg-*rmd* mice have been engineered to carry a functional copy of the *Chkb* gene under the control of a skeletal muscle specific promoter-Titin, this gives them a rescued phenotype in the skeletal muscles but a retains the CHKB-null phenotype in brain tissues, making them a good model for the testing of cognitive impairments.

Choline and phosphatidylcholine in normal brain development:

It has been shown that the deficiency of CDP-choline, a downstream metabolic product of phosphorylation of choline can detrimentally affect neuronal cells and more specifically the glial cells of the hippocampus (Zweigner et al., 2004)(Sanders & Zeisel, 2007). Lack of choline impairs PC production, an important compound for normal brain development. Administration of PC in mice with dementia have a neuroprotective effect and improves memory by increasing brain acetylcholine concentration (S. Chung, et al., 1994). Single nucleotide polymorphisms (SNPs) close to the choline kinase beta gene influences neurobehavior and can cause susceptibility to narcolepsy (Miyagawa et al., 2008). Previous literature suggests that deficiencies in PC production influences neuronal and neuro-behavioral phenotypes.

Choline is an essential nutrient with an average intake for men being around 600 mg/day and that for women at about 450 mg/day. It is required to make phospholipids, especially phosphatidylcholine, and is an important precursor for the biosynthesis of neurotransmitter acetylcholine. Choline deficiency has been reported to cause disorders in the muscle, liver, kidney, pancreas, developing brain and nervous system. Though choline can be synthesized *de novo*, the minute quantities synthesized are not sufficient to carry out synthesis of phospholipids and neurotransmitters and hence *de novo* synthesis of choline is supplemented with dietary intake by absorption from food like organ meats, milk, eggs and peanuts. (Zeisel SH, 1992)(Sanders & Zeisel, 2007). *De novo* synthesis of choline is carried out by the sequential methylation of phosphatidylethanolamine (PE) to PC, catalyzed by phosphatidylethanolamine N-methyltransferase (PEMT) using S-adenosylmethionine (AdoMet) as a methyl-group donor. Choline can also be generated *de novo* by the metabolism of PC via phospholipases.

(Lin & Gant, 2014). Choline synthesized or absorbed from food can then pass through the intercellular tight junctions in the brain, where it is phosphorylated to form phosphocholine and later PC. It has been suggested that deficiency of choline and hence that of PC triggers apoptosis in the brain (Zweigner et al., 2004). PC deficiency also results in muscular dystrophy as reported by Sher et al. and outlined in chapter 2 (Sher et al., 2006)(Wu et al., 2009)(Zeisel, 1992). PC cannot be transported through the blood brain barrier and hence neuronal tissue is dependent on the synthesis of PC from transported choline.

Differences in brain lipid profile in normal and cognitively impaired humans and rodents.

The human brain is about 60% lipid, making lipids important regulators of brain function. Studies on post mortem brain tissue from Alzheimer's disease (AD) patients show that patients with late onset Alzheimer's disease (LOAD) have a distinctly different lipid profile than unaffected humans. After free cholesterol, phospholipids form the second major lipid component in brain with PC and phosphatidylethanolamine (PE) being the most abundant components within the phospholipid group. It has been shown that LOAD patients show a 1.8 fold increase in diacylglycerols (DAGs) in the prefrontal cortex (PFC) with a significant decrease of about 25% in PE species. LOAD patients also show significant changes in sphingolipid metabolism, monoacylglyceryl phosphate and sphingomyelins, with higher plasma levels of sphingomyelins being predictors of slower disease progression in AD patients. The concentration of free fatty acids in plasma was 43% lower in persons with mild cognitive impairments (MCI) and 52% lower in AD patients. AD patients showed significant lower levels of DHA. Analysis of familial Alzheimer's disease (FAD) on three different transgenic mouse models showed fatty acyl long chain remodeling with a decrease in long-chain phospholipid and long-chain sphingolipids

balanced by increases in short and long medium length species. Selective accumulation of medium-chain length SM was observed. Even though similar trends in changes in brain lipid profiles were observed in humans and mice, these changes were not identical within different regions of the brain in humans and mice exemplifying changes in different lipid species (R. B. Chan et al., 2012)(Cunnane et al., 2012)(Wood, 2012).

Results:

***rmd* mutant mice have lower muscle strength than WT littermates:** *rmd* mice begin dragging their feet at about 8 weeks of age. Since behavioral assays for memory and learning are validated for mice aged 8-10 weeks and require considerable physical activity like mobility in a Y-maze and rearing activity for touchscreen, it was imperative to test for muscle strength and function in *rmd* mice at an earlier age. Testing at wean age of 4 weeks was selected as the earliest time point at which the mice can be tested and run on all the behavioral assays. The *rmd* mice were tested against aged-matched WT littermates for muscle strength using open field, rotarod and grip strength assays. The *rmd* males and females showed a small but significant difference from their WT littermates ($p = 0.02$ and 0.04 , respectively) in the total distance travelled (Fig 9 A- B). Males and females also showed a significant difference compared to the WT in the vertical activity with $p=0.001$ and 0.003 , respectively (Fig 9 C-D). The *rmd* mice show decreased fore-paw (males and females, $p < 0.0001$) and all-paw (males and females, $p < 0.0001$) grip strength (Fig 10 A-D). In the rotarod assay, the *rmd* mice showed a significant latency to fall on an average and in between trails with a P value less than 0.0001 in both males and females (Fig 11 A-B). As observed from these tests, muscle function is impaired at 4-5 weeks, making it

impossible to use *rmd* mice for testing in behavioral assays like paired associates learning or dPAL assay as these assays may continue for a period of > 3months.

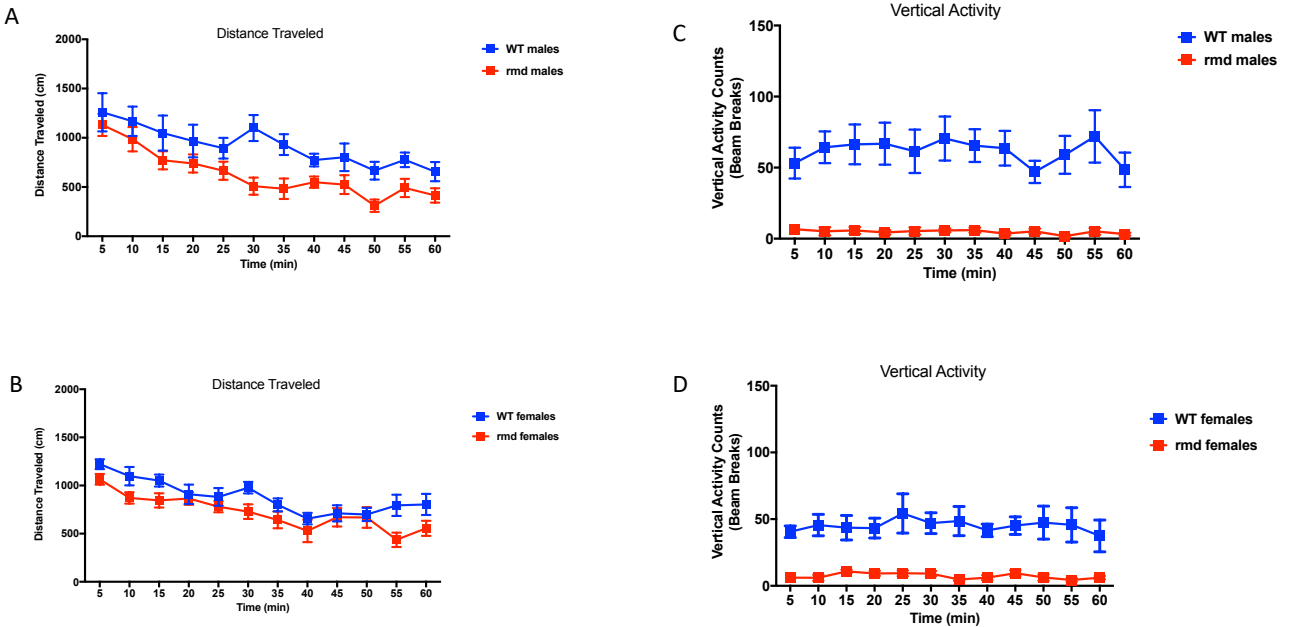


FIG 9. Measurement of open field activity in *rmd* mice. The *rmd* males and females showed a significant difference compared to the WT in the total distance travelled ($p=0.02$ in males and 0.04 in females) and in the vertically activity shown ($p=0.001$ in males and 0.003 in females). $N= 5$ mice/sex/genotype aged 4-5 weeks. Error bars represent SD.

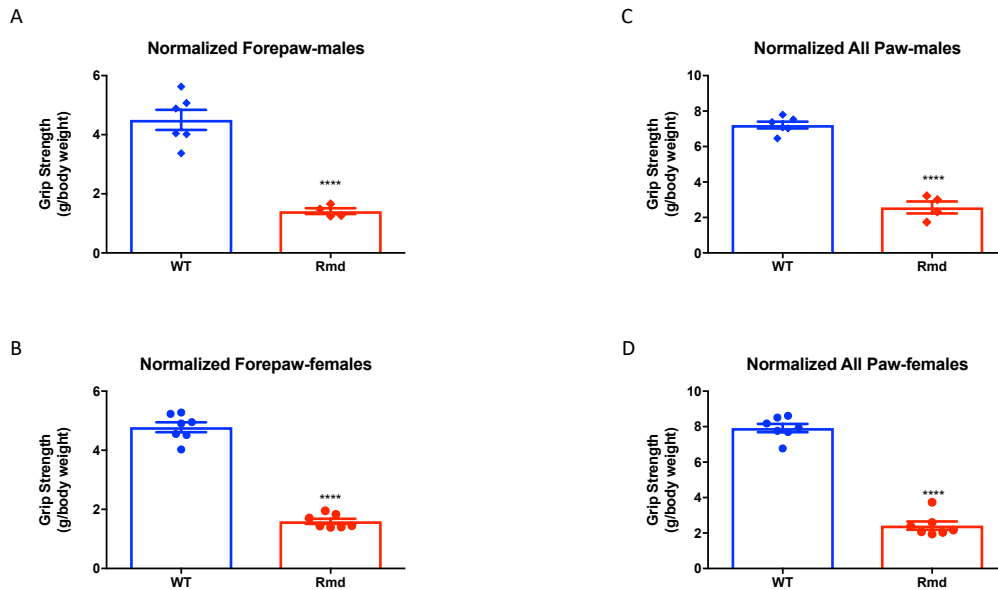
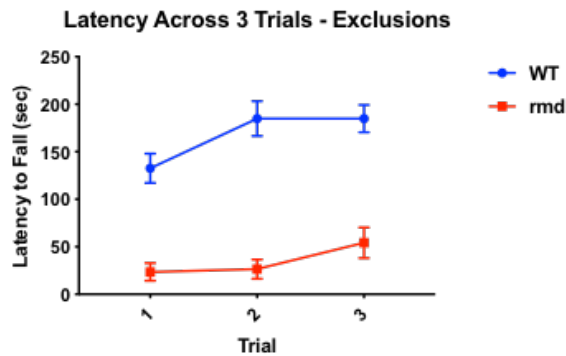


FIG 10. Measurement of grip strength in *rmd* mice. *rmd* mice show significantly decreased fore-paw and all-paw grip strength when compared to their unaffected (WT) littermates with males and females showing p values less than 0.0001 in each of the tests (A-D), suggesting lower grip and hence muscle strength. N= 5 mice/sex/genotype aged 4-5 weeks. Error bars represent SD.

A



B

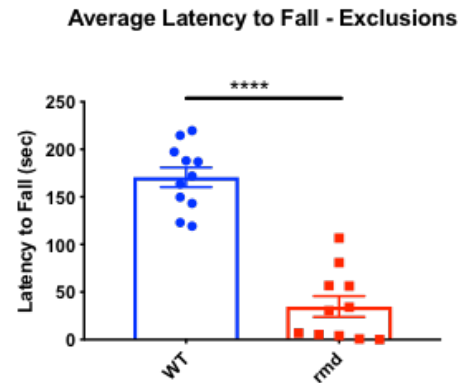


FIG 11. Measurement of rotarod activity in *rmd* mice. *rmd* mice show a significant difference from WT in latency across trials in the rotarod test with $p < 0.0001$ (A) and a significant difference of $p < 0.0001$ in the average latency to fall (B) in a grouped analysis of males and females. $N = 5$ mice/sex/genotype aged 4-5 weeks. Error bars represent SD.

***rmd* mutant mice show significant changes in lipid profile:** Tissue from the cerebellum, cortex and Mid + Hind brain region of *rmd* mice ($N = 2$ mice/sex) were compared with those of WT mice ($N = 2$ mice/sex) in order to test for any changes in the lipid profile as observed in LOAD and MCI patients. These mice were aged and were 56-58 weeks old at the time of brain tissue harvest. MS/MS^{ALL} employs a sequential stepping through a user pre-defined mass range that isolates and fragments all ions within that mass range, resulting in the collection of more than a thousand MS/MS spectra that covers every precursor in the mass range of each cycle. MS/MS^{ALL} is hence, more robust and efficient form of collection of mass spectra data. Lipid profiling with MS/MS^{ALL} mass spectra suggests significant differences in the major lipid molecules like triacylglycerols (TAGs), sphingomyelins (SMs), diacylglycerols (DAGs), monoalk(en)yl

diacylglycerol (MADAGs) and glycerophospholipids (GPLs). Changes within species of lipid molecules are reflected via changes in number of branches, branch length and in saturation.

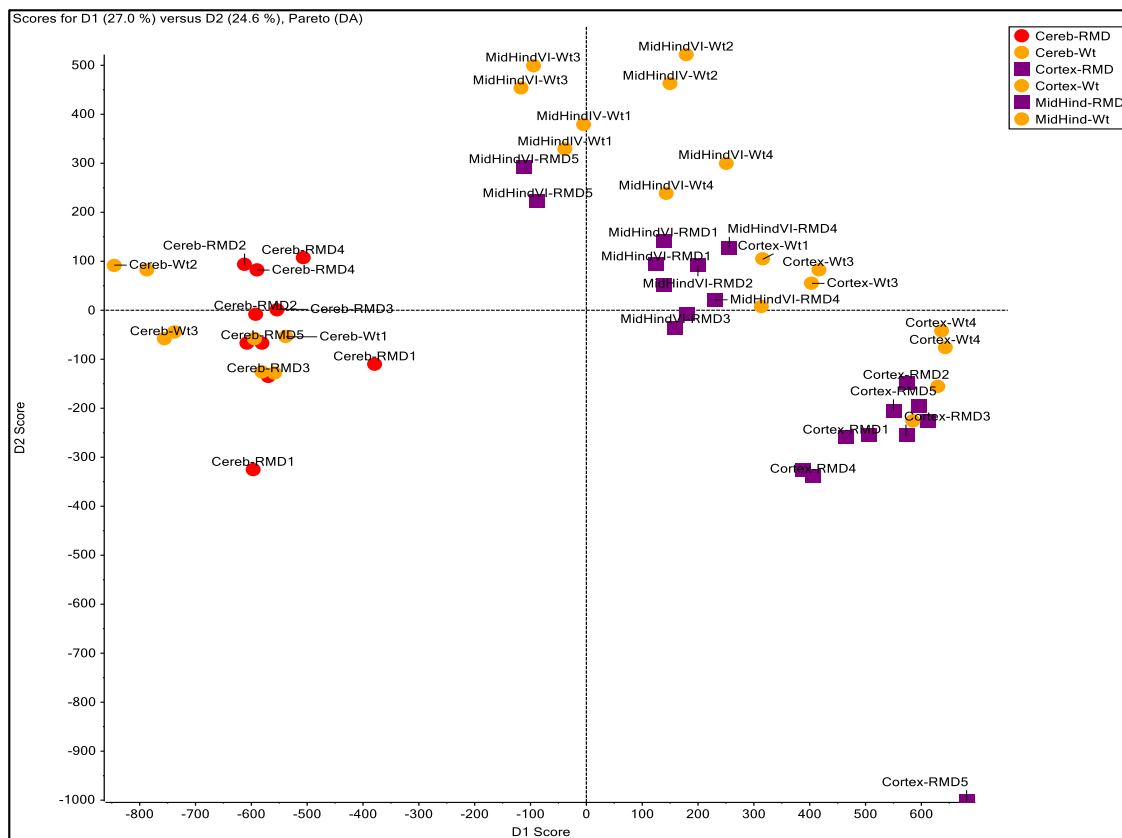


FIG 12. PCA of TAGs in brain. Principal component analysis with Pareto scaling on MS/MS^{ALL} Triacylglycerol (TAGs) in the brain region, showing significant differences across genotype.

A PCA analysis of the TAG molecules in the cortex, cerebellum and mid-hind brain region shows a significantly different clustering in *rmd* and WT cortex and mid-hind brain region. The cerebellum too shows a slightly different clustering in the PCA (Fig 12). Table (1.1-1.3) represents the ten most significantly altered TAG molecules in the above-mentioned brain regions. It can be seen that there alterations in long chain, unsaturated MDAG (54:9/54:10)

molecules which is balanced by an increase in the number of medium-chain MDAG (46:2/48:1) molecules. The same can be found true for TAG (56:7 and 46:7) and DAG (38:5 and 36:1) molecules.

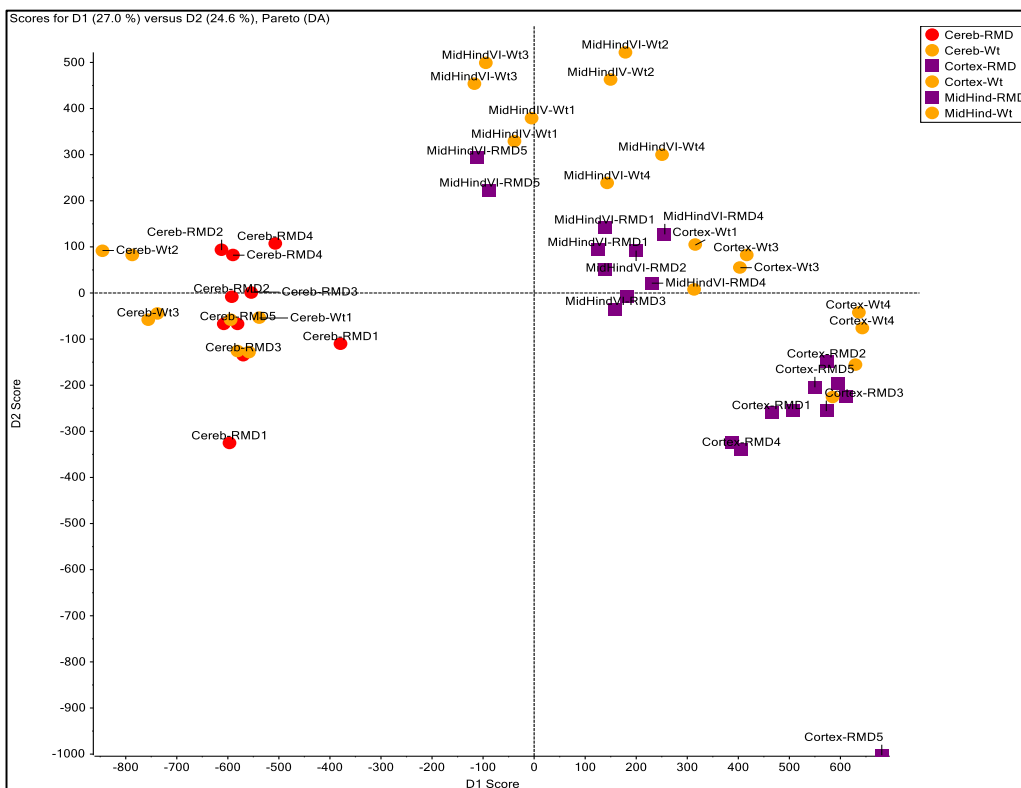


FIG 13. PCA of SMs in brain. Principal component analysis with Pareto scaling on MS/MS^{ALL} Sphingomyelins (SMs) in the brain region, showing significant differences across genotype.

SMs in the cerebellum, cortex and mid-hind brain region of *rdm* and WT mice show significantly separate clustering as observed for DAG molecules (Fig 13). Upon sorting the delta values of the different species identified using MS/MS^{ALL}, from highest to lowest, it can be seen that ten most significantly differing SM molecules differ in their number of side chain/ chain branches (Table 1.4 -1.6).

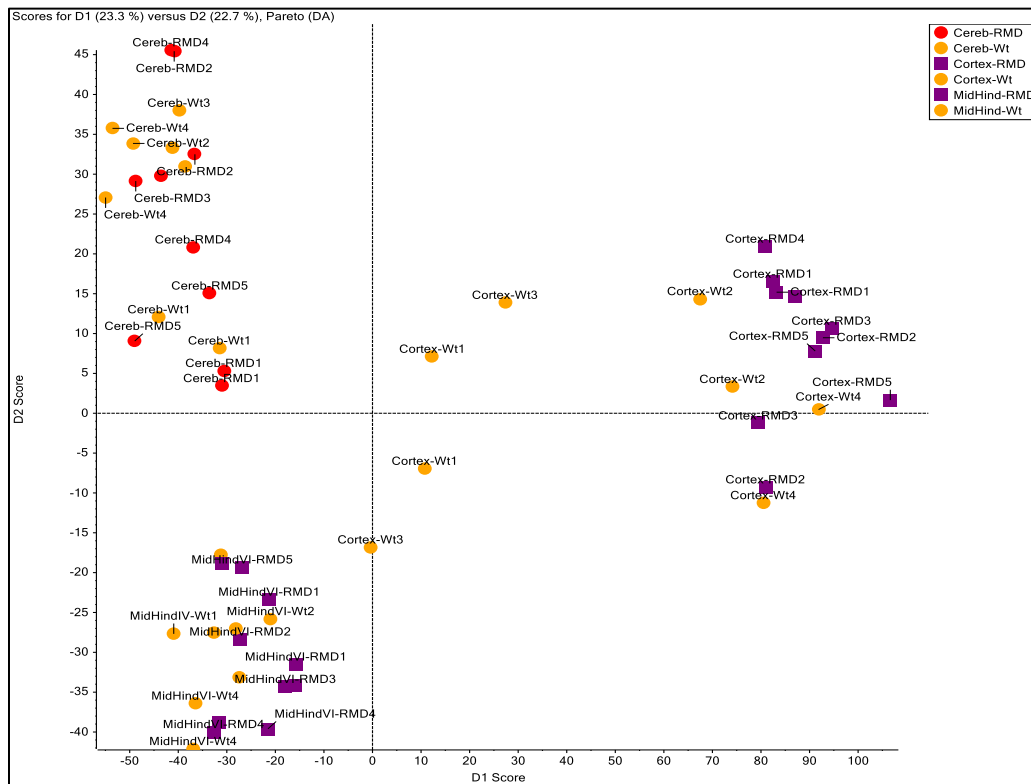


FIG 14. PCA of DAGs in brain. Principal component analysis with Pareto scaling on MS/MS^{ALL} diacylglycerol (DAGs) and monoalk(en)yl diacylglycerol (MADAGs) in the brain region, showing significant differences across genotype.

DAGs analyzed in the cortex of the brain show a clear separation in the PCA for *rmd* and WT mice (Fig 14). The cortex showed higher number of long and medium chain molecules with fewer branches whereas the mid-hind brain region showed an increased number of molecules with small to medium chain length and higher number of chain branches (Table 2.1-2.3).

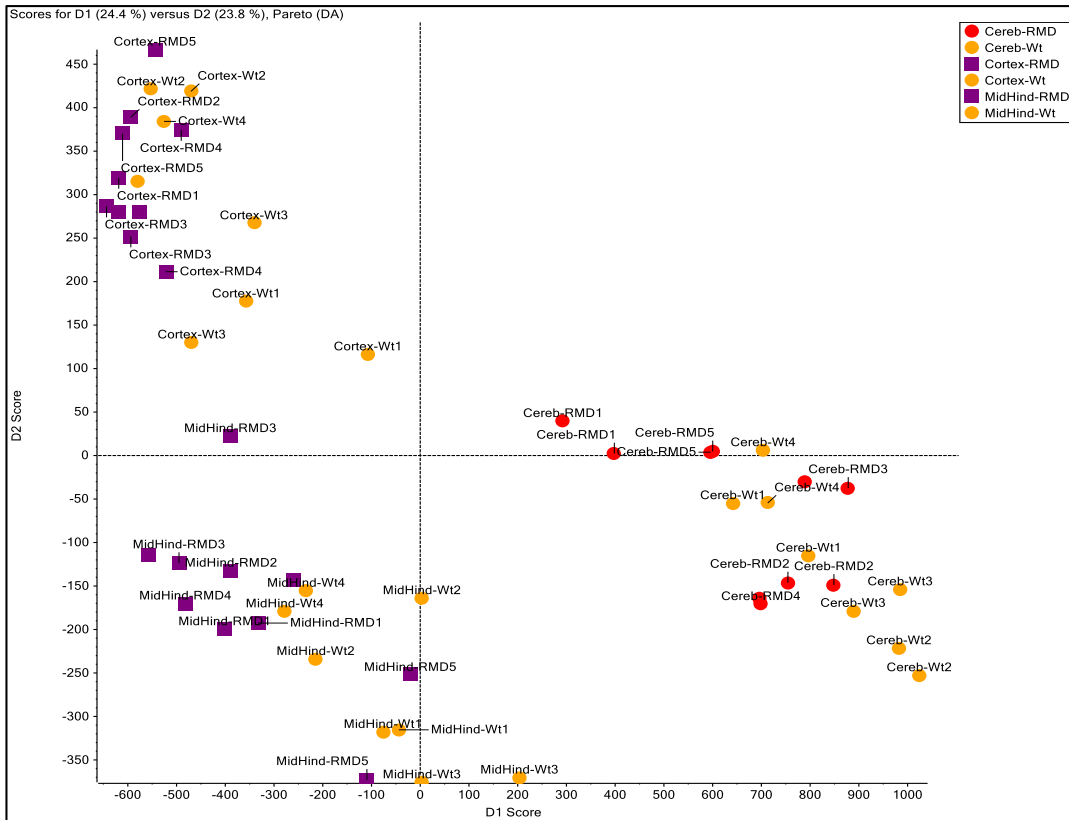


FIG 15. PCA of glycerophospholipids in the brain. Principal component analysis with Pareto scaling on MS/MS^{ALL} glycerophospholipids in the brain region, showing significant differences across genotype.

A PCA of GPLs in the brain region of *rmc* and WT mice showed clear separation in all three analyzed regions with maximum separation in the mid-hind brain region (Fig 15). Major differences were noted in the PE and phosphatidylserine (PS) molecules, with most differences within these molecules lying in the fatty acid chains (Table 2.4-2.6).

Together with previous literature, our data suggests there is a biochemical basis for anticipating cognitive impairments in the *rmc* mice, similar to the spectrum of cognitive impairments demonstrated by MDCMC patients.

1	Top 10 most significantly different TAG species in cerebellum	p value
	TAG 54:6+NH4 (-FA 22:6 (NH4))	0.99924
	MADAG 48:7+NH4 (-FA 19:3 (NH4))	0.98857
	MADAG 48:0+NH4 (-FA 15:0 (NH4))	0.97427
	MADAG 44:5+NH4 (-FA 20:4 (NH4))	0.9724
	DAG 36:4+NH4 (-FA 16:0 (NH4))	0.96115
	MGDG 38:12+NH4 (-MGDG (NH4))	0.94583
	DAG 34:1+NH4 (-FA 16:1 (NH4))	0.94491
	MADAG 54:8+NH4 (-FA 18:1 (NH4))	0.94436
	MADAG 48:0+NH4 (-FA 15:0 (NH4))	0.94347
	MADAG 52:10+NH4 (-FA 14:1 (NH4))	0.93988

2	Top 10 most significantly different TAG species in cortex	p value
	DAG 34:1+NH4 (-FA 16:1 (NH4))	0.98907
	MADAG 52:10+NH4 (-FA 14:0 (NH4))	0.98092
	MADAG 48:7+NH4 (-FA 16:0 (NH4))	0.97418
	TAG 48:8+NH4 (-FA 14:0 (NH4))	0.96965
	TAG 46:3+NH4 (-FA 17:2 (NH4))	0.95001
	TAG 54:5+NH4 (-FA 18:3 (NH4))	0.94092
	TAG 54:6+NH4 (-FA 16:0 (NH4))	0.91744
	MADAG 36:1+NH4 (-FA 16:1 (NH4))	0.91506
	MADAG 48:8+NH4 (-FA 12:0 (NH4))	0.91495
	MADAG 52:11+NH4 (-FA 14:0 (NH4))	0.90907

3	Top 10 most significantly different TAG species in Mid-Hind brain	p-value
	MADAG 50:5+NH4 (-FA 12:3 (NH4))	5.27E-08
	MGDG 38:3+NH4 (-MGDG (NH4))	2.01E-06
	MADAG 50:2+NH4 (-FA 20:1 (NH4))	2.86E-06
	MADAG 52:10+NH4 (-FA 12:1 (NH4))	4.75E-06
	MADAG 54:11+NH4 (-FA 20:4 (NH4))	2.08E-05
	MADAG 52:8+NH4 (-FA 16:1 (NH4))	2.62E-05
	MADAG 46:2+NH4 (-FA 19:2 (NH4))	2.77E-05
	TAG 54:4+NH4 (-FA 18:2 (NH4))	2.80E-05
	TAG 54:4+NH4 (-FA 18:1 (NH4))	4.72E-05
	TAG 54:6+NH4 (-FA 14:0 (NH4))	6.35E-05

4	Top 10 most significantly different SM species in cerebellum	p-value
	HexCer 40:2;4 (LCB 18:1;2-2H2O,LCB 18:0;3-3H2O)	9.47E-06
	HexCer 40:2;4 (LCB 18:1;2-H2O,LCB 18:0;3-2H2O)	5.80E-05
	SM 44:1;3 (SM)	0.0001
	SM 44:4;2 (SM)	0.00011
	SM 44:0;4 (SM)	0.00019
	SM 34:2;3 (SM)	0.00022
	SM 38:2;3 (SM)	0.00029
	SM 44:2;2 (LCB 18:1;2-2H2O,LCB 18:0;3-3H2O)	0.00033
	SM 42:3;2 (SM)	0.00034

5	Top 10 most significantly different SM species in cortex	p-value
	HexCer 42:2;3 (LCB 18:2;2-2H2O,LCB 18:1;3-3H2O)	3.16E-06
	SM 34:0;2 (SM)	8.54E-06
	SM 38:3;2 (SM)	1.50E-05
	HexCer 26:1;3 (LCB 18:0;2-2H2O)	2.25E-05
	HexCer 40:3;3 (LCB 18:2;2-2H2O,LCB 18:1;3-3H2O)	2.96E-05
	SM 38:3;2 (LCB 18:1;2-2H2O,LCB 18:0;3-3H2O)	3.80E-05
	HexCer 40:3;4 (LCB 18:2;2-2H2O,LCB 18:1;3-3H2O)	5.40E-05
	SM 38:4;3 (SM)	9.17E-05
	HexCer 40:2;4 (LCB 18:1;2-H2O,LCB 18:0;3-2H2O)	0.00013
	Cer 34:4;4 (LCB 18:1;2-2H2O,LCB 18:0;3-3H2O)	0.00013

6	Top 10 most significant different SM species in Mid-Hind brain region	p-value
	SM 41:4;2 (LCB 18:1;2-2H2O,LCB 18:0;3-3H2O)	5.27E-08
	SM 41:4;2 (LCB 18:2;2-2H2O,LCB 18:1;3-3H2O)	2.01E-06
	SM 40:4;3 (LCB 18:1;2-2H2O,LCB 18:0;3-3H2O)	2.86E-06
	SM 40:4;3 (LCB 18:1;2-H2O,LCB 18:0;3-2H2O)	4.75E-06
	SM 42:4;2 (LCB 18:1;2-2H2O,LCB 18:0;3-3H2O)	2.08E-05
	SM 40:1;3 (SM)	2.62E-05
	SM 38:2;2 (SM)	2.77E-05
	SM 42:4;3 (LCB 18:1;2-H2O,LCB 18:0;3-2H2O)	2.80E-05
	SM 42:4;3 (LCB 18:1;2-2H2O,LCB 18:0;3-3H2O)	4.72E-05
	HexCer 40:2;4 (LCB 18:1;2-H2O,LCB 18:0;3-2H2O)	6.35E-05

Table 1: Top10 significantly altered TAG (1-3) and SM (4-6) lipid species in the cerebellum, cortex and Mid-Hind brain region of *rmd* mice.

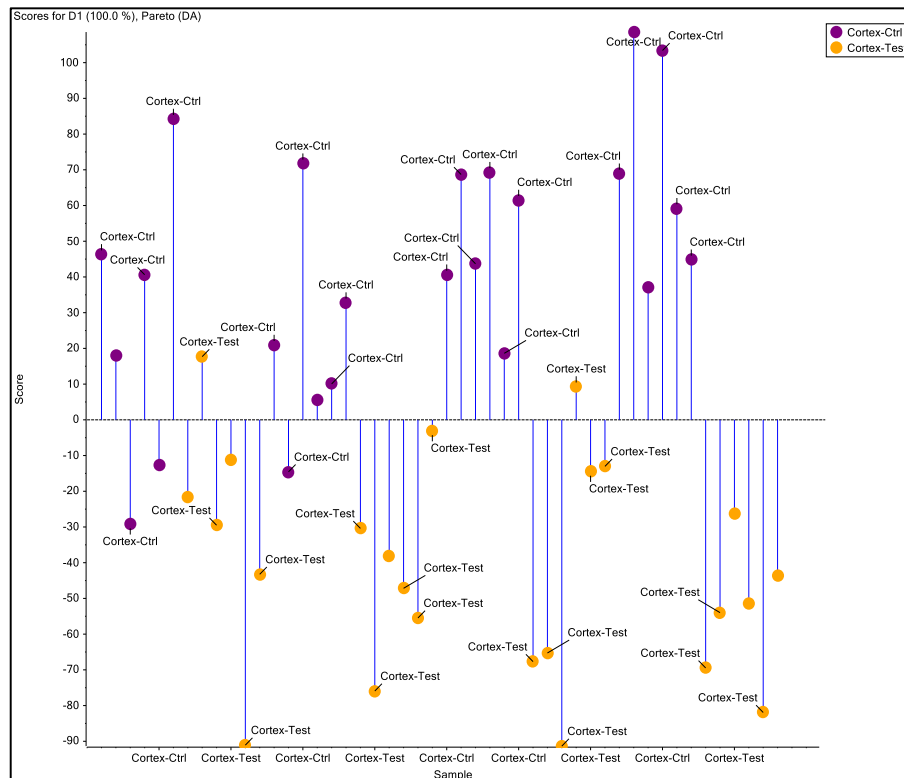
1	Top 10 most significantly different	
	MDAG species in cerebellum	p-value
	MADAG 46:3+NH4 (-FA 24:0 (NH4))	0.00033
	MADAG 46:4+NH4 (-FA 20:4 (NH4))	0.0205
	MADAG 44:4+NH4 (-FA 12:3 (NH4))	0.02207
	MADAG 44:4+NH4 (-FA 20:4 (NH4))	0.02326
	DGDG 24:1+NH4 (-FA 12:1 (NH4))	0.03178
	MGDG 36:3+NH4 (-MGDG (NH4))	0.04507
	MADAG 42:0+NH4 (-FA 17:0 (NH4))	0.04554
	MGDG 36:5+NH4 (-FA 16:3 (NH4))	0.04852
	MADAG 46:0+NH4 (-FA 13:0 (NH4))	0.05581
MADAG 38:2+NH4 (-FA 16:0 (NH4))	0.06819	
2	Top 10 most significantly different	
	MDAG species in cortex	p-value
	MADAG 46:5+NH4 (-FA 17:2 (NH4))	0.02421
	MGDG 36:4+NH4 (-FA 19:3 (NH4))	0.03798
	MGDG 36:4+NH4 (-FA 16:0 (NH4))	0.04239
	MGDG 36:4+NH4 (-MGDG (NH4))	0.04267
	MADAG 46:5+NH4 (-FA 18:3 (NH4))	0.04425
	MGDG 34:2+NH4 (-FA 17:1 (NH4))	0.05998
	MADAG 46:2+NH4 (-FA 20:0 (NH4))	0.07857
	MADAG 46:2+NH4 (-FA 19:1 (NH4))	0.07962
	MADAG 38:1+NH4 (-FA 18:1 (NH4))	0.0814
MADAG 48:7+NH4 (-FA 19:1 (NH4))	0.08166	
3	Top 10 most significantly different	
	MDAG species in Mid-Hind brain	p-value
	MGDG 36:3+NH4 (-MGDG (NH4))	1.89E-06
	MGDG 36:4+NH4 (-MGDG (NH4))	5.88E-06
	MGDG 36:6+NH4 (-MGDG (NH4))	0.00161
	MGDG 36:6+NH4 (-FA 14:0 (NH4))	0.00214
	MGDG 36:10+NH4 (-MGDG (NH4))	0.00236
	MGDG 34:2+NH4 (-MGDG (NH4))	0.00244
	MGDG 36:8+NH4 (-MGDG (NH4))	0.00284
	MGDG 32:2+NH4 (-MGDG (NH4))	0.00386
	DGDG 22:7+NH4 (-DGDG (NH4))	0.0039
MGDG 34:4+NH4 (-FA 14:2 (NH4))	0.00687	
4	Top 10 most significantly different	
	GPL species in cerebellum	p-value
	PE 35:2 (FA 17:1)	1.39E-07
	PE 40:4 (FA 22:4)	1.40E-07
	PE 40:4 (FA 18:0)	3.02E-07
	CL 72:3 (FA 18:1)	7.34E-07
	CL 78:7 (FA 22:4)	3.24E-06
	PE 40:3 (FA 22:3)	6.49E-06
	PS 44:8 (FA 22:4)	1.97E-05
	PS 42:4 (FA 22:0)	2.16E-05
	PE 44:8 (FA 22:4)	3.11E-05
PE 38:4 (FA 16:0)	3.20E-05	
5	Top 10 most significantly different	
	GPL species in cortex	p-value
	PS 42:4 (FA 20:3)	6.73E-08
	PE 36:2 (PE)	3.08E-06
	PC 32:2;1+HCOO (LPC pe)	7.83E-06
	PC 37:0+HCOO (FA 19:0)	9.02E-06
	PS 42:4 (FA 22:1)	1.36E-05
	PS 42:4 (FA 20:4)	2.67E-05
	PE 38:4 (FA 16:1)	3.05E-05
	PC 32:0+HCOO (FA 14:0)	4.92E-05
	CL 88:5 (FA 16:1)	6.80E-05
PS 42:4 (-PS)	6.80E-05	
6	Top 10 most significantly different	
	GPL species in Mid-Hind brain	p-value
	PC 38:6;1+HCOO (LPC pe)	2.44E-07
	PS 42:4 (FA 20:4)	1.52E-06
	CL 78:5 (FA 21:1)	2.08E-06
	PE 36:2 (FA 19:1)	6.10E-06
	OAHFA_18:0/34:1 (18:0 FA)	9.06E-06
	PS 42:5 (-PS)	9.24E-06
	PS 43:3 (-PS)	1.70E-05
	PE 34:1 (FA 18:0)	1.70E-05
	PC 38:6;1+HCOO (LPC pe)	1.91E-05
PS 42:4 (FA 22:0)	3.58E-05	

Table 2: Top10 significantly altered DAG, MDAG (1-3) and GPL (4-6) lipid species in the cerebellum, cortex and Mid-Hind brain region of *rmd* mice.

Tg-*rmd* mice as test models for cognitive impairments in *rmd* mutant mice: As described in chapter 2, the Tg-*rmd* mice are engineered to express a functional copy of the *Chkb* gene under a muscle specific promoter-Titin. These Tg-*rmd* mice, as shown in chapter 2, have muscle strength similar to those of the WT mice. Hence, the Tg-*rmd* mice can be used to test for cognitive impairments in the CHKB-deficient mice.

Tg-*rmd* mice show significantly different lipid profile when compared to controls: Tissue from the cortex and Mid + Hind brain region of *rmd* mice were compared with those of *rmd*^{+/-} control mice in order to test for any changes in the lipid profile. Since lipidomic analysis of *rmd* mice showed maximum differences in the cortex and mid-hind brain region, we selected these two brain regions for a detailed lipid profiling using the MS/MS^{ALL} technique. Lipid profiling with MS/MS^{ALL} mass spectra suggests significant differences in the major lipid molecules like TAGs, PE, cardiolipin (CL), phosphatidic acid (PA), SM and MDAG in both positive and negative mode. Principal component analysis with Pareto scaling shows a distinct separation of lipid profiles in the test (Tg-*rmd*) and control (*rmd*^{+/-}) mice (Fig 16 A-B and 17 A-B). Table number 3 shows the 10 most significantly altered lipid molecule species with differences in molecular chain length, branching and saturation.

A



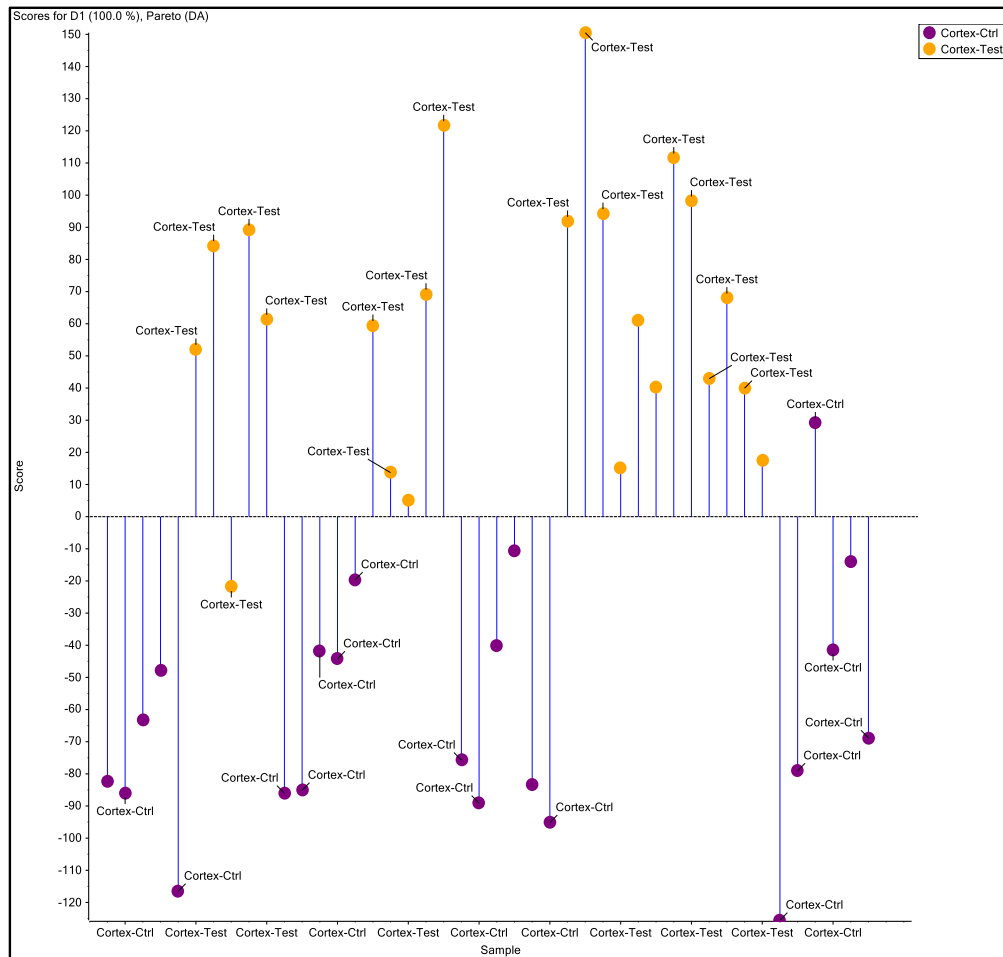
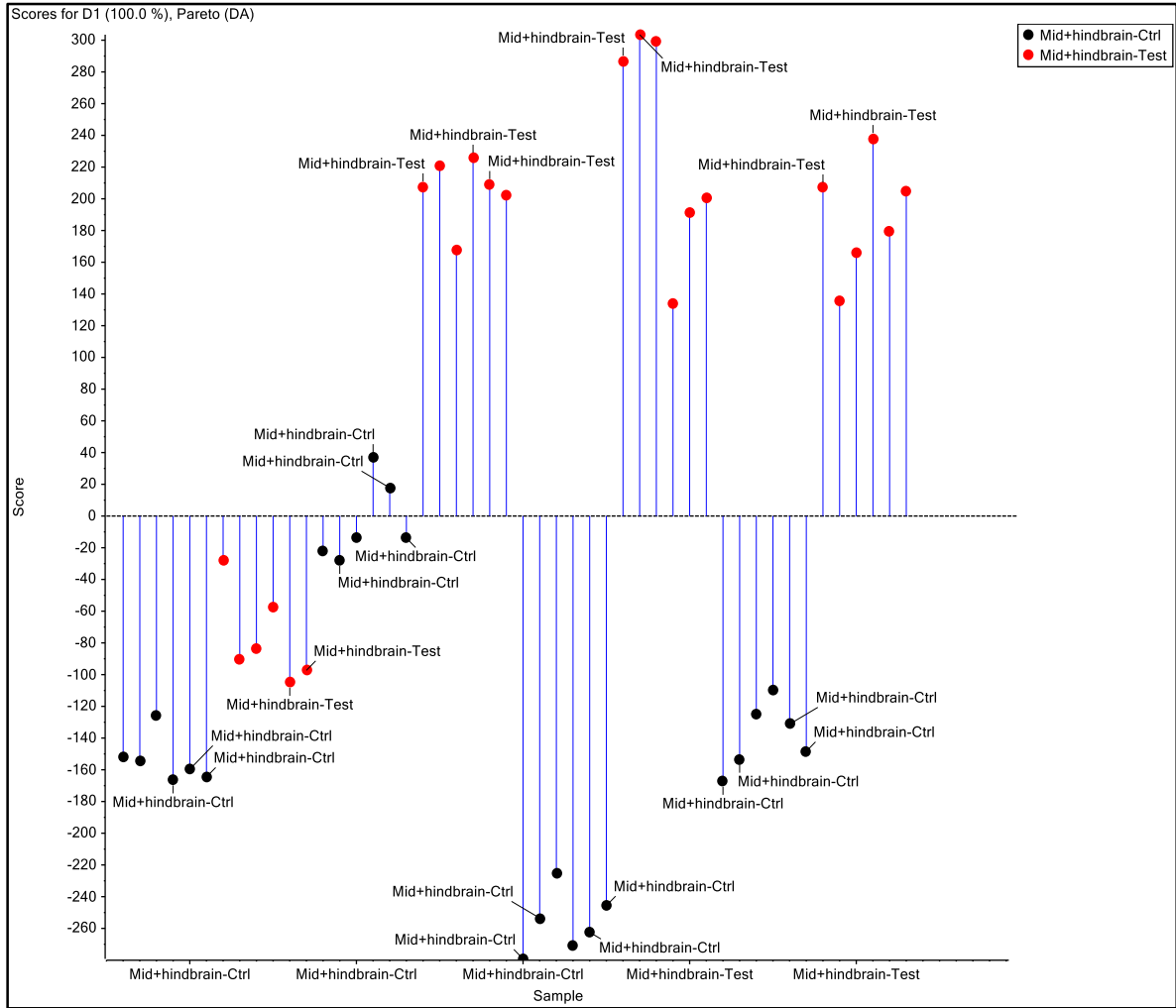
B

FIG 16. Lipid differences in the cerebral cortex across genotypes. Principal component analysis with Pareto scaling in positive (A) and negative (B) ion mode showing significant differences across genotype of test (Tg-rmd) and control (*rmd*^{+/-}) mice in cortex region of brain.

A



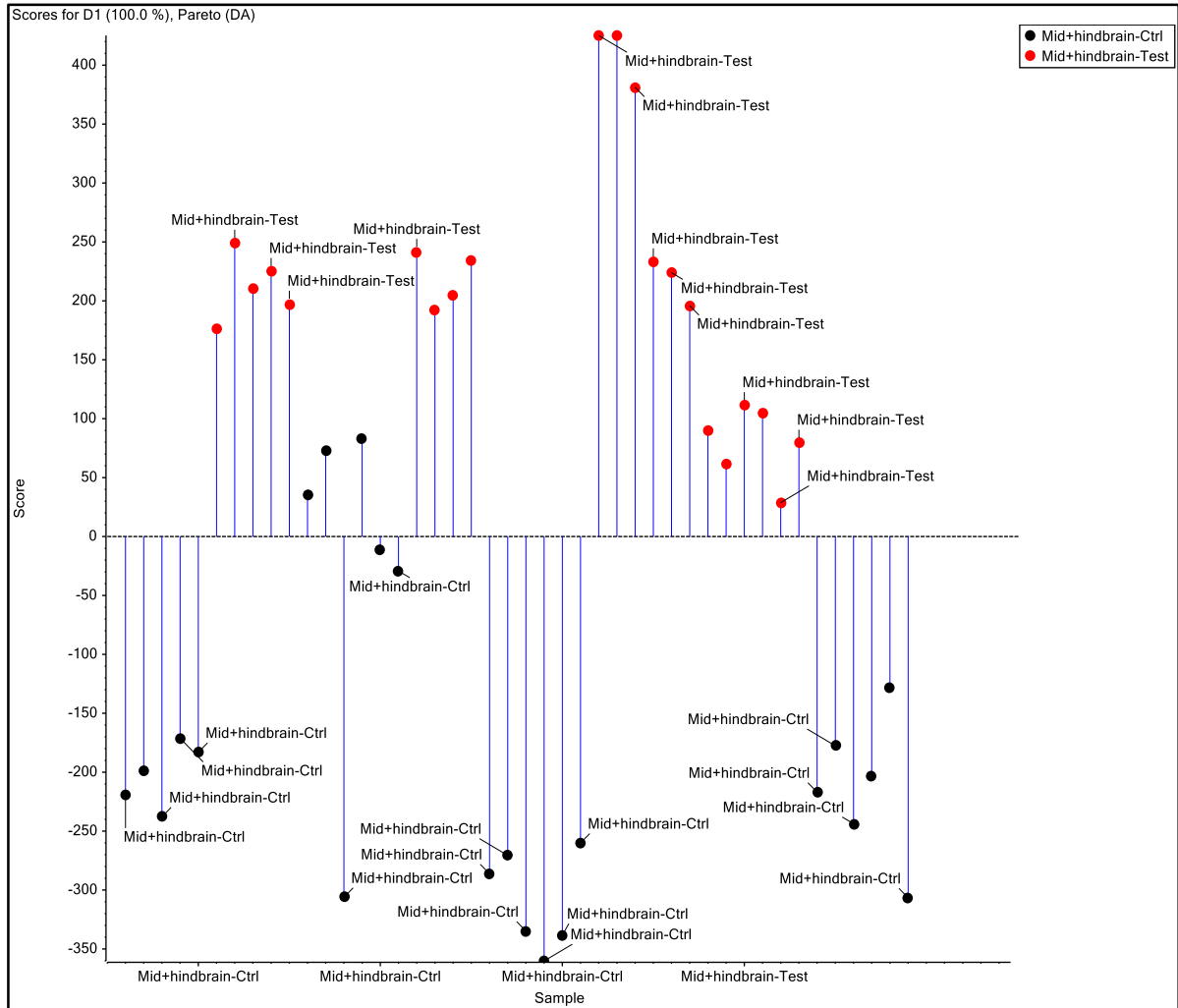
B

FIG 17. Lipid differences in the Mid and Hind brain region across genotypes. Principal component analysis with Pareto scaling in positive (A) and negative (B) ion mode showing significant differences across genotype of test (Tg-rmd) and control ($rmd^{+/-}$) mice in Mid+Hind brain region.

1

Top 10 most significantly different lipid species identified in positive ion mode in cortex	p-value
MADAG 44:5+NH4 (-FA 18:1 (NH4))	0.00054
TAG 54:5+NH4 (-FA 20:4 (NH4))	0.00075
MADAG 46:2+NH4 (-FA 20:0 (NH4))	0.00883
SM 42:4;2 (SM)	0.00884
TAG 56:7+NH4 (-FA 16:0 (NH4))	0.01264
TAG 52:2+NH4 (-FA 16:0 (NH4))	0.01733
HexCer 41:3;2 (LCB 18:2;2-2H2O,LCB 18:1;3-3H2O)	0.01775
MADAG 46:4+NH4 (-FA 19:0 (NH4))	0.01845
GM1 28:1;2 (LCB 18:1;2-H2O,LCB 18:0;3-2H2O)	0.01924
TAG 54:4+NH4 (-FA 16:0 (NH4))	0.02124

2

Top 10 most significantly different lipid species identified in positive ion mode in Mid-Hind brain	p-value
Cer 36:1;2 (LCB 18:0;2-H2O)	3.25E-06
GM1 28:1;2 (LCB 18:1;2-H2O,LCB 18:0;3-2H2O)	3.61E-06
Cer 36:1;2 (LCB 18:1;2-2H2O,LCB 18:0;3-3H2O)	6.47E-06
SM 36:1;2 (SM)	6.58E-06
SM 38:0;4 (SM)	1.09E-05
TAG 54:4+NH4 (-FA 18:2 (NH4))	1.51E-05
Cer 36:1;2 (LCB 18:1;2-H2O,LCB 18:0;3-2H2O)	1.64E-05
GM1 48:1;4 (LCB 18:1;2-2H2O,LCB 18:0;3-3H2O)	1.84E-05
TAG 52:4+NH4 (-FA 18:2 (NH4))	2.37E-05
SM 36:1;4 (SM)	2.90E-05

3

Top 10 most significantly different lipid species identified in negative ion mode in cortex	p-value
LPIP 25:5 (PI,PS,CL,PIP,PIP2,PIP3)	0.00058
PS 44:8 (FA 22:2)	0.00125
CL 78:7 (FA 17:1)	0.00248
PE 34:1 (FA 20:1)	0.00285
PE 38:6;1 (PE)	0.00433
PC 36:5;1+HCOO (LPC pe)	0.00468
PS 44:8 (FA 22:6)	0.00506
PE 38:1;2 (PE)	0.00768
PE 34:1 (FA 18:0)	0.00849
PA 36:2 (PA,PG,PI,CL,PIP,PIP2)	0.00861

4

Top 10 most significantly different lipid species identified by negative ion mode in Mid-Hind brain	p-value
LPIP2 20:2 (PA,PG,PI,CL,PIP,PIP2,PIP3)	5.52E-11
PE 37:1 (FA 17:0)	9.34E-11
PS 42:0 (-PS)	3.58E-10
PS 40:2 (FA 18:0)	4.15E-10
PE 37:1 (FA 18:0)	4.47E-10
CL 84:5 (FA 20:1)	8.16E-10
CL 84:4 (FA 20:1)	1.95E-09
PE 37:1 (FA 20:0)	2.65E-08
PS 34:2 (FA 18:1)	4.45E-08
PE 37:1 (FA 19:1)	5.15E-08

Table 3: Top 10 significantly altered lipid species in the cortex and Mid-Hind brain region of test (*rm*d) and control (*rm*d^{+/-}) mice, demonstrating changes in branch length, side chains and saturation.

Absence of cognitive defects in Tg-*rm*d mice: Mass spectrometry MS/MS^{ALL} analysis shows significant differences in the lipid profiles of Tg-*rm*d when compared to the test (*rm*d^{+/-}) mice. To test the possible impact of these changes on cognitive performance, we ran the Tg-*rm*d mice on assays including spontaneous alternation, spontaneous alternation with delay and on paired associates learning to test them for working and short-term memory and learning. When placed in a maze with multiple arms, mice tend to alternate arm entry and not re-enter an arm. Hence, this Y-maze set-up can be used to assess working memory dependent primarily on the intact hippocampus (Sukoff Rizzo et al., 2018). Spontaneous alternation, as a test for working memory, in Tg-*rm*d mice showed no significant differences in percent alternation between the arms

(males, $p=0.59$ and females, $p=0.80$) (Fig 18 A-B) and no significant differences in the total arm entries (males, $p=0.21$ and females, $p=0.90$) (Fig 18 C-D).

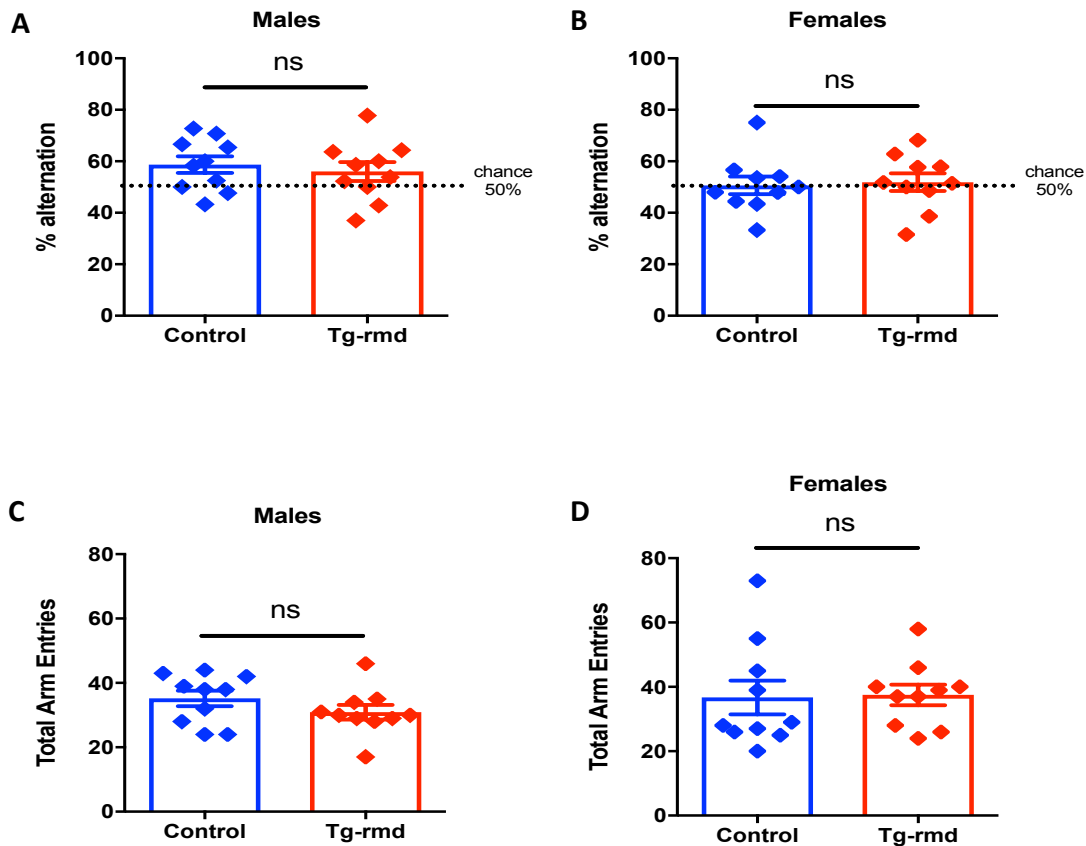
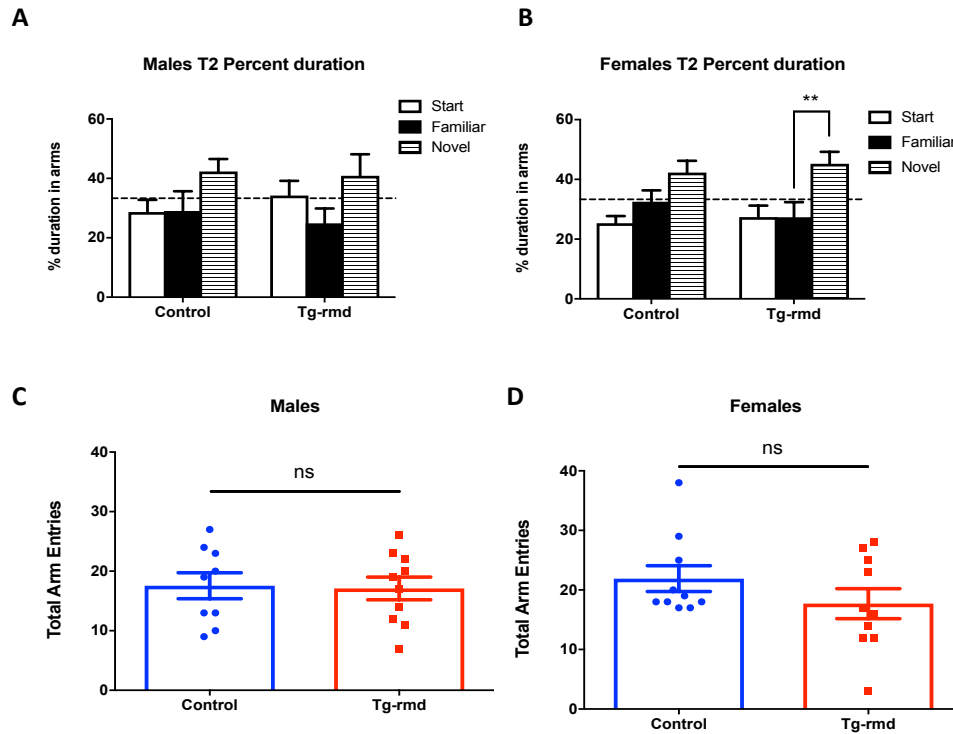


FIG 18. Testing working memory in *Tg-rmd* mice. Spontaneous alternation to test working memory in *Tg-rmd* mice shows no significant differences between *Tg-rmd* and control (*rmd*^{+/-}) mice. Percent alternation between arms in males ($p=0.59$) and females ($p=0.80$) is not significantly different between *Tg-rmd* and control mice (A-B). Total arm entries in males ($p=0.21$) and females (0.90) are not significantly different between *Tg-rmd* and control mice (C-D).

Short-term recognition memory in mice is assessed using novel spatial recognition using the Y-maze with visual cues at the end of each arm. In this test, mice tend to prefer exploring the “novel” arm after the 10 min break in the test as opposed to the two arms it was previously allowed to explore. In the spontaneous alternation with delay test, the percent duration of time spent in each arm after the 10 min break was not significantly different between the two groups in males ($p>0.99$) and females ($p=0.98$) (Fig 19 A-B). The *Tg-rmd* males ($p=0.88$) and females ($p=0.22$) did not show significant differences in the total arm entries when compared to the control mice (Fig 19 C-D).



19. Testing for short-term memory in *Tg-rmd* mice. *Tg-rmd* mice do not show significant differences when compared to the controls in the percent duration of time spent in each arm with the males showing $p>0.99$ and females showing $p=0.98$ (A-B). The total arm entries for males ($p=0.88$) and females ($p=0.22$) were also not significantly different between the two groups (C-D).

Both the Y-maze tests suggest that there is an absence of impairments in working memory and short-term memory in the *Tg-rmd* mice.

Paired associates learning test was used to test for learning impairments in *Tg-rmd* mice. In this test, the mice are required to learn to associate a given object with a particular location. The mice were trained until they attained an 85% correct criterion over three consecutive sessions. Post the pre-training period, the mice are required to complete all trials of the test with 80% accuracy over three consecutive days.

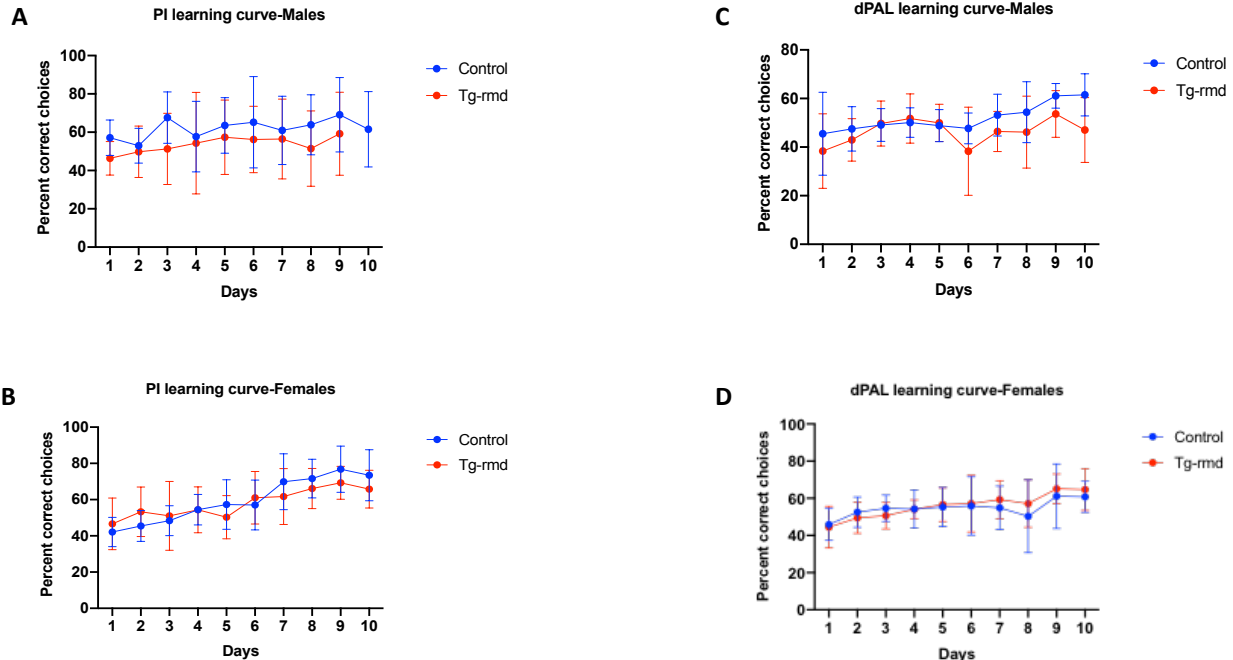


FIG 20. Learning curves of *Tg-rmd* mice in the PI and dPAL tasks. *Tg-rmd* males show a significant difference from the controls in the first 10 days of learning on the PI task with a p of 0.0010 (A) while the females have a learning curve similar to that of the controls with a p value of 0.72 (B). In the dPAL task the *Tg-rmd* males were slightly different (p=0.037) from the controls, whereas the females did not perform differently from the controls (p=0.53).

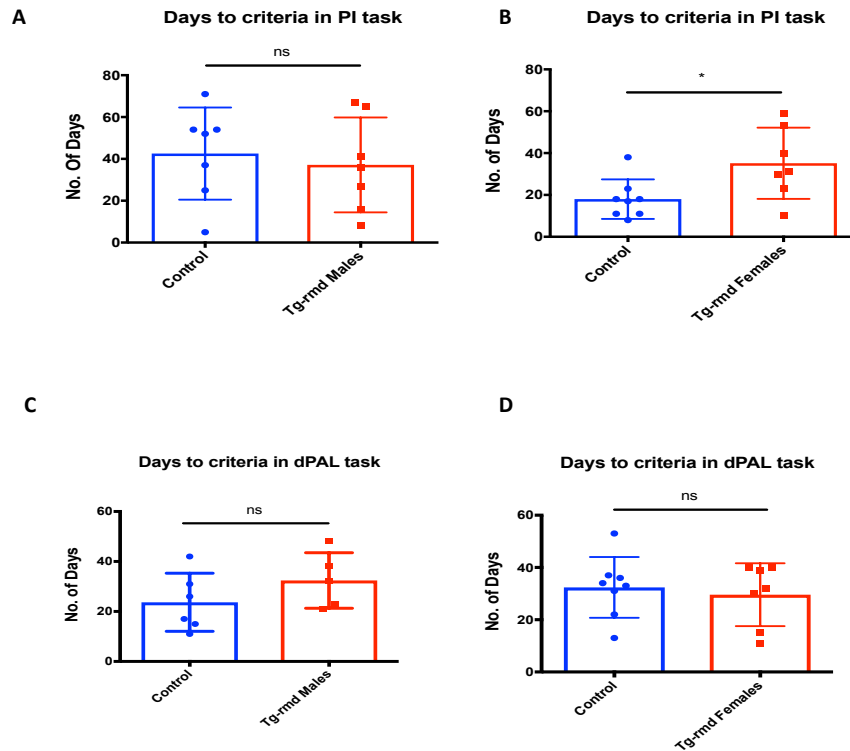


FIG 21. Testing for learning impairments in *Tg-rmd* mice. *Tg-rmd* males did not show any significant differences from controls in the PI task, $p=0.66$ and in the dPAL task, $p=0.24$. *Tg-rmd* females show slower response with a significant difference in the PI task, $p=0.029$ and no significant differences in the dPAL task, $p=0.65$.

Days to criteria for the punish incorrect (PI) task and the paired associates analysis (dPAL) were analyzed post the pre-training period, in order to test for cognitive impairments (Bartko, Vendrell, Saksida, & Bussey, 2011)(Bussey, Dias, Amin, Muir, & Aggleton, 2001). The Punish incorrect task was used as a pre-dPAL assessment, in which mice were trained to select a square that was lit. Failure to do so resulted in no reward and a period of 'light out'. An 85% correct selection in the punish incorrect task for three consecutive days resulted in progressing to the

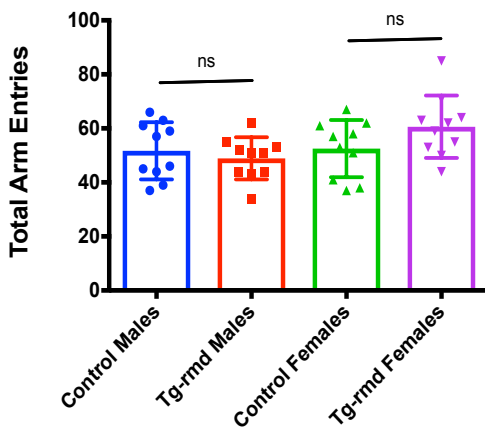
paired associates learning (dPAL) task where the mice tasked to choose a particular object at a particular location on the screen. A rate of 80% correct choices for three consecutive days resulting in completion of the task. It was observed that the *Tg-rmd* males were not significantly different from the controls in the PI ($p=0.66$) and dPAL ($p=0.24$) task (Fig 21 A-C). The *Tg-rmd* females on the other hand, completed the PI task in a slightly shorter span of time ($p=0.029$) (Fig 22 B) but did not perform any different in the dPAL task ($p=0.65$) (Fig 21 D). This was further confirmed by the learning curve demonstrated in the first 10 days of the PI and dPAL tasks. The males showed a difference in rate of learning in both the PI and dPAL task learning curves in the first 10 days but this did not affect the outcome of the two assays (Fig 20 A-D).

These behavioral tests suggest that the *Tg-rmd* mice do not show any signs of cognitive impairments.

Aging does not lead to memory deficits in *Tg-rmd* mice.

The initial testing for memory deficits were performed with mice aged 8-10 weeks. In order to test whether *Tg-rmd* mice show spatial awareness deficits or memory deficits with aging, we repeated the spontaneous alternation and spontaneous alternation with delay assays on them, post completion of the dPAL test at around 9 months of age.

A



B

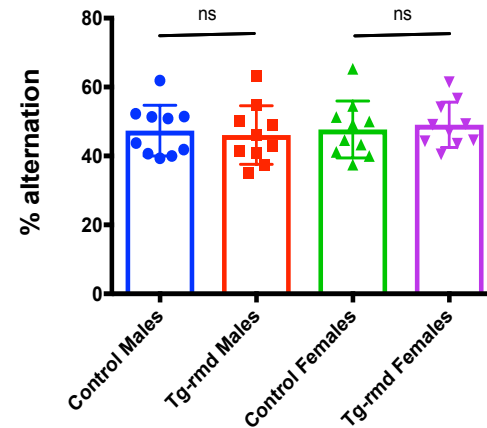


Fig 22. Testing working memory in aged *Tg-rmd* mice. Aged *Tg-rmd* males and females did not show any significant differences from controls in total arm entries ($p=0.51$ and $p=0.12$, respectively) and in the percent alternation between arms ($p=0.72$ and $p=0.69$, respectively).

Spontaneous alternation test results showed no significant differences in total arm entries between *Tg-rmd* males or females and their respective controls with males showing a $p=0.51$ and females that of 0.12 , respectively (Fig 22 A). In percent alternation males showed a P value of 0.72 and females that of 0.69 respectively, suggesting no significant differences from control group (Fig 22 B).

For spontaneous alternation with delay, the delay time for re-introduction into the Y-maze was reduced from 10 min to 5 min, to take into consideration delay dependent effects in aged mice.

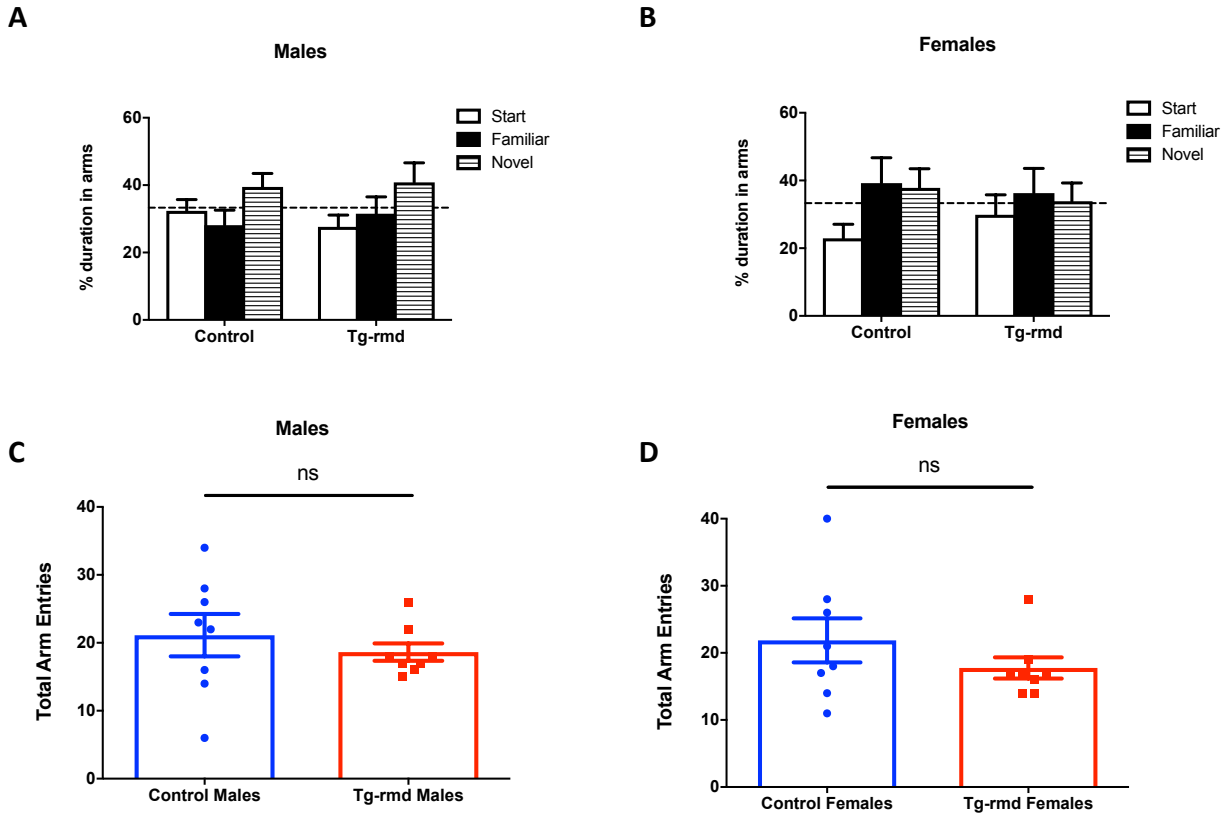


FIG 23. Testing short-term memory in aged *Tg-rmd* mice. Aged *Tg-rmd* males and females did not show any significant differences in the percent duration spent in the arms (males, $p=0.64$ and females, $p=0.62$) (A-B) and in the total arm entries (males, $p=0.47$ and females, $p=0.28$) (C-D).

Spontaneous alternation performed on aged *Tg-rmd* and control mice showed no significant differences in the percent duration spent in each arm of the Y-maze ($p=0.64$) (Fig 23 A) and in the total arm entries ($p=0.62$) (Fig 23 C). The *Tg-rmd* females too showed no significant differences when compared to the aged matched controls in the percent duration spent in each arm of the Y-maze ($p=0.47$) (Fig 23 B) and in the total arm entries ($p=0.28$) (Fig 23 D). In the spontaneous alternation with delay, the control females do not show preference for the novel arm, thus failing the assay and hence cannot be used to draw conclusions with certainty.

The males used in these assays suggest that even in >6 months aged *Tg-rmd* mice, there are no working or short-term memory deficits observed from these tests conducted. Together, the results indicate that from these particular behavioral tests, no spatial awareness, memory deficits or cognitive impairment could be modelled in the *Tg-rmd* mice.

Expression of *Chkb* transgene does not influence spatial awareness and memory in mice.

Addition of a transgene may result in impairments in cognition and memory which are apparent in the spontaneous alternation and delayed spontaneous alternations tests

(<https://med.stanford.edu>). In order to test this, the *Tg-WT* mice were tested for spatial awareness on the Y-maze through the spontaneous alternation and spontaneous alternation with delay tests.

For this test, *Tg-Wt* and *WT* mice (N=10 mice/sex/genotype) were acclimatized and tested for spontaneous alternation on the y-maze as previously described. The *Tg-WT* mice did not perform any differently than the *WT* controls with the total number of arm entries and percent spontaneous alternation between the two groups being similar (Fig 24 A-D).

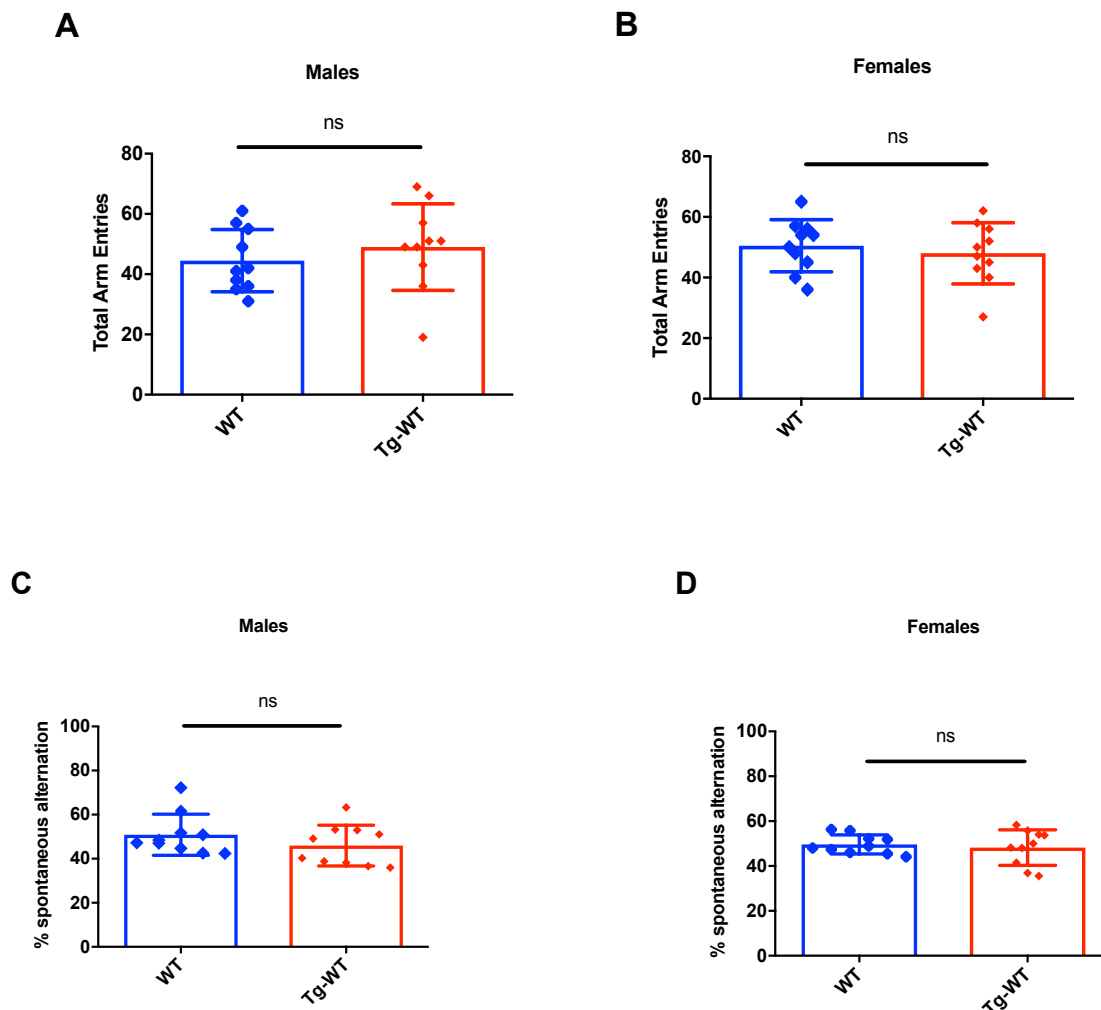


Fig 24. Testing of spatial awareness in *Tg-WT* mice. The *Tg-WT* mice when tested on the y-maze for spontaneous alternation were not significantly different from the control *WT* mice in the total number of arm entries with *p* values of 0.43 and 0.56 in males (A) and females (B) respectively. The *Tg-WT* mice were not significantly different from the controls in the percent spontaneous alternation with *p* values of 0.25 and 0.63 in males (C) and females (D) respectively. *N*=10 mice/sex/genotype aged 8-10 weeks. Error bars represent SD.

Young *rmd* mice do not show impairments in spatial awareness and memory

When tested for short-term memory on the y-maze using the spontaneous alternation with delay assay, the male and female controls did not show preference for the novel arm and hence did not pass the test. In this test, too an N of 10 mice/sex/genotype aged 8-10 weeks were used and were acclimatized as per the testing protocol previously described (Fig 25 A-D).

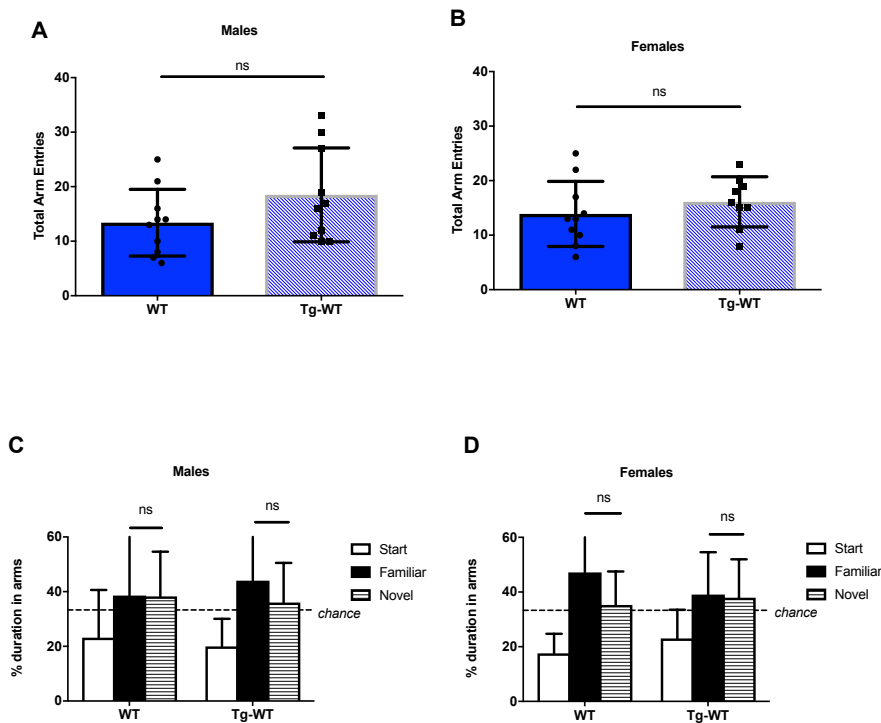


Fig 25. Testing for short-term memory in *Tg-WT* mice. The *Tg-WT* mice when tested for short-term memory on the y-maze test did not show any difference from the controls. The *Tg-WT* mice had similar arm entries, when compared to WT controls with $p=0.14$ in males (A) and $p=0.38$ in females (B). *Tg-WT* mice did not show any preference to the novel arm with $p > 1$ in both males (C) and females (D). $N=10$ mice/sex/genotype aged 8-10 weeks. Error bars represent

The spontaneous alternation assay and the percent spontaneous alternation in the spontaneous alternation with delay test suggest the transgene has no detrimental effect on the spatial awareness and short-term memory of the mice.

Since Tg-*rmd* and Tg-WT mice do not show any differences in their spatial awareness and memory when compared to control mice, we decided to test *rmd* mutant mice directly for differences in these abilities. However, since the *rmd* mice become physically impaired due to their hindlimb dragging at 8 weeks of age, we tested for the presence of these impairments at 4-5 weeks of age.

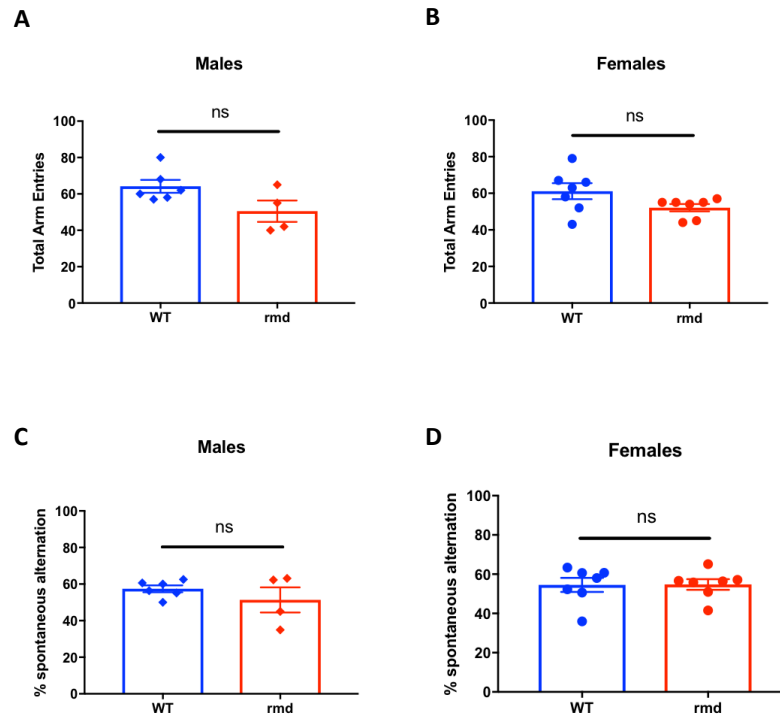


FIG 26. Testing working memory in young *rmd* mice. *rmd* mutant mice are not significantly different from their WT controls in total arm entries (males, $p=0.07$) and (females, $p=0.09$) (A-B) and in the percent of spontaneous alternation (males, $p=0.33$ and females, $p=0.96$) (C-D).

Spontaneous alternation showed *rmd* are not significantly different from their age-matched controls (WT mice). The males and females showed a P value of 0.07 and 0.09 respectively in the total number of arm entries (Fig 26 A-B). The percent alternation between arms of the Y-maze were also not significantly different in the *rmd* males and females with a P value of 0.33 and 0.96 respectively (Fig 26 C-D).

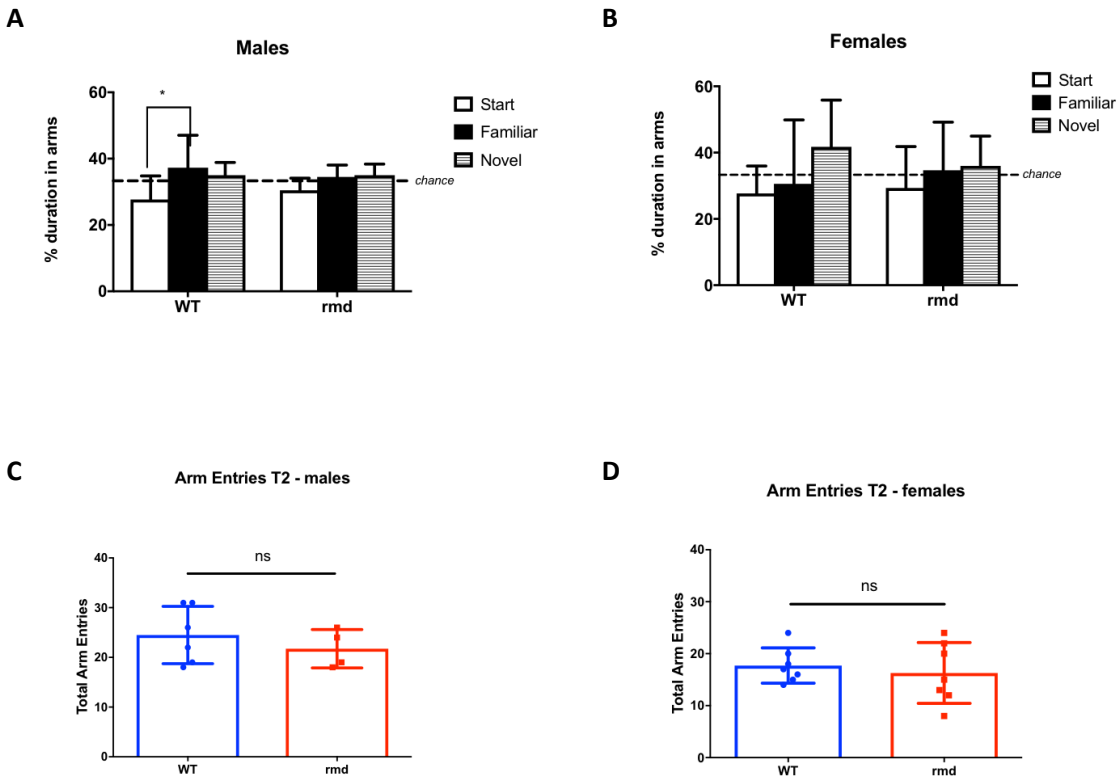


FIG 27. Testing short-term memory in young *rmd* mice. *rmd* mice when tested for spontaneous alternation with delay did not show preference for the novel arm greater than chance percent in both males and females with no significant differences between the *rmd* and control groups (males, $p=0.62$ and females, $p=0.61$) (A-B). *rmd* mutant mice did not show significant differences in the total number of arm entries when compared to controls (males, $p=0.43$ and females, $p=0.59$) (C-D).

The *rmd* mutant mice were tested for deficits in memory using the spontaneous alternation with delay test on the Y-maze. The *rmd* mice did show a preference to spend greater time in the novel arm. The control mice, on the other hand, showed a greater preference for the familiar arm. Both the *rmd* and the control mice did not any significant differences to each other (males, $p=0.62$ and females, $p=0.61$) (Fig 27 A-B). The *rmd* mice did not show any significant differences in the total arm entries when compared to their aged-matched controls (males, $p=0.43$ and females, $p=0.59$) (Fig 27 C-D).

This suggests that the *rmd* mice do not model cognitive impairments at a very young age (immediately post-wean).

Discussion:

Changes in brain lipid composition has been indicated in cognitive impairments, anxiety and depression (Müller et al., 2015)(Vitali, Wellington, & Calabresi, 2014). Previous literature shows that there lies a direct correlation between the lipid composition of brain tissue and cognitive impairments, with persons suffered from brain trauma and diseases like Alzheimer's, mild cognitive impairments and dementia showing a greater percent of short chain, unsaturated fatty acids in their brain tissue when compared to brain tissue from unaffected population (R. B. Chan et al., 2012)(Wood, 2012)(Cunnane et al., 2012). It has been shown that choline and hence PC are important molecules in normal brain development(G. B. ANSELL, 1971)(Zeisel SH, 1992)(Zweigner et al., 2004)(Sanders & Zeisel, 2007). Not much is known about the lipid profiles in the brain of C57BL/6J mice or in that of AD mouse models and additional insights in this filed are necessitated by the recent progress in Alzheimer's and mild cognitive impairment research.

We have shown that significant lipid profile differences exist in brain tissue from *rmd* and Tg-*rmd* mice when compared to unaffected mice, justifying the use of these mice in order to model the cognitive impairments seen in MDCMC patients in these mouse models. We have shown that since the *rmd* mice lack muscle strength required for performing certain basic behavioral tasks, the Tg-*rmd* mice were used as test subjects for behavioral tests including spontaneous alternation, spontaneous alternation with delay and dPAL, all of which require considerable physical activity. Besides this, tests like the dPAL can continue for more than 6 months by the time of which the *rmd* mice would be unable to perform at the same level as at 4-5 weeks of age, further justifying the use of Tg-*rmd* mice as test subjects. Behavioral testing for spatial awareness, memory and associated learning in the Tg-*rmd* mice did not show any significant differences from their controls. Tests for spatial awareness and short-term memory failed to show significant differences between >6 months aged Tg-*rmd* and aged-matched controls. A repeat of the spatial awareness and short-term memory tests on young *rmd* mice did not show cognitive impairments at 4-5 weeks of age. Together, it has been shown that across different genotypes and at different ages, the differences in brain lipid profiles could not be translated behaviorally using the specified methods of analysis and testing. The Cortex and in particular the hippocampus plays an important part in memory, speech and spatial awareness. The hippocampus and the lipids within has been shown to be affected with increasing age and in conditions like AD (Delion et al., 1997). The y-maze assay, mainly tests the hippocampal region of the brain and has been used to correlate changes in hippocampus with memory, spatial awareness and aging (Ira et al., 1999).

Our research has helped bridge the gap in knowledge pertaining to lipid profiles of brain in B6 mouse models. Additionally, we have also profiled the *rmd* mouse model that lacks *Chkb*

gene necessary for production of PC, an important lipid molecule required for normal brain function and development. Our data used the MS/MS^{ALL} technique to meticulously identify all the different lipid molecules at different chain lengths and saturation levels, contributing to the building repository of information pertaining to lipid profiles in mouse models of cognitive impairments. This can help correlate information from aging, drug use and diet and obesity studies in order to gain more perspective on treatment methods and effects on human population.

Cognitive impairments demonstrated by MDCMC patients fall in a broad spectrum ranging from low IQ, speech deficits, memory loss, inability to learn and lack of social cues resulting in failure to interact and integrate in a social environment (Gutiérrez Ríos et al., 2012)(Castro-Gago et al., 2014)(Oliveira et al., 2015)(Cabrera-Serrano et al., 2015)(S. Sparks & Harper, 2001). The assays I used tested only a few aspects within this spectrum. We have shown that the *rmd* and *Tg-rmd* mice do not demonstrate deficits in spatial awareness or memory and learning, however, this covers only a part of the cognitive spectrum observed in MDCMC patients and hence does not imply a lack of speech and social interaction difficulties.

It has been shown that background strains of mice influence their performance in cognitive tasks thus impacting their phenotype. C57BL/6J mice perform better in the Morris water maze task but have a greater predominance of approach towards a DBA/2J females whereas DBA mice perform worse than C57BL/6J on the Morris water maze but have a greater predominance of avoidance towards a DBA/2J female. Different strains like Friend Virus B NIH Jackson (FVB), DBX, 129, DBA SJL, each has a different effect over cognitive functions of the mouse (Hall & Roberson, 2012)(Brodkin, Hagemann, Nemetski, & Silver, 2004)(Lassalle, Halley, Dumas, Verret, & Francés, 2008). Our *rmd* and *Tg-rmd* mice have been bred on a C57BL/6J background and it may be possible that changing this background could result in

changes in the outcome of the behavioral assays performed above. These background strains also influence the effects of aging on the mice, thus indirectly influencing cognitive functions.

In summary we conclude that there are significant differences in lipid profiles in the brain of *rmd* and *Tg-rmd* mice compared to WT and *rmd*^{+/-} mice and that these differences do not translate to observable differences in the behavioral assays for learning and memory. This study is impactful since it is one of the first that compares dynamic and detailed lipid profiles amongst different ages and phenotypes of mice in a CHKB deficient environment, providing the first of its kind study for further characterization of MDCMC patients.

Materials and Methods:

Lipidomic analysis: Brain and liver from *Tg-rmd*, *rmd*, WT and *rmd*^{+/-} were harvested (N=4 mice/sex/genotype). The brain was separated into cortex, cerebellum and mid+hind brain region. The samples were homogenized and process as described by Liaw et al. Unbiased MS/MS^{ALL} lipidomic shotgun analysis was performed on these samples using the method described by Liaw et al.(Liaw et al., 2016).

Behavioral Assays for cognition: Spontaneous alternation, Novel spatial recognition and Paired Associates Learning (dPAL) were used to assess working memory, short-term memory and learning.

Spontaneous alternation: Spontaneous alternation tests the working memory of mice and depends on their intact hippocampus. For this test 5-10 mice/sex/genotype were used. The mice were placed in a three-armed Y-shaped maze with no visual cues inside the maze and a perimeter curtain to minimize extra maze cues (Sukoff Rizzo et al., 2018). An 8 min trial was run on each

mouse under a 50 lux environmental lighting conditions. Behavioral tracking software was used to track the movement of the mouse based on its center point, thus recording its entry into each arm. Total arm entries and time spent in each arm are calculated.

Novel spatial recognition/ Spontaneous alternation with delay: This test assesses short-term memory in mice. 10 mice/sex/genotype were used for this assay. The mice were tested in a three-armed Y-shaped maze with dimensions as specified by Rizzo et al. (Sukoff Rizzo et al., 2018). The three arms are designated as start arm, familiar arm and novel arm. The novel arm is closed off using a black polycarbonate wall and the mice are allowed to explore in the start and familiar arm for 10 minutes. After this the mice are removed and allowed a delay time of 10 minutes post which they are re-introduced in the maze with access to the novel arm, thus giving access to all three arms of the maze, and are allowed to explore for 5 minutes. Behavioral tracking software is used to track the movements of the mice with their center point as reference point and is used to calculate total arm entries, total time spent in each arm in the first 10 minutes and during the 5 minutes of re-introduction in the maze. For calculations of learning curve, first 10 days were calculated as during this period only one mouse finished the test, the data from this mouse was impugned from day 7 to day 10 in order to maintain consistency.

Paired associates learning (dPAL): The dPAL assay was used to assess learning in mice (N= 8 mice/sex/genotype). The mice were food restricted and their body weights reduced prior to the test and then maintained at about 80%-85% free feeding throughout the testing period (Bussey et al., 2001). The testing chamber consists of a black opaque plastic triangular space with the touchscreen placed at the base of the triangle. An opaque plastic screen with three windows is placed ahead of the touchscreen, facilitating three options that the animal can nose-poke and choose from. A pellet chamber is present at the apex of the triangle. This chamber is attached to

a vacuum pump that dispenses about 20 μ l of strawberry milk into the chamber as a reward. For selection, three novel stimuli (picture) were presented to the animal, one per window. The animal has to select the correct stimuli at the correct location (window) in order to receive the reward (Brigman et al., 2008). Correct choice would lead to a cue and dispensing of strawberry milk in the pellet chamber while an incorrect choice would lead. The mice were trained until they attained an 80% correct criterion over three consecutive sessions. Post the pre-training period, the mice are required to complete all trials of the test with 80% accuracy over three consecutive days. The tracking software is used to measure time taken to complete each trial, percent correct and many other values. For calculations of learning curve, first 10 days were calculated as during this period only one mouse finished the test, the data from this mouse was impugned from day 7 to day 10 in order to maintain consistency.

Statistical analysis: All the experiments were performed at the Jackson Laboratory, Bar Harbor. All mouse handling, testing, and analysis were performed blinded for mouse genotype. Where appropriate, statistical significance was calculated using Student's t-test or 2-way ANOVA with post-hoc Bonferroni corrections unless otherwise noted. Calculations were performed using Prism 7.0c software for Mac OS X and any significant differences ($p < 0.05$) between test and control strains are denoted by an asterisk symbol. For behavioral assays, each mouse is treated as a biological control and each test has a different number of statistical control experiments run on one mouse.

Protocols for open field, rotarod, spontaneous alternation, spontaneous alternation with delay were conducted as described in chapter 2.

CHAPTER 4

GENETIC AND THERAPEUTIC MECHANISMS TARGETED TOWARDS THE RESCUE OF *RMD* MUTANT PHENOTYPE

1. Mitofusin as a modifier gene for the rescue of *rmd* muscular dystrophy

In WT mice, many muscle cells or myofibers come together forming a bundle that forms an entire muscle. Each muscle fiber is bound by a plasma membrane called sarcolemma. The sarcolemma forms invaginations called Transverse tubules (T-tubules) that penetrate the muscle fiber and tightly associate with the sarcoplasmic reticulum (SR), forming the junctional SR (Al-Qusairi & Laporte, 2011). A T-tubule associated with a terminal cisternae on each side forms a structure called the triad (Fig 28 A-B). In a muscle fiber, the excitation-contraction (EC) coupling is mediated by Ca^{2+} ions that are stored and provided by the SR. These Ca^{2+} form the secondary messengers and play an important role in the contraction of muscle fibers. Due to its structure and close contact with the SR, the muscle triad plays a principle role in EC coupling and hence in muscle contraction (Al-Qusairi & Laporte, 2011). In a *rmd* mouse, the triad structure is destroyed due to the sheer size of the mitochondria (Fig 29). All the other proteins involved in EC coupling are shifted thus negatively impacting Ca^{2+} ion storage and exchange and thus abilities of the muscle to contract (Fig 30 A-B).

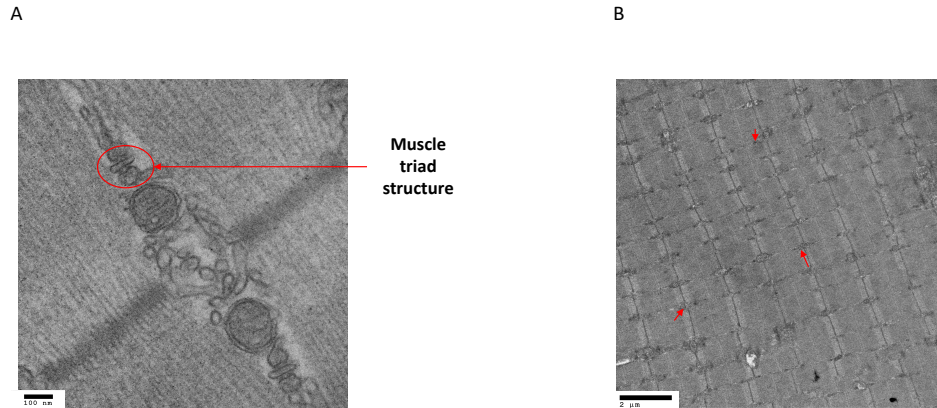


FIG 28. TEM images of muscle triad structure. (A) Shows the muscle triad structure which plays a principle role in EC coupling and hence in muscle contraction. (B) Represents a birds eye view of a general muscle structure with intact muscle triads at 10000X.

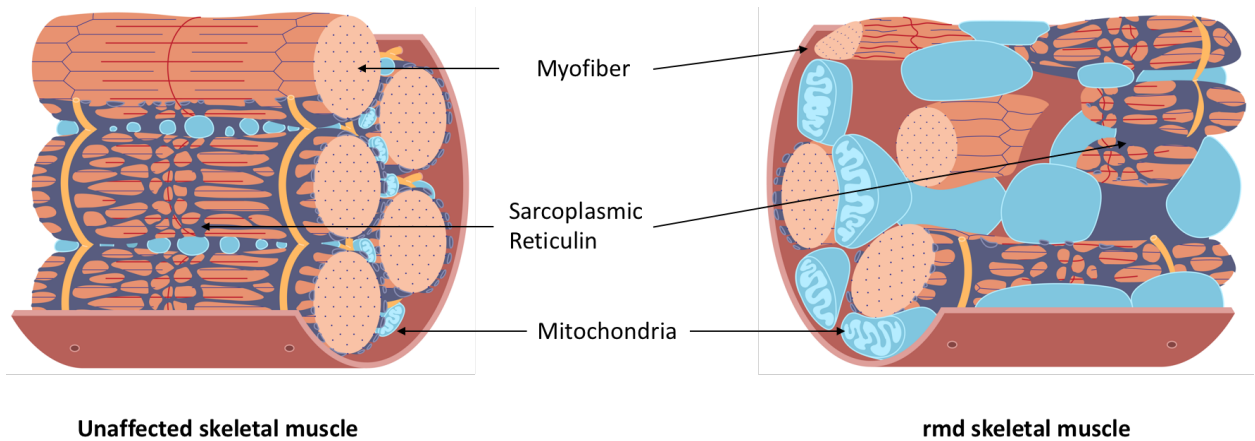
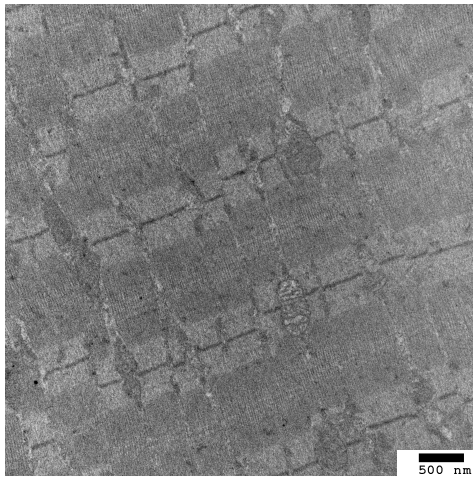


FIG 29. Representational image of WT and rmd muscle structure. A representation of the difference in muscle structure of an unaffected and rmd mouse.

A



B

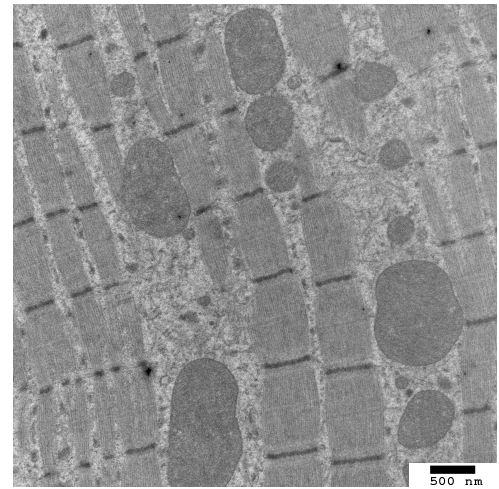


FIG 30. TEM images of gastrocnemius muscle from WT and *rmd* mice. (A) Represents skeletal muscle from an unaffected WT mouse, showing normal mitochondrial phenotype and distribution (B) Represents skeletal muscle from a *rmd* mutant mouse, showing megamitochondria and disrupted muscle architecture as a result of the megamitochondria. N= 4 mice/sex/genotype aged 4-6 weeks.

As seen in chapter 2, *rmd* mutant mice show an increase in mitochondrial area but a decrease in mitochondrial numbers. We hypothesize that this phenomenon directly correlates to a defect in mitochondrial fission or fusion, the correction of which, may enable normal sized mitochondria, which will in turn normalize the disrupted muscle architecture and will thus enable regular Ca^{2+} ion exchange and muscle contraction, thus rescuing the *rmd* phenotype.

In mammals, both mitochondrial fission and fusion are important events in maintaining mitochondrial morphology, mitochondrial DNA (mtDNA) stability, respiratory capacity, response to cellular stress and apoptosis. In mammals, there are three important fusion proteins- mitofusin 1 (*Mfn1*), mitofusin 2 (*Mfn2*) and optic atrophy 1 (OPA1) that facilitate proper

mitochondrial fusion. *Mfn* 1 and 2 are transmembrane GTPases embedded in the mitochondrial outer membrane, whereas OPA1 is a dynamin related GTPase associated with the mitochondrial inner membrane or intermembrane space (D. C. Chan, 2012).

Depletion of any one of the three fusion proteins results in a decrease in mitochondrial fusion (D. C. Chan, 2012). Previous literature shows that *Mfn* 1 and 2 can exist as both homotypic and heterotypic oligomers and can cooperate as well as act individually to promote mitochondrial fusion (H. Chen et al., 2003). Mice heterozygous for *Mfn1* or *Mfn2* null mutations demonstrate full viability and fertility but homozygous mutants for either gene are embryonically lethal. Preliminary studies by Chen, et al. indicate that double homozygous embryos show greater developmental delay and die earlier than either single mutant. Hybrid cell fusion assays (PEG fusion assays) determined that *Mfn1* or *Mfn2* deficient cells have severely fragmented mitochondria with deficient mobility. This fragmentation is caused by a reduction in fusion caused by loss of *Mfn1* or *Mfn2*. Additionally, it was noted that in 10% of fused *Mfn1* mutant cells, the mitochondria did not spread readily throughout the cytoplasm but instead remained in distinct sectors of red and green fluorescence showing a ‘sectoring effect’ (H. Chen et al., 2003).

Hence, in order to test our hypothesis, that reducing the size of megamitochondria in our *rmd* mice would have a positive effect on muscle morphology and function, we engineered a muscle-specific *Mfn1* null mouse and a separate muscle-specific *Mfn2* mouse that we bred separately to our *rmd* strain resulting in a *Mfn1*^{-/-}HSA.Cre.Tg^{+/-}*rmd/rmd* and a *Mfn2*^{-/-}HSA.Cre.Tg^{+/-}*rmd/rmd* strain respectively. The HSA.Cre transgenic mouse has a Human Alpha-Skeletal Actin promoter driven Cre recombinase. This when bred to a loxp flanked sequence of interest, will result in a Cre mediated deletion of the sequence of interest in the skeletal muscle only. We hypothesized that the megamitochondria of *rmd* mice when coupled with the

fragmented mitochondria of the $Mfn1/2^{-/-}$ HSA.CreTg^{+/-} mouse will result in normal (WT) sized mitochondria which would restore muscle architecture and hence the dystrophic phenotype in the *rmd* mutant mice. This strategy would serve as a proof of concept for the possible strategy for the knockdown of *Mfn1* and 2 genes in MDCMC patients for a restoration of their muscle fiber structure and hence disease phenotype.

Results:

Partial rescue of mitochondrial dimensions in $Mfn1^{-/-}$ HSA.CreTg^{+/-}*rmd/rmd* and $Mfn2^{-/-}$

HSA.CreTg^{+/-}*rmd/rmd* mice: $Mfn1/2^{-/-}$ HSA.Cre.Tg^{+/-}*rmd/rmd* mice were generated using the breeding scheme represented in Fig 30.

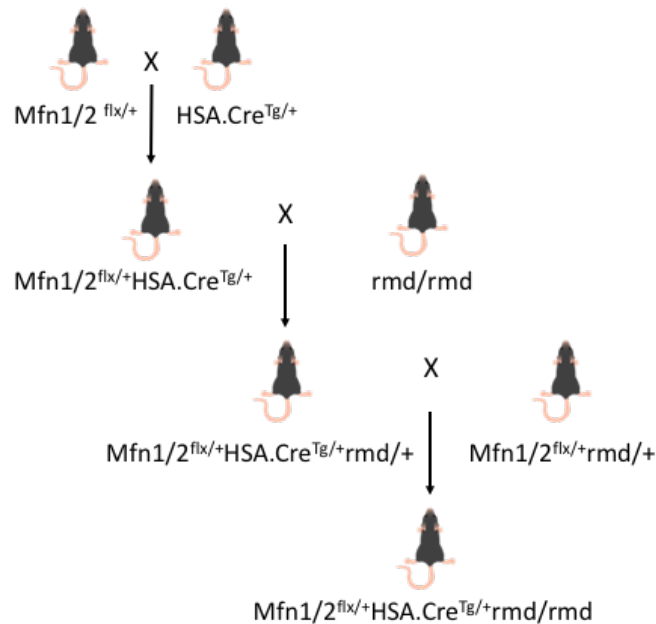


FIG 31. Breeding scheme to obtain $Mfn1/2^{-/-}$ HSA.Cre.Tg^{+/-}*rmd/rmd* mice.

Mfn1^{-/-}HSA.Cre.Tg^{+/-}*rmd/rmd* mitofusin mice were analyzed for mitochondrial areas to test for histological changes in cellular phenotype. Gastrocnemius skeletal muscles were harvested and stained for TEM analysis (4 mice/sex/genotype aged 4-6 weeks). It can be seen that the mitochondria in *Mfn1*^{-/-}HSA.Cre.Tg^{+/-}*rmd/rmd* mice have area in between that of *Mfn1*^{-/-}HSA.Cre.Tg^{+/-}*rmd*^{+/+} and *rmd* mice (Fig 32 A-C) and (Fig 33 A-C). Quantitative analysis shows that the mitochondrial areas of *Mfn1*^{-/-}HSA.Cre.Tg^{+/-}*rmd/rmd* are significantly greater ($p < 0.0001$) than those from *Mfn1*^{-/-}HSA.Cre.Tg^{+/-}*rmd*^{+/+} mice and significantly smaller than those from *rmd* mutant mice ($p < 0.0001$) (Fig 34 A-B).

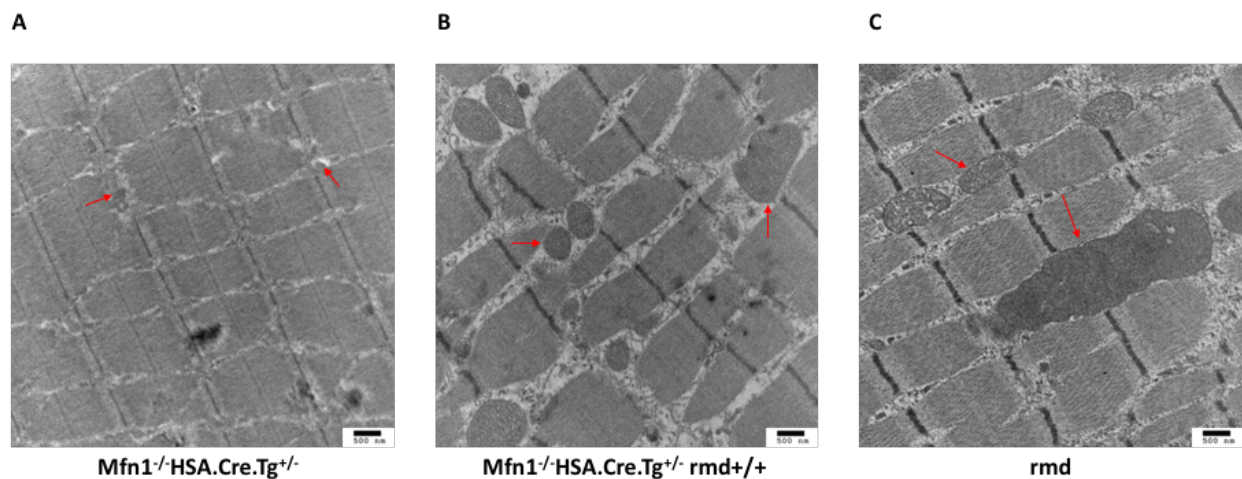


FIG 32. Mitochondrial dimensions across *Mfn1* genotypes. (A) represents skeletal muscle from *Mfn1*^{-/-}HSA.Cre.Tg^{+/-} mouse with highly fragmented mitochondria and (B) represents skeletal muscle from *Mfn1*^{-/-}HSA.Cre.Tg^{+/-} *rmd*^{+/+} mice with mitochondria in between that of *Mfn1*^{-/-}HSA.Cre.Tg^{+/-} and *rmd* mice. (C) represents skeletal muscle from a *rmd* mouse showing megamitochondria. N=4 mice/sex/genotype aged 4-6 weeks.

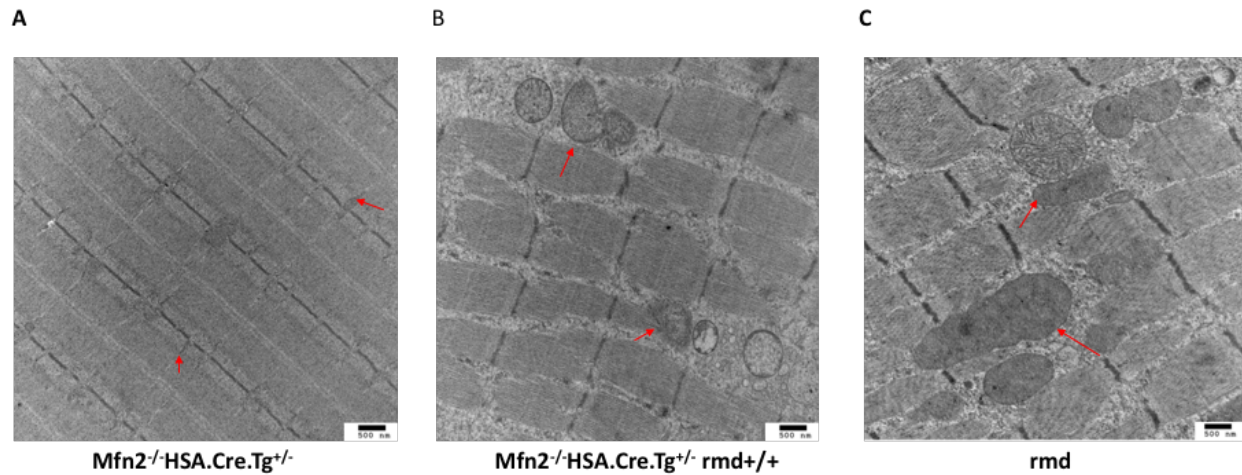


FIG 33. Mitochondrial dimensions across *Mfn2* genotype. (A) represents skeletal muscle from Mfn2^{-/-}HSA.Cre.Tg^{+/-} mouse with highly fragmented mitochondria and (B) represents skeletal muscle from Mfn2^{-/-}HSA.Cre.Tg^{+/-} rmd^{+/+} mice with mitochondria in between that of Mfn2^{-/-}HSA.Cre.Tg^{+/-} and rmd mice. (C) represents skeletal muscle from a rmd mouse showing megamitochondria. N=4 mice/sex/genotype aged 4-6 weeks.

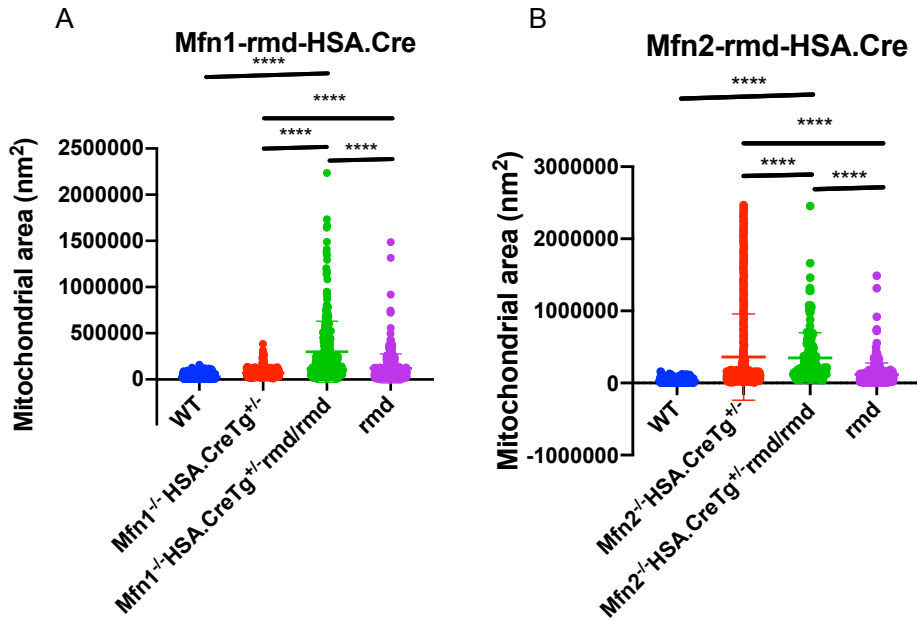


FIG 34. Mitochondrial areas across *Mfn1* and *Mfn2* genotypes. (A-B) show a statistical analysis for mitochondrial areas in the different genotypes of analyzed mice. In summary, *Mfn1*^{2^{-/-}}HSA.Cre.Tg^{+/-} *rmd*^{+/+} mice show mitochondrial area significantly larger than those of *Mfn1*^{2^{-/-}}HSA.Cre.Tg^{+/-} mice but smaller than those of *rmd* mice, indicating a partial rescue in mitochondrial dimensions. N=4 mice/sex/genotype aged 4-6 weeks. Error bars represent mean with SD.

Mitochondrial area analysis (performed as described in chapter 2) indicated a partial rescue in the areas of *Mfn1*^{2^{-/-}}HSA.Cre.Tg^{+/-}*rmd*/*rmd* mice compared to the *rmd* and *Mfn1*^{2^{-/-}}HSA.Cre.Tg^{+/-}*rmd*^{+/+} mice.

Changes in mitochondrial dimensions do not rescue body weights and grip strength: $Mfn1^{-/-}$ HSA.CreTg^{+/-}*rmd/rmd* and $Mfn2^{-/-}$ HSA.Cre.Tg^{+/-}*rmd/rmd* mice were weaned at 3 weeks of age and then weighed and tested for wire hang abilities for a period of 7 weeks post wean. Body weight curves show that $Mfn1^{-/-}$ HSA.Cre.Tg^{+/-}*rmd/rmd* or $Mfn2^{-/-}$ HSA.Cre.Tg^{+/-}*rmd/rmd* mice were not significantly different from the *rmd* mice (Fig 35, 36) and showed no gross improvements in overt phenotype (Table 4, 5). Testing for grip strength on the wire hang apparatus showed no significant differences in the hang time between $Mfn1^{-/-}$ HSA.Cre.Tg^{+/-}*rmd/rmd* or $Mfn2^{-/-}$ HSA.Cre.Tg^{+/-}*rmd/rmd* and *rmd* mice indicating that a muscle specific deletion of *Mfn* 1 or *Mfn* 2 gene in a *rmd* mouse did not rescue muscle strength phenotype (Fig 37, 38) (Table 6,7). A muscle specific deletion of mitofusin did not rescue the forelimb deformity seen in the *rmd* mice, affecting their ability to perform on the hanging wire assay.

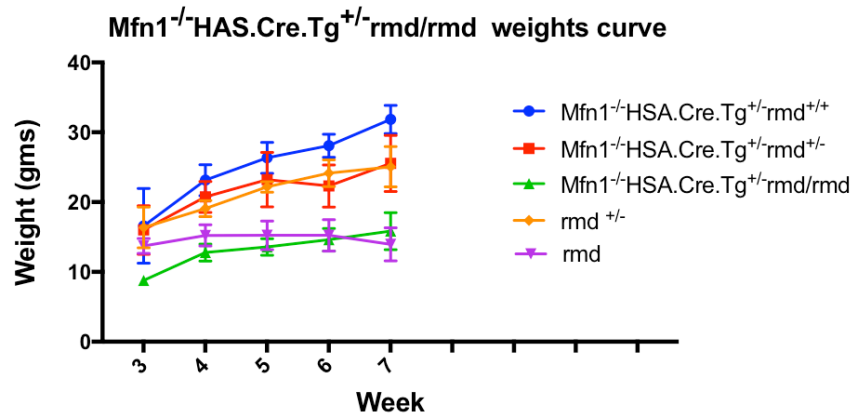


FIG 35. Growth curve across *Mfn1* genotypes. $Mfn1^{-/-}$ HSA.Cre.Tg^{+/-}*rmd/rmd* weights curve
There are no significant differences in the weights of $Mfn1^{-/-}$ HSA.Cre.Tg^{+/-}*rmd/rmd* and *rmd* mutant mice. N= 4 mice/sex/genotype.

Tukey's multiple comparisons test	Mean Diff.	95.00% CI of diff.	Significant?	Summary	Adjusted P Value
Mfn1 ^{-/-} HSA.Cre.Tg ^{+/-} rmd ^{+/+} vs. Mfn1 ^{-/-} HSA.Cre.Tg ^{+/-} rmd ^{+/-}	3.103	0.5921 to 5.614	Yes	**	0.0081
Mfn1 ^{-/-} HSA.Cre.Tg ^{+/-} rmd ^{+/+} vs. Mfn1 ^{-/-} HSA.Cre.Tg ^{+/-} rmd/rmd	11.55	9.039 to 14.06	Yes	****	<0.0001
Mfn1 ^{-/-} HSA.Cre.Tg ^{+/-} rmd ^{+/+} vs. rmd	9.984	7.748 to 12.22	Yes	****	<0.0001
Mfn1 ^{-/-} HSA.Cre.Tg ^{+/-} rmd ^{+/-} vs. rmd ^{+/-}	3.296	0.7854 to 5.807	Yes	**	0.0042
Mfn1 ^{-/-} HSA.Cre.Tg ^{+/-} rmd ^{+/-} vs. Mfn1 ^{-/-} HSA.Cre.Tg ^{+/-} rmd/rmd	8.447	5.896 to 11	Yes	****	<0.0001
Mfn1 ^{-/-} HSA.Cre.Tg ^{+/-} rmd ^{+/-} vs. rmd	6.881	4.6 to 9.163	Yes	****	<0.0001
Mfn1 ^{-/-} HSA.Cre.Tg ^{+/-} rmd ^{+/-} vs. rmd ^{+/-}	0.1933	-2.358 to 2.744	No	ns	0.9995
Mfn1 ^{-/-} HSA.Cre.Tg ^{+/-} rmd/rmd vs. rmd	-1.565	-3.847 to 0.7164	No	ns	0.3136
Mfn1 ^{-/-} HSA.Cre.Tg ^{+/-} rmd/rmd vs. rmd ^{+/-}	-8.253	-10.8 to -5.702	Yes	****	<0.0001
rmd vs. rmd ^{+/-}	-6.688	-8.97 to -4.406	Yes	****	<0.0001

Table 4: Tukey's multiple comparisons test for weights on different Mfn1 genotypes.

This table shows that there are no significant differences in the weights of Mfn1^{-/-}HSA.Cre.Tg^{+/-}rmd/rmd and rmd mice showing no improvements in the wire hang / grip strength by a muscle specific deletion of Mfn1 gene in rmd mice.

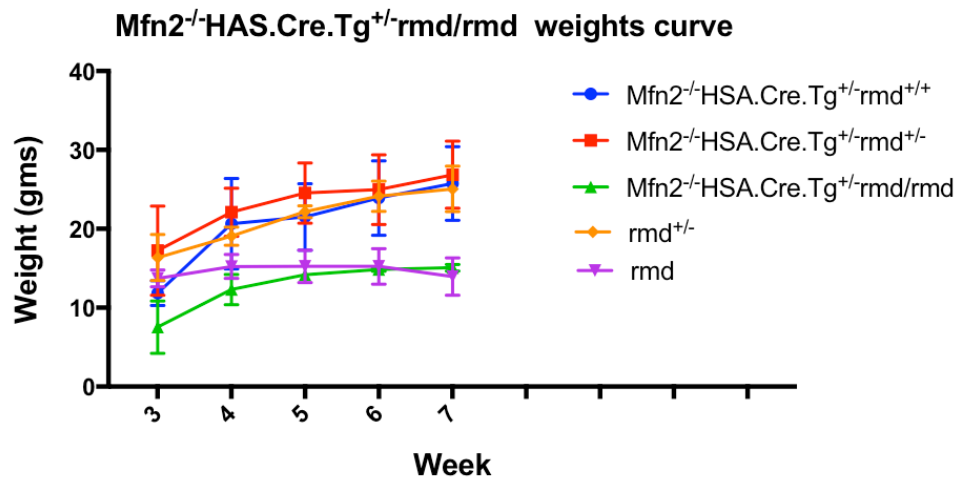


FIG 36. Growth curves across Mfn2 genotypes. Mfn2^{-/-}HSA.Cre.Tg^{+/-}rmd/rmd weights curve

There are no significant differences in the weights of Mfn2^{-/-}HSA.Cre.Tg^{+/-}rmd/rmd and mutant rmd mice. N= 4 mice/sex/genotype.

Tukey's multiple comparisons test	Mean Diff.	95.00% CI of diff.	Significant?	Summary	Adjusted P Value
Mfn2 ^{-/-} HSA.Cre.Tg ^{+/-} rmd ^{+/+} vs. Mfn2 ^{-/-} HSA.Cre.Tg ^{+/-} rmd ^{+/-}	-2.41	-5.385 to 0.5654	No	ns	0.1671
Mfn2 ^{-/-} HSA.Cre.Tg ^{+/-} rmd ^{+/+} vs. Mfn2 ^{-/-} HSA.Cre.Tg ^{+/-} rmd/rmd	7.95	4.975 to 10.93	Yes	****	<0.0001
Mfn2 ^{-/-} HSA.Cre.Tg ^{+/-} rmd ^{+/+} vs. rmd	6.058	3.445 to 8.671	Yes	****	<0.0001
Mfn2 ^{-/-} HSA.Cre.Tg ^{+/-} rmd ^{+/+} vs. rmd ^{+/-}	-0.63	-3.605 to 2.345	No	ns	0.9755
Mfn2 ^{-/-} HSA.Cre.Tg ^{+/-} rmd ^{+/-} vs. Mfn2 ^{-/-} HSA.Cre.Tg ^{+/-} rmd/rmd	10.36	7.179 to 13.54	Yes	****	<0.0001
Mfn2 ^{-/-} HSA.Cre.Tg ^{+/-} rmd ^{+/-} vs. rmd	8.468	5.623 to 11.31	Yes	****	<0.0001
Mfn2 ^{-/-} HSA.Cre.Tg ^{+/-} rmd ^{+/-} vs. rmd ^{+/-}	1.78	-1.401 to 4.961	No	ns	0.5216
Mfn2 ^{-/-} HSA.Cre.Tg ^{+/-} rmd/rmd vs. rmd	-1.892	-4.737 to 0.953	No	ns	0.3459
Mfn2 ^{-/-} HSA.Cre.Tg ^{+/-} rmd/rmd vs. rmd ^{+/-}	-8.58	-11.76 to -5.399	Yes	****	<0.0001
rmd vs. rmd ^{+/-}	-6.688	-9.533 to -3.843	Yes	****	<0.0001

Table 5: Tukey's multiple comparisons test for weights on different Mfn2 genotypes.

This table shows that there are no significant differences in the weights of Mfn2^{-/-} HSA.CreTg^{+/-}rmd/rmd and rmd mice showing no improvements in the wire hang / grip strength by a muscle specific deletion of Mfn2 gene in mutant rmd mice.

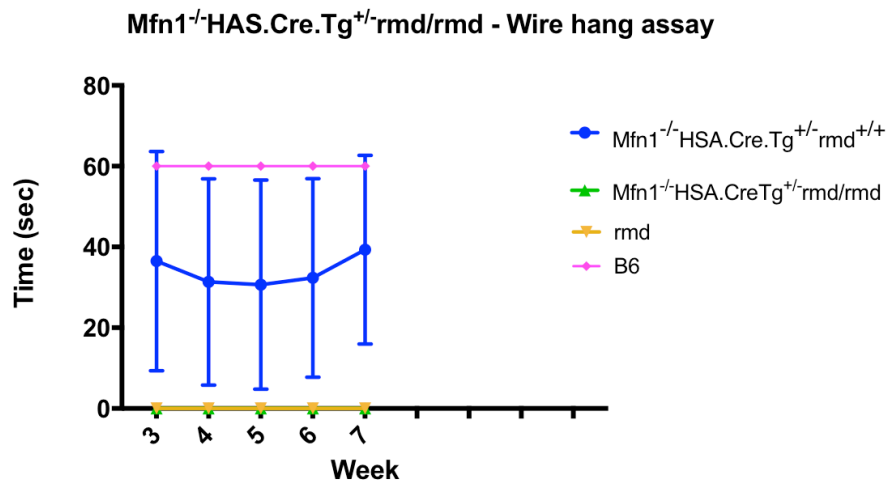


FIG 37. Wire hang assay on *Mfn1*^{-/-}HSA.Cre.Tg^{+/-}*rmd/rmd* mice. Wire hang assay in *Mfn1*^{-/-}HSA.Cre.Tg^{+/-}*rmd/rmd* mice. Wire hangs show no significant differences in hang time of *Mfn1*^{-/-}HSA.Cre.Tg^{+/-}*rmd/rmd* and *rmd* mice. *Mfn1*^{-/-}HSA.Cre.Tg^{+/-}*rmd*^{+/-} mice show hanging times in between those of WT (B6) mice and *Mfn1*^{-/-}HSA.Cre.Tg^{+/-}*rmd/rmd* mice indicating probable partial effect of muscle specific deletion of *Mfn1* gene in WT mice. N= 4 mice/sex/genotype.

Tukey's multiple comparisons test	Mean Diff.	95.00% CI of diff.	Significant?	Summary	Adjusted P Value
<i>Mfn1</i> ^{-/-} HSA.Cre.Tg ^{+/-} <i>rmd</i> ^{+/+} vs. <i>Mfn1</i> ^{-/-} HSA.Cre.Tg ^{+/-} <i>rmd/rmd</i>	34.19	22.24 to 46.14	Yes	****	<0.0001
<i>Mfn1</i> ^{-/-} HSA.Cre.Tg ^{+/-} <i>rmd</i> ^{+/+} vs. <i>rmd</i>	34.19	23.04 to 45.34	Yes	****	<0.0001
<i>Mfn1</i> ^{-/-} HSA.Cre.Tg ^{+/-} <i>rmd</i> ^{+/+} vs. B6	-25.81	-37.76 to -13.86	Yes	****	<0.0001
<i>Mfn1</i> ^{-/-} HSA.Cre.Tg ^{+/-} <i>rmd/rmd</i> vs. <i>rmd</i>	0	-11.36 to 11.36	No	ns	>0.9999
<i>Mfn1</i> ^{-/-} HSA.Cre.Tg ^{+/-} <i>rmd/rmd</i> vs. B6	-60	-72.14 to -47.86	Yes	****	<0.0001
<i>rmd</i> vs. B6	-60	-71.36 to -48.64	Yes	****	<0.0001

Table 6: Tukey's multiple comparisons test for *Mfn1*^{-/-}HSA.Cre.Tg^{+/-}*rmd/rmd* mice on wire hang assay.

The table summarizes the statistical significance between the different genotypes for *Mfn1* gene tested. There are no significant differences between the wire hang time of *Mfn1*^{-/-}HSA.Cre.Tg^{+/-}*rmd/rmd* and *rmd* mice, indicating the muscle specific deletion of *Mfn1* gene in *rmd* mutant mice does not rescue muscle strength phenotype.

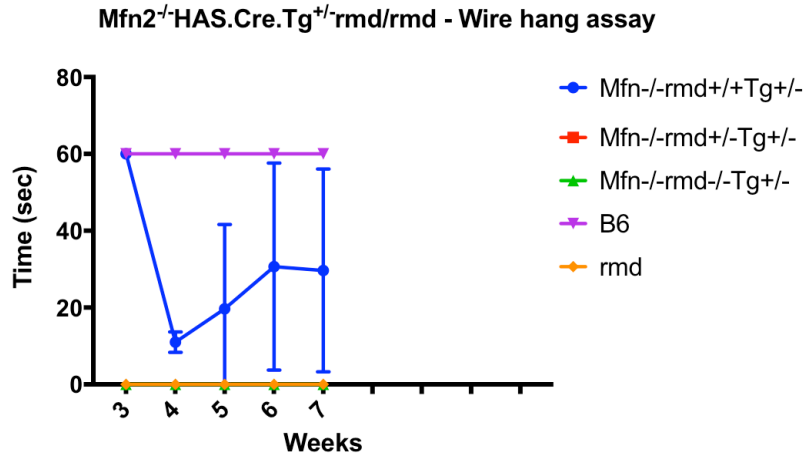


FIG 38. Wire hang assay on *Mfn2^{-/-}HSA.Cre.Tg^{+/-}rmd/rmd* mice. Wire hang assay in *Mfn2^{-/-}HSA.Cre.Tg^{+/-}rmd/rmd* mice. Wire hangs show no significant differences in hang time of *Mfn2^{-/-}HSA.Cre.Tg^{+/-}rmd/rmd* and *rmd* mice. *Mfn2^{-/-}HSA.Cre.Tg^{+/-}rmd^{+/-}* mice show hanging times in between those of WT (B6) mice and *Mfn2^{-/-}HSA.Cre.Tg^{+/-}rmd/rmd* mice indicating probable partial effect of muscle specific deletion of *Mfn2* gene in WT mice. N= 4 mice/sex/genotype.

Tukey's multiple comparisons test	Mean Diff.	95.00% CI of diff.	Significant?	Summary	Adjusted P Value
<i>Mfn2^{-/-}HSA.Cre.Tg^{+/-}rmd^{+/-}</i> vs. <i>Mfn2^{-/-}HSA.Cre.Tg^{+/-}rmd/rmd</i>	30.2	20.63 to 39.77	Yes	****	<0.0001
<i>Mfn2^{-/-}HSA.Cre.Tg^{+/-}rmd^{+/-}</i> vs. B6	-29.8	-39.37 to 20.23	Yes	****	<0.0001
<i>Mfn2^{-/-}HSA.Cre.Tg^{+/-}rmd^{+/-}</i> vs. <i>rmd</i>	30.2	20.63 to 39.77	Yes	****	<0.0001
<i>Mfn2^{-/-}HSA.Cre.Tg^{+/-}rmd/rmd</i> vs. B6	-60	-69.57 to 50.43	Yes	****	<0.0001
<i>Mfn2^{-/-}HSA.Cre.Tg^{+/-}rmd/rmd</i> vs. <i>rmd</i>	0	-9.567 to 9.567	No	ns	>0.9999
B6 vs. <i>rmd</i>	60	50.43 to 69.57	Yes	****	<0.0001

Table 7: Tukey's multiple comparisons test for *Mfn2^{-/-}HSA.Cre.Tg^{+/-}rmd/rmd* mice on wire hang assay.

The table summarizes the statistical significance between the different genotypes for *Mfn2* gene tested. There are no significant differences between the wire hang time of *Mfn2*^{-/-} HSA.Cre.Tg^{+/-}*rmd/rmd* and mutant *rmd* mice, indicating the muscle specific deletion of *Mfn2* gene in mutant *rmd* mice does not rescue muscle strength phenotype.

2. S107 compound for the treatment of muscular dystrophy

Ryanodine receptor 1 (RyR1) is the calcium release channel in the sarcoplasm of the skeletal muscle required for muscle contraction. Calstabin1 is a sub-unit that stabilized this RyR1 and has been shown to decrease with age, making RyR1 unstable and hence leaky. It has been shown that S107 preserves RyR1-calstabin1 binding, stabilizing RyR1, reducing Ca²⁺ sparks and hence restoring muscle specific force for improved exercise capacity in aged WT mice (Andersson et al., 2011)(Mei et al., 2013). Similar RyR1-calstabin1 binding instability has been observed in the *mdx* mouse model for Duchenne muscular dystrophy and is predicted to be a major reason for decreased muscle function in this disease. When *mdx* mice were supplied 25mg/100ml of S107 compound through drinking water for 7-9 days they showed increased running speed and duration on the running wheel (Andersson et al., 2012). In a separate study, *mdx* mice administered S107 were found to have increased muscle function, voluntary activity and improved muscle histopathology (Blat & Blat, 2015).

Previous literature provides strong evidence of the involvement in RyR1-calstabin1 binding integrity in prevention of muscular dystrophy and provides evidence for the effect of S107 in preserving RyR1 and calstabin1 binding. Hence, we decided to test the effects of supplementation of S107 to our *rmd* mice via diet. The experimental set-up was similar to that of the CDP-choline and 50mg/Kg/day of S107 was administered to *rmd* mice via Clear H₂O diet

gel. Diet gel spiked with the same amount of S107 was also fed to WT mice to test for toxic effects of S107 in healthy conditions.

Results:

S107 administration did not improve body weight and growth curve of *rmd* mutant mice

3 week mice were administered 50 mg/Kg/day of S107 compound by mixing 8.75 mg of S107 compound in 56gms of Clear H₂O diet gel and available to the mice for ad libitum consumption. Clear H₂O diet gel was prepared fresh and administered daily. Mice were weighed every week from the start of the study at 3 weeks and up to 5 weeks of age. No significant improvements in growth rate were observed in the *rmd* (MUT) S107 treated mice when compared with historic data from *rmd* mice on plain Clear H₂O diet gel (p=0.10, 0.26 and 0.56 at 3, 4 and 5 weeks respectively). *rmd* S107 administered mice showed a significantly decreased (p<0.0001) growth curve when compared WT mice administered S107 compound. No significant differences were observed between the S107 administered WT mice and WT mice on Clear H₂O diet gel (historic data) indicating no toxic effects of supplementation of S107 in healthy conditions (Fig 39).

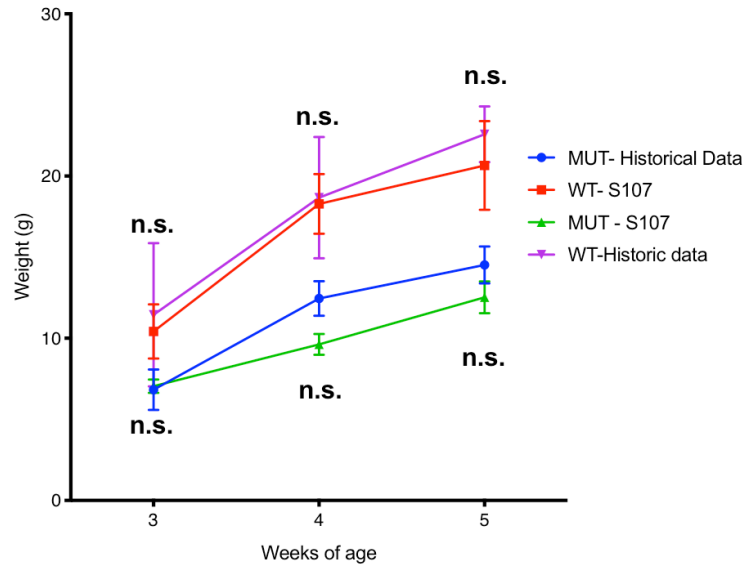


FIG 39. Growth curve of *rmd* mice on S107 supplement: Growth curve of *rmd* mice on S107 supplementation. No significant improvements in growth curve was observed in the *Mfn1/2^{-/-}HAS.Cre.Tg^{+/-}rmd/rmd* S107 treated mice when compared with historic data from *rmd* mice on plain Clear H₂O diet gel (p=0.10, 0.26 and 0.56 at 3, 4 and 5 weeks respectively). *Mfn1/2^{-/-}HAS.Cre.Tg^{+/-}rmd/rmd* S107 administered mice showed a significantly decreased (p<0.0001) growth curve when compared with *Mfn1/2^{-/-}HAS.Cre.Tg^{+/-}rmd^{+/+}* (WT) mice administered S107 compound. The *Mfn1/2^{-/-}HAS.Cre.Tg^{+/-}rmd^{+/+}* mice were not significantly different from the WT mice on plain diet gel, as seen from historic data. Where; MUT=mutant, WT=wild type. N= 4 mice/sex/genotype.

Discussion:

It can be seen that even though the use of mitofusin as a genetic modifier helps partially restore mitochondrial area and hence mitochondrial phenotype, this does not have any effect on the life-span / growth curve and wire hang abilities of the *Mfn1/2^{-/-}HSA.Cre.Tg^{+/-}rmd/rmd* mice. A major reason for the inability to perform the wire hang tests is the forelimb deformities in the *Mfn1/2^{-/-}HSA.Cre.Tg^{+/-}rmd/rmd* mice that do not seem to be corrected, resulting in inability to grip and hang on to the wire grid in the test. *rmd* mice show defects in membrane integrity as seen from Evans Blue Fluorescent staining and JC-1 fluorescence assay (Sher et al., 2006)(Wu et al., 2010). The mitochondria in the *Mfn1/2^{-/-}HSA.Cre.Tg^{+/-}rmd/rmd* mice have not been tested for membrane integrity. Rescue of mitochondrial size could rescue membrane function and integrity, which remains to be tested using the above-mentioned assays or the Seahorse cell analysis technology.

This forelimb deformity was not corrected after the administration of S107 and hence these mice were not tested for wire hang. S107 when administered to *rmd* mice did not seem to improve growth curves as previously reported with the *mdx* mice, suggesting that oral supplementation of S107 through Clear H₂O diet gel did not show any improvement in *rmd* phenotype. An alteration to the supplementation strategy via introducing the drug earlier in gestation to the pregnant mothers in order to target muscular dystrophy of their mutant *rmd* offspring before its onset might show a better response.

Materials and Methods:

Growth Curve: In order to measure the body weight and hence the growth curve of mice an N of 4 mice/sex/genotype were used for the experiments. The mice were weighed one at a time at approximately the same time once a week. For weighing, an empty Lilly tub was pre-weighed and used as a holder for mice in the weighing scale. The mice were then weighed and the weight of the Lilly tub was subtracted to give the weight of the mice.

Wire hang: The wire hang assay was performed once a week at around the same time of day. For this assay, the mice were placed on a wire mesh and the mesh then inverted. The stop watch was started at the time when the wire mesh was inverted. The number of seconds for which a mouse could hold on the mesh was recorded. An N of 4 mice/sex/genotype was used for each experiment.

Mitochondria area analysis: For analysis of mitochondrial area, n=4 mice/sex/genotype were used. Gastrocnemius muscles from the mice were prepared for TEM analysis as described in chapter 2. About 5 pictures from each mouse were analyzed for mitochondrial areas. All the mitochondrial areas analyzed from each group were pooled together and student's t-test was used to assess differences between mitochondrial areas between groups.

Transmission electron microscopic sample preparation, image analysis, were performed as described in chapter 2.

CHAPTER 5

CONCLUSION AND FUTURE DIRECTIONS

Medical management of muscular dystrophy

MD continues to affect many Americans (1 in 250,000) (Mercuri et al., 2002) (www.mda.org, www.ninds.nih.gov). However, no cure exists. Medical management techniques like cardiac care, provision of self-feeding support, implementation of techniques for safe swallowing, physical therapy and other palliative care can be provided. Treatments are generally tailored specific to patient needs by a team of physicians and they include occupational therapy to improve muscle strength and function and speech therapy (National Organization of Rare Disorders). Depending on the type and stage of MD, corrective surgery like cataract removal or adding a pacemaker in cases of cardiac failure can be performed. Current medications used to slow down the progression of MD symptoms are glucocorticoids like prednisone and Emflaza that helps increase muscle strength, agility and slows down the progression of MD, anticonvulsants to help with muscle spasms, immunosuppressants to help slow down the death of muscle cells and antibiotics to treat respiratory infections, drugs like angiotensin converting enzyme (ACE) inhibitors and beta blockers (www.nichd.nih.gov, www.muscular dystrophynews.com). Intraperitoneal injections of protease inhibitor leupeptin in dy/dy mouse model for dystrophy prevented the development of any histological features of muscular dystrophy (Tsuji & Matsushita, 1986). However, no further research has been conducted in this therapeutic area. Myoblast transfer as a technique to replace dystrophin in Duchenne's muscular dystrophy patients showed no significant difference in muscle strength and a low percentage of donor-derived dystrophin (Mendell et al., 1995). In the past decade,

gene therapy as a method of treatment of muscular dystrophy has gained momentum. Many efforts have been made in the treatment of Duchenne muscular dystrophy (DMD) one of the most common types of MD. Efforts for delivery of the mini or micro-dystrophin gene in DMD patients are being made using vectors like adenoviruses, retroviruses plasmids and adeno-associated viruses with AAV vector mediated gene delivery being the most feasible with many positive results in pre-clinical trials (Chamberlain, 2002) (Hollinger & Chamberlain, 2015)(Ramos et al., 2015). In another effort to help cure Duchenne muscular dystrophy, Serepta therapeutics has been working on increasing expression of GALGT2 gene by AAV mediated injections (www.musculardystrophynews.com). GALGT2 encodes for the protein GalNAc transferase (beta 1,4 N-acetylgalactosamine galactosyltransferase) that transfers a complex sugar molecule on to dystroglycan. In an mdx mouse, upregulation of GALGt2 gene via AAV vector upregulates utrophin, which in turn prevents dystrophy (www.parentprojectmd.org)(Hirst, McCullagh, & Davies, 2005). However, none of these therapies are FDA approved yet.

AAV mediated gene therapy for MDCMC

AAV is increasingly being used as a vector of choice for gene therapy in the alleviation of MD symptoms. Retroviruses effectively integrate into the host genome but are difficult to grow in large quantities thus inhibiting their use in gene therapy. Use of retroviruses for gene therapy can be problematic in cases where retroviruses have been known to integrate into promoter regions of oncogenic genes and cause tumorigenesis (RS, BF, SRW, P, & Chen H, 2004). Adenoviruses and plasmids have poor transduction properties when compared to AAV vectors, making AAV vectors one of the most suitable forms of gene transfer systems. On the other hand, AAV vectors can be used to carry genes up to 4.7Kb in size and can transduce post-

mitotic cells, thus gaining specific importance in the field of MD therapy. Although not common, studies have reported the generation of cellular immune response against protein delivered by AAV. These immune responses can be limited by using muscle specific promoters in case of muscular dystrophy patients (Cordier et al., 2001). For each case, a tissue specific promoter can be inserted upstream of the AAV vector so as to have tissue specific effects and lower host immune responses (Zeng et al., 2008)(B. Wang et al., 2008). Each AAV vector is designed to carry a specific gene that the patient lacks making each vector specialized and specific for the treatment of that particular MD (Chamberlain, 2002).

Therapeutic rescue of dystrophy in *rmd* mice

While our data contributes immensely to the current knowledge in the field of MDCMC, many questions still remain unanswered. Deficiency of CHKB gene results in MDCMC as was discovered from the study of the *rmd* mice. The *rmd* mice form a good model for MDCMC, demonstrating most of the features of this disorder as seen from biochemical (Sher et al., 2006), histology and muscle strength analysis. It is not known as to why deletion of a ubiquitously present gene like choline kinase beta affects the mitochondria of the skeletal muscles exclusively. Choline kinase beta deficiency should have effects on the membranes of all cellular organelles but this is not apparent from histology of tissues like brain and heart of *rmd* mice, whereas the skeletal muscles of the forelimbs show a less severe dystrophic phenotype. Levels of PC in the hind limb skeletal muscles of *rmd* mutant mice are not depleted but severely reduced (Sher et al., 2006), indicating that the hindlimb skeletal muscle tissues possibly derive PC via some other pathway like the PE pathway in the liver. It will be interesting to know which pathway compensates in choline kinase beta deficient conditions. Components of that pathway

can then be regulated using drugs to increase PC levels in MDCMC patients. As part of my thesis, I have worked on the therapeutic rescue of *rmd* phenotype using mitofusin1 and 2 as genetic modifier, using CDP-choline as a dietary supplement to bypass the defects in the Kennedy pathway for PC synthesis, Using S107 as a dietary supplement to stabilize RyR1-calstabin binding and thus improve *rmd* phenotype and by using gene therapy for the up-regulation of choline kinase alpha and choline kinase beta in *rmd* muscle.

Therapeutic intervention using CDP-choline and S107 as oral supplements. Therapeutic intervention in the form of oral supplementation of a Kennedy pathway intermediate like CDP-choline and that of a known RyR1-calstabin1 binding stabilizer-S107, failed to prevent dystrophy in *rmd* mice. CDP-choline did not benefit life span of *rmd* mice and failed to rescue *rmd* phenotype. Previous studies have shown that CDP-choline helps decrease creatinine kinase levels in skeletal muscles of *rmd* mice (Wu et al., 2010). The pharmacokinetics of absorption of CDP-choline in different tissues and testing of serum creatinine kinase levels in *rmd* mice supplemented with CDP-choline will help determine improvements in muscle condition that were not visible through gross phenotype studies. Analysis of muscle force of contraction in fast-twitch muscle groups like the EDL can sensitively determine improvements in muscle force and contraction which are not visible in tests like wire hang.

S107 has been shown to help improve muscle excitation and contraction force in mouse models of Duchenne muscular dystrophy (Andersson et al., 2011)(Andersson et al., 2012)(Blat & Blat, 2015). Supplementation of S107 compound in diet did not lead to improvements in gross wire hang abilities or weights of the *rmd* mice. Like with the CDP-choline supplemented mice, it will be beneficial to assess the muscle force of contraction in fast-twitch muscle groups like the

EDL muscle. These tests will help determine if improvements in muscle force and contraction abilities will help translate to better quality life in MDCMC patients.

Use of Mitofusin 1 and Mitofusin 2 as genetic modifiers in *rmd*: Use of *Mfn1/2* as a gene modifier, led to partial rescue of the mitochondria, with mitochondrial areas in between that of *rmd* and WT mice but failed to rescue dystrophy and increase life span of *rmd* mice. Mitochondria in *rmd* mice show decreased membrane potential and are not as efficient as mitochondria in WT mice (Sher et al., 2006)(Wu et al., 2010). The partially rescued mitochondria in *Mfn1/2*HSA.Cre^{+/+}*rmd/rmd* mice have not been tested for membrane integrity or function. Performing these tests on the Seahorse cell analysis machine can help understand if the partial mitochondria showed a rescue in function. Improvements in membrane function would lead to further confirmation of our findings; that, megamitochondria, by itself does not rescue *rmd* but may contribute to other characteristics of the disorder arising due to choline kinase beta and hence PC deficiency.

Gene therapy by up-regulation of *Chkb*: The Tg-*rmd* showed muscle strength, mitochondrial phenotype and life span comparable to that of WT mice. A 14-fold increased expression of *Chkb* gene does not cause cellular damage and hence, systemic overexpression of *Chkb* can be targeted as a possible gene therapy. This led to testing of AAV mediated gene therapy for the rescue of dystrophy in *rmd* mice. For treating *rmd* in our mouse models, I have not used a muscle specific promoter but have conducted intra-muscular injections, in order to circumvent the construct size restrictions, since our *Ttn* promoter along with our *Chka* or *Chkb* gene far exceeds the 4.7 kb carrying capacity of the AAV vector (Maddatu et al., 2005b). AAV-*Chkb* gene therapy,

intramuscular injections in the gastrocnemius muscles of *rmd* mice improved muscle fiber regeneration, leading to increased fiber area, decrease in the number of centralized nuclei and increased muscle weight. This indicates that upregulation of AAV-*Chkb* in MDCMC can be targeted as a potential therapy, however, in order to design a therapy that can be FDA approved, testing of a few more factors is necessary. It is essential to test for effects of systemic injections in *rmd* mice. Even though, my experiments indicate that over-expression of *Chkb* gene in *Chkb* deficient *rmd* mice does not cause immediate toxic effects, it is essential to perform an aging study on systemically injected mice, in order to test for long-term toxic or immunogenic effects that may occur. Along with this study, it will be interesting to note whether, AAV-*Chkb* injections in 8 week *rmd* mice would result in similar improvements in muscle health and phenotype. This experiment can test for percent regeneration of muscle fibers compared to 3-week injected mice and help understand if injection of adult MDCMC patients can be beneficial for delaying progression of dystrophy and can help with increased muscle strength.

Gene therapy by up-regulation of *CHKA*: AAV mediated injections of *CHKA* gene resulted in similar improved muscle regeneration, decreased number of centralized nuclei and increased muscle weight as with the AAV-*Chkb* injections, indicating that *Chka* can also be a potential target for the rescue of dystrophy. Since MDCMC is caused due to deficiency in choline kinase beta gene, upregulation of choline kinase beta will be the preferred mode of therapy in MDCMC patients. AAV-*Chka* injections can be administered in the rare possibility of development of an immune reaction to AAV-*Chkb* injections or in the event, that a second injection is required after a few years of administering the first injection with AAV-*Chkb*. For use as a gene therapy

vector, it is necessary to test for long-term effects of systemic injections of *Chka* in *rmd* and unaffected mice.

In order to minimize off-target transduction, AAV vectors carrying *Chka* or *Chkb* gene of interest under a muscle specific promoter, other than *Ttn* can be used. Thus, the vector can be made specific for treatment of muscular dystrophy caused as a result of *Chkb* deficiency. Muscle creatinine kinase (MCK) has been shown to have success as a muscle specific promoter in gene therapy for Duchenne muscular dystrophy (Cordier et al., 2001)(B. Wang et al., 2008).

Implication of choline kinase alpha in cancer: Choline kinase alpha gene has been studied more extensively than choline kinase beta gene due to its implication in cancer. *CHKA* expression is the lowest in adult human skeletal muscle (GETx Portal Version V7). Interestingly, in mice, *Chka* expression in skeletal muscle tissues decreases in a rostro-caudal gradient with an increase in mouse age (Wu et al., 2010) (Gallego-Ortega et al., 2009). Decrease in choline kinase alpha expression in adult skeletal muscle tissues implies that choline kinase alpha is detrimental to healthy skeletal muscle tissues. Choline kinase alpha is overexpressed in 40-60% of human tumors (X. Chen et al., 2017). Transfecting Hek293T with choline kinase alpha leads to anchorage independence similar to that obtained with Rho-A induction. However, up-regulating *CHKA* expression in adult skeletal muscle tissues using AAV mediated gene therapy does not show any immediate toxic effects in the *rmd* or unaffected mice. This implies that choline kinase alpha may not be the causative agent in tumorigenesis but a possible indicator of the same. Hence, up-regulation of Choline kinase alpha to rescue can be a potential therapeutic strategy for the rescue of *rmd* phenotype.

The mechanism behind decrease in *CHKA* expression in adult skeletal muscles of humans and a complete shut-down of *Chka* expression in adult skeletal muscles of mice is not known. Epigenetic changes like DNA methylation can bring about a decrease in gene expression. *De novo* methylation of CpG islands has been known to contribute to gene silencing (Jaenisch & Bird, 2003). Many diverse classes of RNA have been shown to recruit histone and DNA methyltransferases, thus silencing DNA/gene expression (Holoch & Moazed, 2015). Methylation of choline kinase alpha gene sequence can be determined with array of bead hybridization followed by a higher resolution method like HPLC and mass spectrometry to determine the exact percentage of sequence methylated. These assays can be performed at 1, 2, 4, 6 and 8 week old mice on order to determine the period when these epigenetic changes begin to occur in mice (Kurdyukov & Bullock, 2016). DNA methylation has been shown to be inhibited in vitro in cell culture using chemical compounds like 5-Aza-2'-deoxycytidine, caffeic acid and chlorogenic acid. It will be interesting to see whether these compounds can help inhibit DNA methylation of choline kinase alpha, preventing its shut down and thus rescuing rmd phenotype in choline kinase beta deficiency. This strategy can also be applied to MDCMC patients in order to decrease shut down of *CHKA* expression, prevent drastic decrease in PC levels and hence prevent or reverse muscular dystrophy caused as a result of *CHKB* deficiency.

Differential function of *Chka* and *Chkb*: enzymatic properties of Choline kinase alpha and beta have shown that choline kinase beta has a Michaelis constant (K_m) for choline 2.8 times higher than choline kinase alpha 1. The K_m of choline kinase beta is lower than that of choline kinase alpha 1 for ethanolamine. This suggests that in cell free systems, choline is a better substrate for choline kinase alpha 1 and ethanolamine is a better substrate for choline kinase beta (Gallego-

Ortega et al., 2009). This is different for different tissues. In mice, we know that choline kinase beta is responsible for the phosphorylation of choline since choline kinase alpha is shut down (Wu et al., 2010b). The activity of choline kinase in a given cell type is regulated not by its amounts but by the combination of each isoform subunit to form functional homodimers or heterodimers (Aoyama et al., 2004). It has been speculated that the alpha/beta heterodimer may have a specific activity in between that of the two respective homodimers. A common conclusion from in vitro and in vivo studies suggests that the main fate of choline is the synthesis of PC via the Kennedy pathway, accounting for the use of 95% of total choline pool in most tissues (Gibellini & Smith, 2010).

Expression patterns of *Chka* and *Chkb* in different tissues: Though research on the expression levels of different homo and heterodimers of choline kinase alpha and beta need to be performed, it can be implied that alpha and beta paralogs can compensate for each other. Thus, in the skeletal muscles of mice, where there is shut down of choline kinase alpha expression, complete lack of choline kinase beta results in extremely low levels of PC and hence muscular dystrophy. The forelimb shows low/remnant levels of choline kinase alpha expression and hence are less affected in choline kinase beta deficient conditions. In *rmd* mice, the cortex and mid-hind brain tissues shows undetectable levels of *Chkb* expression but show minute levels of *Chka* expression in comparison to C57BL/6 mice (0.24 and 0.0005 fold, respectively) (Supplemental fig 5-6) . Tg-*rmd* mice show 0.23 fold and 0.8 fold expression of *Chka* compared to C57BL/6 mice in the Mid-Hind brain region. *Chkb* expression levels for the Mid-Hindbrain region are 0 and 0.38 for *rmd* and Tg-*rmd* mice. This data indicates that different regions of the brain have a specific pattern of *Chka* and *Chkb* expression which influence cognition, membrane fluidity and

structure. This data along with the cognitive analysis on the Tg-rmd and *rmd* mice suggests that in *Chkb* deficient conditions, there remains expression of *Chka* in regions of the brain and while it has not been identified whether this *Chka* expression is from neural cells or vasculature, it can be suggested that this expression influences development of cognitive phenotype in these mice.

Absence of cognitive impairments in rmd mice

Based on my thesis research, the *rmd* mutant mice do not show signs of cognitive impairment in any of the behavioral assays I examined them on. This could be because these mice were tested at a very early age, not having developed working memory or learning problems. However, children at the age of about 5 years were shown to have a lower performance on certain learning tests and tests for IQ (Mitsuhashi, Ohkuma, et al., 2011)(S. Sparks et al., 2012). MDCMC patients showed prominent speech defects which were not tested for in *rmd* mice. Going further, we could test the Tg-rmd mice for other disorders within the spectrum of cognitive impairments observed in MDCMC patients such as speech impairments and interaction with a strange mouse or object in order to gain a better understanding of social interaction and hence, of the presence of multiple aspects within the cognitive impairment spectrum. As mentioned in chapter 3, background strains have a significant influence over behavioral assays. Using a different background strain like FVB or DBX could significantly alter the results of the spontaneous alternation, spontaneous alternation with delay and paired associates learning tests (Hall & Roberson, 2012)(Brodkin et al., 2004)(Lassalle et al., 2008). Real time PCR analysis on the cortex and mid-hind brain tissue showed a 0.4 fold expression of *Chkb* gene in the cortex and a 0.8 fold expression in the mid-hind brain region in the Tg-rmd mice when compared to C57BL/6J (Supplemental Fig 5). This expression is absent in the *rmd* mice. Further tests need to

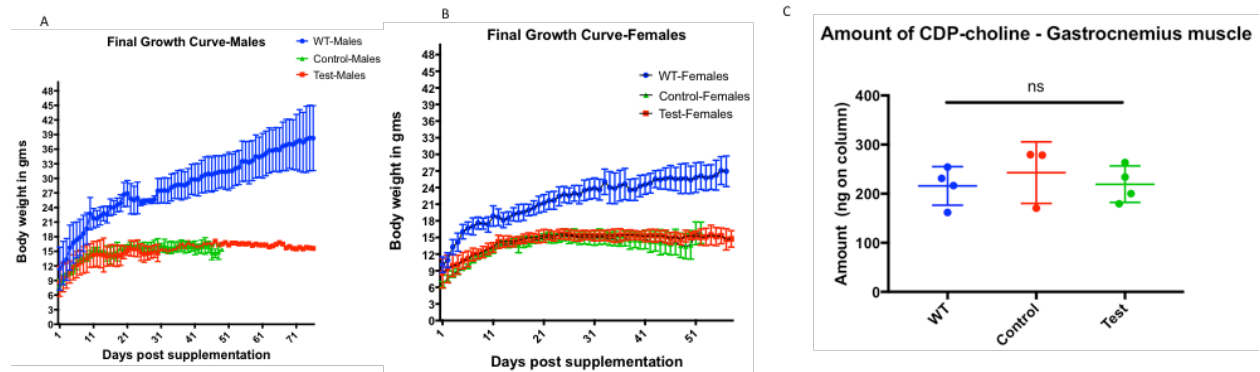
be performed in order to determine if this expression of transgenic *Chkb* gene is within a certain population of neuronal cells or in the glial, endothelial or vascular smooth muscle cells of the brain. Culturing neurons from Tg-*rmd* mice and testing them for the expression of *Chkb* gene would help determine expression in that cell population alone. PCR markers specific to transgenic *Chkb* and endogenous *Chkb* will help distinguish between the two expressed genes in the cells. Presence of reliable antibodies for *Chka* and *Chkb* can enable immunostaining of cross sections of the brain in order to determine the regions of expression of the two respective genes. Another method of determining the regional specific expression of *Chka* and *Chkb* is by using techniques like RNA *in situ* hybridization in which, single stranded RNA probes which bind to complementary nucleic acid sequences are used to help detect the genes or mRNA of interest. This can enable visual detection of *Chka* and *Chkb* in various tissue cross sections.

Summary of contributions to the field

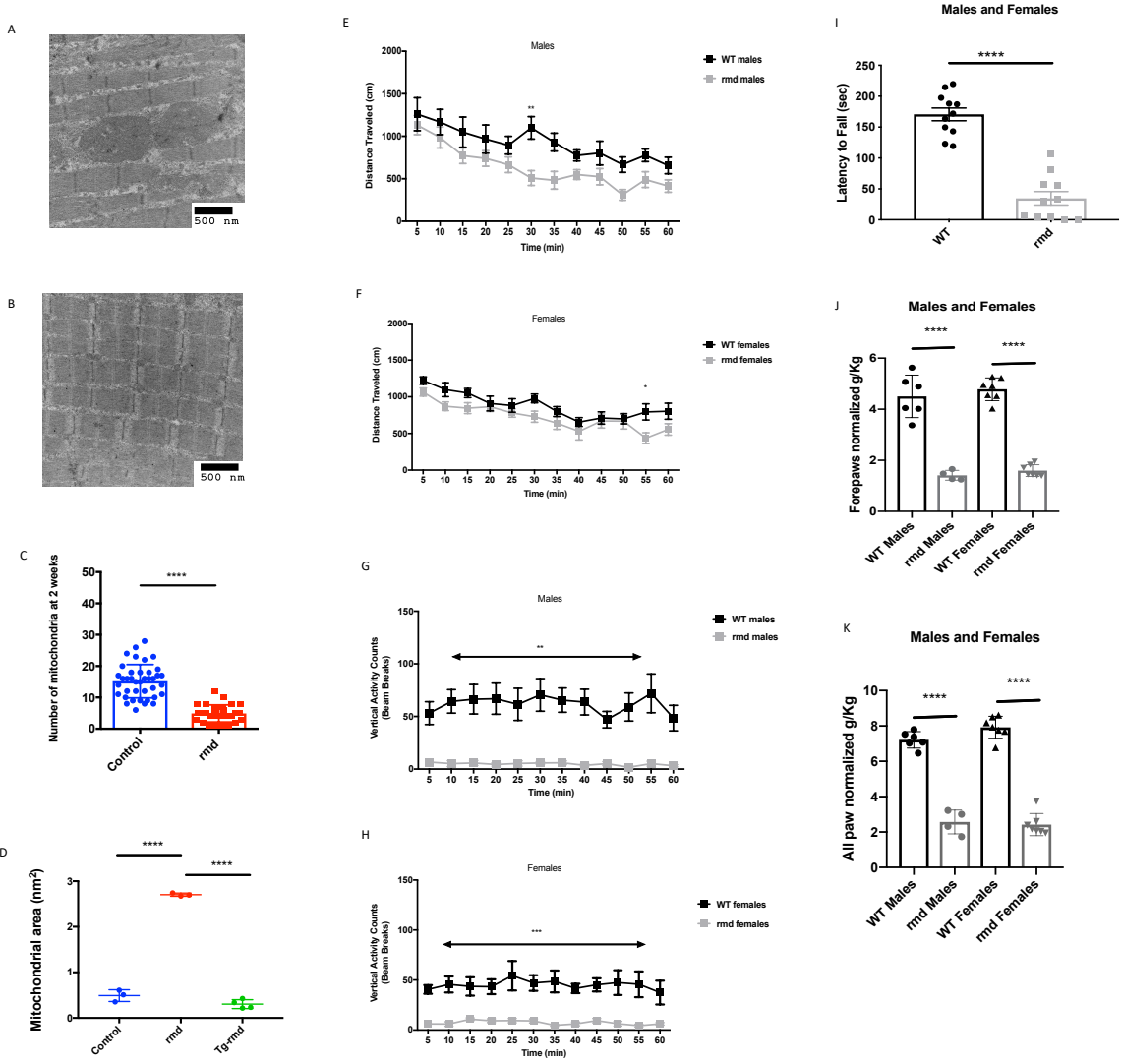
Choline kinase beta deficiency causes lack of PC synthesis which results in muscular dystrophy. The *rmd* mouse discovered in our lab, has a spontaneous 1.5 kb deletion in the choline kinase beta gene, develops muscular dystrophy in a rostro-caudal gradient and shows megamitochondria like the MDCMC patients, providing an excellent model organism for the further study of MDCMC. In the various attempts to rescue *rmd* phenotype in mice, it was observed that, even though oral supplements and compounds do not seem to rescue dystrophy, further analysis can confirm if these compounds can be used for increasing muscle strength and hence the quality of life in MDCMC patients. Rescuing mitochondrial area does not rescue dystrophy in *rmd* mice, providing further confirmation that the dystrophy results due to deficiency in choline kinase beta gene and hence, in, PC synthesis and not as a result of the megamitochondria disrupting normal

muscle architecture. Thus, muscular dystrophy in *rmd* and hence MDCMC can be rescued using gene therapy by upregulating choline kinase beta expression levels for the production of the necessary PC molecule. Even though there is a decrease in the expression of gene paralog *Chka* in adult murine skeletal muscles, there appears no immediate toxic effects of the upregulation of choline kinase alpha in mouse adult skeletal muscles via AAV mediated gene therapy. It appears that choline kinase alpha homodimers can compensate for PC production in *Chkb* deficient conditions. *rmd* mice show brain lipid changes consistent with those observed in Alzheimer's Disease patients, patients with mild cognitive impairments and brain trauma victims, however, these lipid changes do not translate to behavioral differences when tested on a battery of behavioral assays, indicating a secondary mechanism of PC synthesis in *rmd* brain tissue or mouse background strain influence. Correcting for background strain influence can make the *rmd* mouse a complete model for the study of MDCMC. Together, my research has added to the field of knowledge pertaining to MDCMC by way of creating a database of lipid changes occurring in choline kinase beta deficient conditions and by way of engineering and testing a gene therapy for the rescue of muscular dystrophy as a result of choline kinase beta deficiency. This gene therapy study can be further expanded upon for translation into MDCMC patients.

Appendix A: Chapter 2 Supplemental data



SUPPLEMENTAL FIG 1. Dietary supplementation of CDP-choline for the rescue of *rmd* phenotype: Dietary supplementation of CDP-choline *rmd* mice did not show a significant increase in body weights of male or female mice tested (A)(B). Mass spectrometric analysis of the amount of CDP-choline in the muscle of the *rmd* mice post CDP-choline supplementation for a period of 71 days did not show significant differences between the groups analyzed (C) indicating that there were no beneficial effects of CDP-choline supplementation, where WT indicates *+/+* littermates on CDP-choline diet, Control indicates *rmd/rmd* mice on normal diet and Test indicates *rmd/rmd* mice on CDP-choline supplemented diet. N = 4 mice/sex in WT, 4 mice/sex in control and 8 mice/sex in test. Diet supplementation was initialized at 3 weeks of age and continued for a total of 12 weeks.

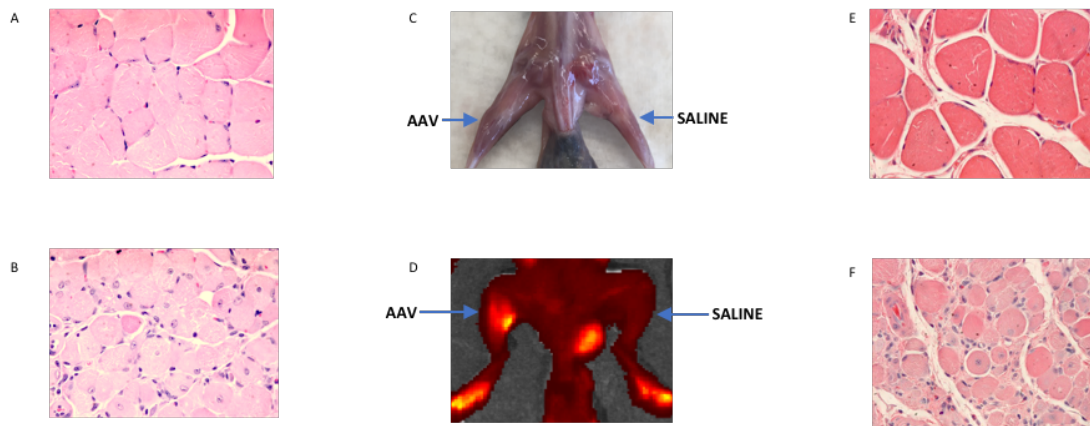


SUPPLEMENTAL FIG 2: Evidence of *rmd* phenotype at 2 and 4 weeks:

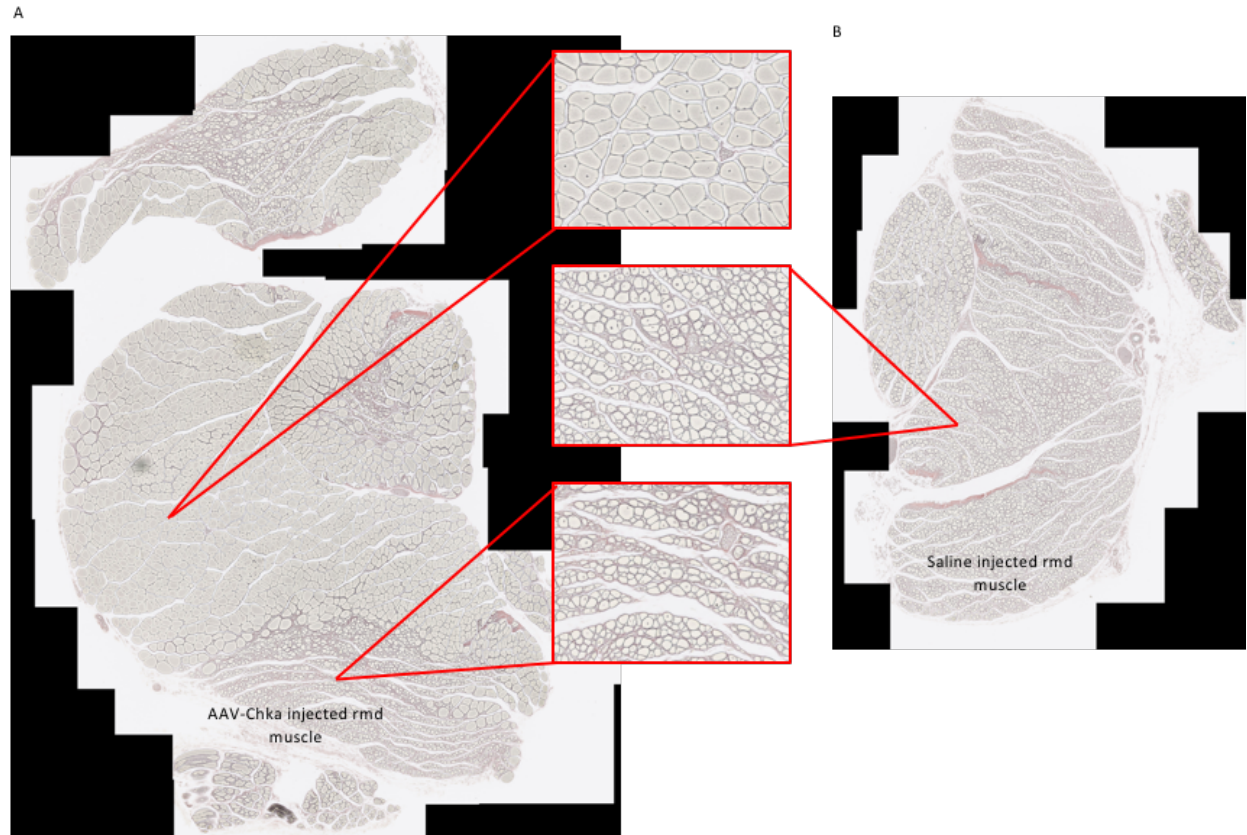
At 2 weeks: *rmd* mice show disturbed muscle fiber architecture with megamitochondria (A) compared to WT mice (B). Number of mitochondria are significantly lower with $p < 0.0001$ (C). Mitochondrial areas are significantly larger in *rmd* mice at 2 weeks with $p < 0.0001$ (D). $N = 4$ mice/sex/genotype. Error bars represent mean and SD.

At 4-5 weeks: The *rmd* males (E) and females (F) showed a significant difference compared to the WT in the total distance travelled ($p = 0.02$ in males and 0.04 in females) and in the vertically activity shown ($p = 0.001$ in males and 0.003 in females) (G-H). On the rotarod

assay, *rmd* mice show a significant difference from WT in latency to fall with $p < 0.0001$ (I) in a grouped analysis of males and females. *rmd* mice show significantly decreased fore-paw and all-paw grip strength when compared to their unaffected (WT) littermates with males and females showing p values less than 0.0001 in each of the tests (J-K), suggesting lower grip and hence muscle strength. $N = 4-6$ mice /sex/genotype. Error bars represent mean and SD.



SUPPLEMENTAL FIG 3: *Effects of gene therapy on rmd muscle: H&E staining of AAV-Chkb injected gastrocnemius muscle in rmd mice shows restoration of muscle structure in injected leg (A) vs in the uninjected leg (B). As seen in AAV-Chkb injected gastrocnemius muscle, AAV-Chka injected gastrocnemius muscle of rmd mice also look bigger and bulkier when compared to saline injected rmd muscle (C). AAV-Chka injected rmd muscles shows presence of fluorescent EGFP reporter, whereas no fluorescence is observed in saline injected rmd muscle (D). Autofluorescence can be detected in the feet and bladder region but is not significant to the study. H&E staining further provides evidence of restoration of muscle phenotype in the AAV-Chka injected muscle (E) compared to the sham injected muscle (F).*

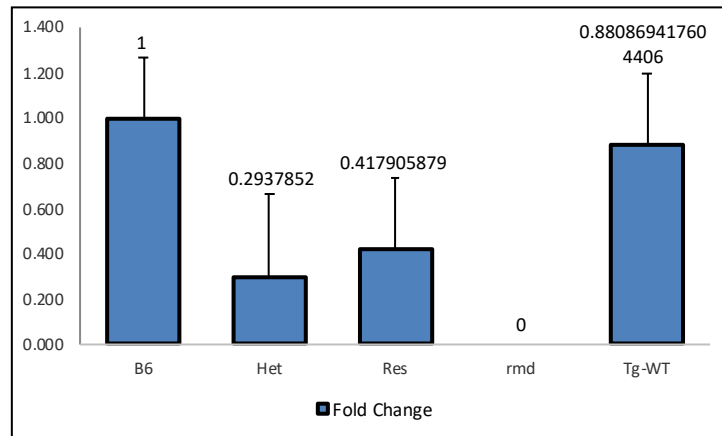


SUPPLEMENTAL FIG 4: *Montaged image of AAV-Chka injected rmd muscle: Cross section of gastrocnemius muscles from AAV-Chka injected rmd mouse shows significant and partial restoration of muscle structure and phenotype in AAV-Chka injected muscle (E) compared to the dystrophic muscle architecture of sham injected muscle (F). Both E and F represent Fiji stitched images whereas, inset pictures are at 20X magnification and indicate the nature of partial restoration of muscle phenotype in AAV-Chka injected rmd muscle.*

Appendix B: Chapter 3 Supplemental data :

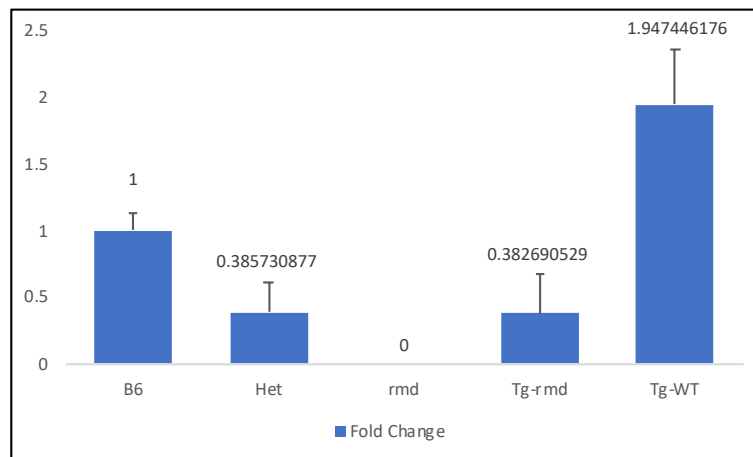
A

***Chkb* gene expression levels in cortex**



B

***Chkb* gene expression levels in Mid+Hind brain region**

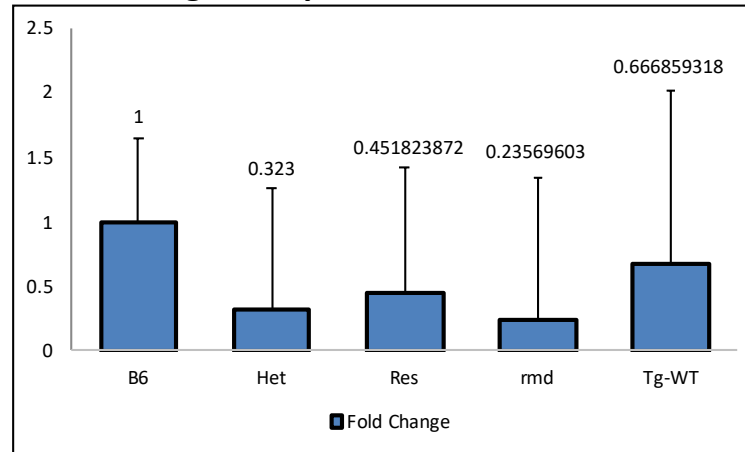


Supplemental Fig 5. *Realtime PCR for detection of Chkb levels in brain tissue*: Real time PCR in the cortical tissue of rmd mice showed a no expression of Chkb, whereas, tissue from rmd/+, Tg-rmd and Tg-WT mice showed levels of 0.29, 0.42 and 0.89 respectively, on comparison to C57BL/6J mice. In the mid+hind brain tissue rmd mice showed no expression of Chkb gene whereas, tissue from rmd/+, Tg-rmd and Tg-WT mice showed levels of 0.39, 0.38 and 1.95 respectively, on comparison to C57BL/6J mice.

Appendix C: Chapter 5 Supplemental data:

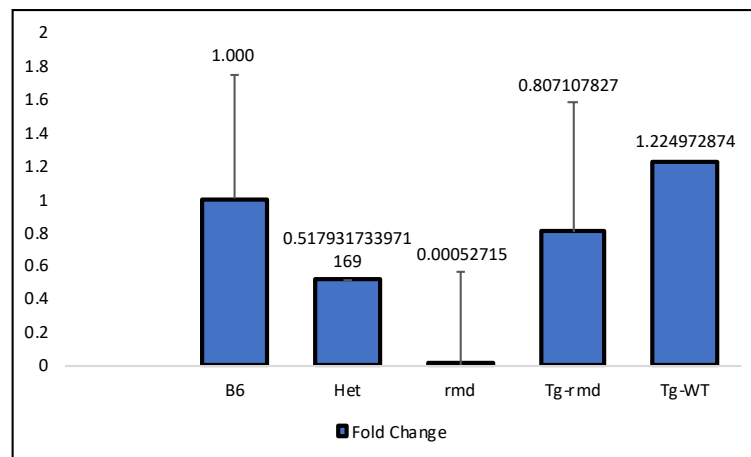
A

***Chka* gene expression levels in cortex**



B

***Chka* gene expression levels in Mid+Hind brain region**



Supplemental Fig 6. *Realtime PCR for detection of Chka levels in brain tissue:*

Real time PCR in the cortical tissue of C57B/6J, rmd/+ (Het), Tg-rmd, rmd and Tg-WT mice showed a 0.45-fold expression in Tg-rmd mice and a 0.23-fold expression in rmd mice. Rmd/+ and Tg-WT mice showed expression levels of 0.32 and 0.67 respectively. In the Mid-Hind brain region Tg-rmd mice showed a 0.81-fold expression of *Chka* and rmd mice showed negligible expression levels of 0.00052. The rmd/+ and Tg-WT mice showed expression levels of 0.52 and 1.22 respectively. This shows that in *Chkb* deficient conditions, rmd mice show expression of *Chka* in some regions of the brain, which may influence cognition, membrane fluidity and structure in the brain.

REFERENCES

- Agut J. (1983). Bioavailability of MethyP4C CDP-Choline by Oral Route. *Arzneimittel-Forschung*, 33(7A), 1045–7.
- Al-Qusairi, L., & Laporte, J. (2011). T-tubule biogenesis and triad formation in skeletal muscle and implication in human diseases. *Skeletal Muscle*, 1(1), 26. <http://doi.org/10.1186/2044-5040-1-26>
- Andersson, D. C., Betzenhauser, M. J., Reiken, S., Meli, A. C., Umanskaya, A., Xie, W., ... Marks, A. R. (2011). Ryanodine receptor oxidation causes intracellular calcium leak and muscle weakness in aging. *Cell Metabolism*, 14(2), 196–207. <http://doi.org/10.1016/j.cmet.2011.05.014>
- Andersson, D. C., Meli, A. C., Reiken, S., Betzenhauser, M. J., Umanskaya, A., Shiomi, T., ... Marks, A. R. (2012). Leaky ryanodine receptors in β -sarcoglycan deficient mice: A potential common defect in muscular dystrophy. *Skeletal Muscle*, 2(1), 1–9. <http://doi.org/10.1186/2044-5040-2-9>
- Aoyama, C., Liao, H., & Ishidate, K. (2004). Structure and function of choline kinase isoforms in mammalian cells. *Progress in Lipid Research*, 43(3), 266–281. <http://doi.org/10.1016/j.plipres.2003.12.001>
- Asinof, S. K., Sukoff Rizzo, S. J., Buckley, A. R., Beyer, B. J., Letts, V. a, Frankel, W. N., & Boumil, R. M. (2015). Independent Neuronal Origin of Seizures and Behavioral Comorbidities in an Animal Model of a Severe Childhood Genetic Epileptic Encephalopathy. *PLoS Genetics*, 11(6), e1005347. <http://doi.org/10.1371/journal.pgen.1005347>
- Bachmanov, A. a., Reed, D. R., Beauchamp, G. K., & Tordoff, M. G. (2002). Food intake, water intake, and drinking spout side preference of 28 mouse strains. *Behavior Genetics*, 32(6), 435–443. <http://doi.org/10.1023/A:1020884312053>
- Bartko, S. J., Vendrell, I., Saksida, L. M., & Bussey, T. J. (2011). A computer-automated touchscreen paired-associates learning (PAL) task for mice: Impairments following administration of scopolamine or dicyclomine and improvements following donepezil. *Psychopharmacology*, 214(2), 537–548. <http://doi.org/10.1007/s00213-010-2050-1>
- Blat, Y., & Blat, S. (2015). Drug discovery of therapies for duchenne muscular dystrophy. *Journal of Biomolecular Screening*, 20(10), 1189–1203. <http://doi.org/10.1177/1087057115586535>

- Brady, L., Giri, M., Provias, J., Hoffman, E., & Tarnopolsky, M. (2016). Proximal myopathy with focal depletion of mitochondria and megaconial congenital muscular dystrophy are allelic conditions caused by mutations in CHKB. *Neuromuscular Disorders*, *26*(2), 160–164. <http://doi.org/10.1016/j.nmd.2015.11.002>
- Brigman, J. L., Feyder, M., Saksida, L. M., Bussey, T. J., Mishina, M., & Holmes, A. (2008). Impaired discrimination learning in mice lacking the NMDA receptor NR2A subunit. *Learn Mem*, *15*(2), 50–54. <http://doi.org/10.1101/lm.777308>
- Brodkin, E. S., Hagemann, A., Nemetski, S. M., & Silver, L. M. (2004). Social approach-avoidance behavior of inbred mouse strains towards DBA/2 mice. *Brain Research*, *1002*(1–2), 151–157. <http://doi.org/10.1016/j.brainres.2003.12.013>
- Brooks, S. P., & Dunnett, S. B. (2009). Tests to assess motor phenotype in mice: a user’s guide. *Nature Reviews. Neuroscience*, *10*(7), 519–29. <http://doi.org/10.1038/nrn2652>
- Bussey, T. J., Dias, R., Amin, E., Muir, J. L., & Aggleton, J. P. (2001). Perirhinal cortex and place-object conditional learning in the rat. *Behavioral Neuroscience*, *115*(4), 776–85. <http://doi.org/10.1037/0735-7044.115.4.776>
- Cabrera-Serrano, M., Junckerstorff, R. C., Atkinson, V., Sivadorai, P., Allcock, R. J., Lamont, P., & Laing, N. G. (2015). Novel CHKB mutation expands the megaconial muscular dystrophy phenotype. *Muscle and Nerve*, *51*(1), 140–143. <http://doi.org/10.1002/mus.24446>
- Castro-Gago, M., Dacruz-Alvarez, D., Pintos-Martínez, E., Beiras-Iglesias, A., Arenas, J., Martín, M. Á., & Martínez-Azorín, F. (2016). Erratum: Corrigendum to “Congenital neurogenic muscular atrophy in megaconial myopathy due to a mutation in CHKB gene” (Brain and Development (2016) 38(1) (167–172) (S0387760415001023) (10.1016/j.braindev.2015.05.008)). *Brain and Development*, *38*(8), 783. <http://doi.org/10.1016/j.braindev.2016.04.009>
- Castro-Gago, M., Dacruz-Alvarez, D., Pintos-Martínez, E., Beiras-Iglesias, A., Delmiro, A., Arenas, J., ... Martínez-Azorín, F. (2014). Exome sequencing identifies a CHKB mutation in Spanish patient with Megaconial Congenital Muscular Dystrophy and mtDNA depletion. *European Journal of Paediatric Neurology*, *18*(6), 796–800. <http://doi.org/10.1016/j.ejpn.2014.06.005>
- Chamberlain, J. S. (2002). Gene therapy of muscular dystrophy. *Human Molecular Genetics*, *11*(20), 2355–62. <http://doi.org/10.1093/HMG/11.20.2355>
- Chan, D. C. (2012). Fusion and Fission: Interlinked Processes Critical for Mitochondrial Health. *Annual Review of Genetics*, *46*(1), 265–287. <http://doi.org/10.1146/annurev-genet-110410-132529>

- Chan, R. B., Oliveira, T. G., Cortes, E. P., Honig, L. S., Duff, K. E., Small, S. A., ... Di Paolo, G. (2012). Comparative lipidomic analysis of mouse and human brain with Alzheimer disease. *Journal of Biological Chemistry*, 287(4), 2678–2688. <http://doi.org/10.1074/jbc.M111.274142>
- Chang, C. C., Few, L. L., Konrad, M., & See Too, W. C. (2016). Phosphorylation of human choline kinase beta by protein kinase A: Its impact on activity and inhibition. *PLoS ONE*, 11(5), 1–23. <http://doi.org/10.1371/journal.pone.0154702>
- Chen, H., Detmer, S. A., Ewald, A. J., Griffin, E. E., Fraser, S. E., & Chan, D. C. (2003). Mitofusins Mfn1 and Mfn2 coordinately regulate mitochondrial fusion and are essential for embryonic development. *Journal of Cell Biology*, 160(2), 189–200. <http://doi.org/10.1083/jcb.200211046>
- Chen, X., Qiu, H., Wang, C., Yuan, Y., Tickner, J., Xu, J., & Zou, J. (2017). Molecular structure and differential function of choline kinases $CHK\alpha$ and $CHK\beta$ in musculoskeletal system and cancer. *Cytokine and Growth Factor Reviews*, 33, 65–72. <http://doi.org/10.1016/j.cytogfr.2016.10.002>
- Cordier, L., Gao, G.-P., Hack, A. A., McNally, E. M., Wilson, J. M., Chirmule, N., & Sweeney, H. L. (2001). Muscle-Specific Promoters May Be Necessary for Adeno-Associated Virus-Mediated Gene Transfer in the Treatment of Muscular Dystrophies. *Human Gene Therapy*, 12(2), 205–215. <http://doi.org/10.1089/104303401750061267>
- Crawley, J. (2000). Defining Behavioral Phenotypes in Transgenic and Knockout Mice, (Dc), 1–10. Retrieved from <http://www.ncbi.nlm.nih.gov/books/NBK100287/>
- Cunnane, S. C., Schneider, J. a., Tangney, C., Tremblay-Mercier, J., Fortier, M., Bennett, D. a., & Morris, M. C. (2012). Plasma and Brain Fatty Acid Profiles in Mild Cognitive Impairment and Alzheimer's Disease. *J Alzheimers Dis.*, 29(3), 691–697. <http://doi.org/10.3233/JAD-2012-110629>. Plasma
- Delion, S., Chalon, S., Guilloteau, D., Lejeune, B., Besnard, J. C., & Durand, G. (1997). Age-related changes in phospholipid fatty acid composition and monoaminergic neurotransmission in the hippocampus of rats fed a balanced or an n-3 polyunsaturated fatty acid-deficient diet. *Journal of Lipid Research*, 38(4), 680–9. Retrieved from <http://www.ncbi.nlm.nih.gov/pubmed/9144083>
- G. B. ANSELL. (1971). The Metabolism of Phosphatidylcholine in Brain Tissue. *PROCEEDINGS OF THE BIOCHEMICAL SOCIETY*.
- Gallego-Ortega, D., Ramirez de Molina, A., Ramos, M. A., Valdes-Mora, F., Barderas, M. G., Sarmentero-Estrada, J., & Lacal, J. C. (2009). Differential role of human choline kinase alpha and beta enzymes in lipid metabolism: implications in cancer onset and treatment. *PloS One*, 4(11), e7819. <http://doi.org/10.1371/journal.pone.0007819>

- Gibellini, F., & Smith, T. K. (2010). The Kennedy pathway-de novo synthesis of phosphatidylethanolamine and phosphatidylcholine. *IUBMB Life*, 62(June), 414–428. <http://doi.org/10.1002/iub.337>
- Gutiérrez Ríos, P., Kalra, A. A., Wilson, J. D., Tanji, K., Akman, H. O., Area Gómez, E., ... DiMauro, S. (2012). Congenital megaconial myopathy due to a novel defect in the choline kinase beta gene. *Archives of Neurology*, 69(5), 657–661. <http://doi.org/10.1001/archneurol.2011.2333>
- Haliloglu, G., Talim, B., Sel, C. G., & Topaloglu, H. (2015). Clinical characteristics of megaconial congenital muscular dystrophy due to choline kinase beta gene defects in a series of 15 patients. *Journal of Inherited Metabolic Disease*, 38(6), 1099–1108. <http://doi.org/10.1007/s10545-015-9856-2>
- Hall, A., & Roberson, E. (2012). Mouse models of Alzheimer's disease. *Brain Res Bull*, 88(1), 3–12. <http://doi.org/10.1016/j.brainresbull.2011.11.017>.Mouse
- Hirst, R. C., McCullagh, K. J. A., & Davies, K. E. (2005). Utrophin upregulation in Duchenne muscular dystrophy . *Acta Myologica : Myopathies and Cardiomyopathies : Official Journal of the Mediterranean Society of Myology* . Italy . Retrieved from http://umaine.summon.serialssolutions.com/2.0.0/link/0/eLvHCXMwtV3LS8MwGA_qRLyI77f0Pipt86IHD-IDUSZM52WXkaYJ7tCuzO2w_94vj251oOjBS2mTEtp8v3zJ90YIJ5dRuMQTCNZU8IRqQhXXKcsyrVMK0gnOiSaZCSXudslzh_T7xoBa-74v2v6V8NAGpDeBtH8g_nxQaIB7gABcAQRw_RUM3ibjUfU-LNvTaufKzvnv
- Hollinger, K., & Chamberlain, J. S. (2015). Viral vector-mediated gene therapies, 28(5), 522–527. <http://doi.org/10.1097/WCO.0000000000000241>
- Holoch, D., & Moazed, D. (2015). RNA-mediated epigenetic regulation of gene expression, 22(4), 328–335. <http://doi.org/10.1038/nrg3863>.RNA-mediated
- Hong, B. S., Allali-Hassani, A., Tempel, W., Finerty, P. J., MacKenzie, F., Dimov, S., ... Park, H. W. (2010). Crystal structures of human choline kinase isoforms in complex with hemicholinium-3: Single amino acid near the active site influences inhibitor sensitivity. *Journal of Biological Chemistry*, 285(21), 16330–16340. <http://doi.org/10.1074/jbc.M109.039024>
- Ira, D., Derek, H. A., Helen, P., Ronald, Y. A., William, B. M., Richard, B. N., & Robert, S. J. (1999). Robustesse de quelques indices de diversité à l'échantillonnage. *Cerebral Cortex*, 25(3), 435–455. <http://doi.org/10.1093/cercor/bhg081>
- Jaenisch, R., & Bird, A. (2003). Epigenetic regulation of gene expression: How the genome integrates intrinsic and environmental signals. *Nature Genetics*, 33(3S), 245–254. <http://doi.org/10.1038/ng1089>

- Kent, C. (1995). Eukaryotic Phospholipid Biosynthesis. *Annual Review of Biochemistry*, 64(1), 315–343. <http://doi.org/10.1146/annurev.bi.64.070195.001531>
- Kurdyukov, S., & Bullock, M. (2016). DNA Methylation Analysis: Choosing the Right Method. *Biology*, 5(1), 3. <http://doi.org/10.3390/biology5010003>
- Lassalle, J. M., Halley, H., Daumas, S., Verret, L., & Francés, B. (2008). Effects of the genetic background on cognitive performances of TG2576 mice. *Behavioural Brain Research*, 191(1), 104–110. <http://doi.org/10.1016/j.bbr.2008.03.017>
- Liaw, L., Prudovsky, I., Koza, R. A., Anunciado-Koza, R. V., Siviski, M. E., Lindner, V., ... Vary, C. P. H. (2016). Lipid Profiling of In Vitro Cell Models of Adipogenic Differentiation: Relationships With Mouse Adipose Tissues. *Journal of Cellular Biochemistry*, 12(February), 2182–2193. <http://doi.org/10.1002/jcb.25522>
- Lin, J. C., & Gant, N. (2014). De novo synthesis Related terms : Metabolic Regulation of Apoptosis in Cancer Energy Metabolism of the Brain TRAIL (TNF-Related Apoptosis-Inducing Ligand). *Magnetic Resonance Spectroscopy*.
- Liu, M., Yue, Y., Harper, S. Q., Grange, R. W., & Jeffrey, S. (2008). Adeno-Associated Virus-Mediated Microdystrophin Expression Protects Young mdx Muscle from Contraction-Induced Injury, *11*(2), 245–256. <http://doi.org/10.1016/j.ymthe.2004.09.013>. Adeno-Associated
- Lu, Y. Y., Wang, L. J., Muramatsu, S. I., Ikeguchi, K., Fujimoto, K. I., Okada, T., ... Nakano, I. (2003). Intramuscular injection of AAV-GDNF results in sustained expression of transgenic GDNF, and its delivery to spinal motoneurons by retrograde transport. *Neuroscience Research*, 45(1), 33–40. [http://doi.org/10.1016/S0168-0102\(02\)00195-5](http://doi.org/10.1016/S0168-0102(02)00195-5)
- Maddatu, T. P., Garvey, S. M., Schroeder, D. G., Zhang, W., Kim, S. Y., Nicholson, A. I., ... Cox, G. A. (2005a). Dilated cardiomyopathy in the nmd mouse: Transgenic rescue and QTLs that improve cardiac function and survival. *Human Molecular Genetics*, 14(21), 3179–3189. <http://doi.org/10.1093/hmg/ddi349>
- Maddatu, T. P., Garvey, S. M., Schroeder, D. G., Zhang, W., Kim, S. Y., Nicholson, A. I., ... Cox, G. A. (2005b). Dilated cardiomyopathy in the nmd mouse: Transgenic rescue and QTLs that improve cardiac function and survival. *Human Molecular Genetics*, 14(21), 3179–3189. <http://doi.org/10.1093/hmg/ddi349>
- Mei, Y., Xu, L., Kramer, H. F., Tomberlin, G. H., Townsend, C., & Meissner, G. (2013). Stabilization of the Skeletal Muscle Ryanodine Receptor Ion Channel-FKBP12 Complex by the 1,4-Benzothiazepine Derivative S107. *PLoS ONE*, 8(1). <http://doi.org/10.1371/journal.pone.0054208>

- Mendell, J. R., Kissel, J. T., Amato, A. A., King, W., Signore, L., Prior, T. W., ... Burghes, A. H. M. (1995). Myoblast Transfer in the Treatment of Duchenne's Muscular Dystrophy. *New England Journal of Medicine*, 333(13), 832–838. <http://doi.org/10.1056/NEJM199509283331303>
- Mercuri, E., Sewry, C., Brown, S. C., & Muntoni, F. (2002). Congenital muscular dystrophies. *Seminars in Pediatric Neurology*, 9(2), 120–31. <http://doi.org/http://dx.doi.org/10.1053/spen.2002.33802>
- Mitsuhashi, S., Hatakeyama, H., Karahashi, M., Koumura, T., Nonaka, I., Hayashi, Y. K., ... Nishino, I. (2011). Muscle choline kinase beta defect causes mitochondrial dysfunction and increased mitophagy. *Human Molecular Genetics*, 20(19), 3841–51. <http://doi.org/10.1093/hmg/ddr305>
- Mitsuhashi, S., Ohkuma, A., Talim, B., Karahashi, M., Koumura, T., Aoyama, C., ... Nishino, I. (2011). A congenital muscular dystrophy with mitochondrial structural abnormalities caused by defective de novo phosphatidylcholine biosynthesis. *American Journal of Human Genetics*, 88(6), 845–51. <http://doi.org/10.1016/j.ajhg.2011.05.010>
- Miyagawa, T., Kawashima, M., Nishida, N., Ohashi, J., Kimura, R., Fujimoto, A., ... Tokunaga, K. (2008). Variant between CPT1B and CHKB associated with susceptibility to narcolepsy. *Nature Genetics*, 40(11), 1324–1328. <http://doi.org/10.1038/ng.231>
- Müller, C. P., Reichel, M., Mühle, C., Rhein, C., Gulbins, E., & Kornhuber, J. (2015). Brain membrane lipids in major depression and anxiety disorders. *Biochimica et Biophysica Acta - Molecular and Cell Biology of Lipids*, 1851(8), 1052–1065. <http://doi.org/10.1016/j.bbalip.2014.12.014>
- Nishino, I., Kobayashi, O., Goto, Y. I., Kurihara, M., Kumagai, K., Fujita, T., ... Nonaka, I. (1998). A new congenital muscular dystrophy with mitochondrial structural abnormalities. *Muscle and Nerve*, 21(January), 40–47. [http://doi.org/10.1002/\(SICI\)1097-4598\(199801\)21:1<40::AID-MUS6>3.0.CO;2-G](http://doi.org/10.1002/(SICI)1097-4598(199801)21:1<40::AID-MUS6>3.0.CO;2-G)
- Oliveira, J., Negrão, L., Fineza, I., Taipa, R., Melo-Pires, M., Fortuna, A. M., ... Sousa, M. (2015). New splicing mutation in the choline kinase beta (CHKB) gene causing a muscular dystrophy detected by whole-exome sequencing. *Journal of Human Genetics*, (October 2014), 1–8. <http://doi.org/10.1038/jhg.2015.20>
- Paumier, K. L., Rizzo, S. J. S., Berger, Z., Chen, Y., Gonzales, C., Kaftan, E., ... Dunlop, J. (2013). Behavioral Characterization of A53T Mice Reveals Early and Late Stage Deficits Related to Parkinson's Disease, 8(8). <http://doi.org/10.1371/journal.pone.0070274>
- Quinlivan, R., Mitsuhashi, S., Sewry, C., Cirak, S., Aoyama, C., Moore, D., ... Straub, V. (2013). Muscular dystrophy with large mitochondria associated with mutations in the CHKB gene in three British patients: Extending the clinical and pathological phenotype. *Neuromuscular Disorders*, 23(7), 549–556. <http://doi.org/10.1016/j.nmd.2013.04.002>

- Ramírez De Molina, A., Gallego-Ortega, D., Sarmentero, J., Bañez-Coronel, M., Martín-Cantalejo, Y., & Lacal, J. C. (2005). Choline kinase is a novel oncogene that potentiates RhoA-induced carcinogenesis. *Cancer Research*, 65(13), 5647–5653. <http://doi.org/10.1158/0008-5472.CAN-04-4416>
- Ramos, J., Chamberlain, J. S., & Muscular, W. (2015). Gene Therapy for Duchenne muscular dystrophy. *Expert Opin Orphan Drugs.*, 3(11), 1255–1266. <http://doi.org/10.1517/21678707.2015.1088780.Gene>
- RS, M., BF, B., SRW, S., P, S., & Chen H, et al. (2004). Nicotine Keeps Leaf-Loving Herbivores at Bay. *PLoS Biology*, 2(8), e250. <http://doi.org/10.1371/journal.pbio.0020250>
- S. Chung, T. Moriyama, E. Uezu, K. Uezu, T. K. and S. Y. (n.d.). Administration of PC increases brain Acetylcholine concentration and improves memory in mice with dementia.
- Sanders, L. M., & Zeisel, S. H. (2007). Choline: Dietary requirements and role in brain development. *Nutrition Today*, 42(4), 181–186. <http://doi.org/10.1097/01.NT.0000286155.55343.fa>
- Secades JJ, F. G. (1995). *Methods and findings in experimental and clinical pharmacology*.
- Seibenhener, M. L., & Wooten, M. C. (2015). Use of the Open Field Maze to Measure Locomotor and Anxiety-like Behavior in Mice. *Journal of Visualized Experiments*, (96), 1–6. <http://doi.org/10.3791/52434>
- Sher, R. B., Aoyama, C., Huebsch, K. a, Ji, S., Kerner, J., Yang, Y., ... Cox, G. a. (2006a). A rostrocaudal muscular dystrophy caused by a defect in choline kinase beta, the first enzyme in phosphatidylcholine biosynthesis. *The Journal of Biological Chemistry*, 281(8), 4938–48. <http://doi.org/10.1074/jbc.M512578200>
- Sher, R. B., Aoyama, C., Huebsch, K. a, Ji, S., Kerner, J., Yang, Y., ... Cox, G. a. (2006b). A rostrocaudal muscular dystrophy caused by a defect in choline kinase beta, the first enzyme in phosphatidylcholine biosynthesis. *The Journal of Biological Chemistry*, 281(8), 4938–48. <http://doi.org/10.1074/jbc.M512578200>
- Sparks, S. E., & Escolar, D. M. (2011). Chapter 4 - Congenital muscular dystrophies. In R. C. Griggs & A. A. B. T.-H. of C. N. Amato (Eds.), *Muscular Dystrophies* (Vol. 101, pp. 47–79). Elsevier. <http://doi.org/https://doi.org/10.1016/B978-0-08-045031-5.00004-9>
- Sparks, S., & Harper, A. (n.d.). Congenital Muscular Dystrophy Overview Definition of CMD Clinical Manifestations of CMD Subtypes of CMD Subtypes of CMD of Known Cause. *GeneReviews® [Internet]*.
- Sparks, S., Quijano-Roy, S., Harper, A., Rutkowski, A., Gordon, E., Hoffman, E. P., & Pegoraro, E. (2012). Congenital muscular dystrophy overview. *NCBI Bookshelf*, 2. <http://doi.org/NBK1291> [bookaccession]

- Sukoff Rizzo, S. J., Anderson, L. C., Green, T. L., McGarr, T., Wells, G., & Winter, S. S. (2018). Assessing Healthspan and Lifespan Measures in Aging Mice: Optimization of Testing Protocols, Replicability, and Rater Reliability. *Current Protocols in Mouse Biology*, 8(2), e45. <http://doi.org/10.1002/cpmo.45>
- Tatem, K. S., Quinn, J. L., Phadke, A., Yu, Q., Gordish-Dressman, H., & Nagaraju, K. (2014). Behavioral and Locomotor Measurements Using an Open Field Activity Monitoring System for Skeletal Muscle Diseases. *Journal of Visualized Experiments*, (91), 1–7. <http://doi.org/10.3791/51785>
- Tsuji, S., & Matsushita, H. (1986). Successful treatment of murine muscular dystrophy with the protease inhibitor bestatin. *Journal of the Neurological Sciences*, 72(2–3), 183–194. [http://doi.org/10.1016/0022-510X\(86\)90006-7](http://doi.org/10.1016/0022-510X(86)90006-7)
- Van Der Giessen, R. S., Koekkoek, S. K., van Dorp, S., De Gruijl, J. R., Cupido, A., Khosrovani, S., ... De Zeeuw, C. I. (2008). Role of Olivary Electrical Coupling in Cerebellar Motor Learning. *Neuron*, 58(4), 599–612. <http://doi.org/10.1016/j.neuron.2008.03.016>
- Van der Vaart, T., van Woerden, G. M., Elgersma, Y., de Zeeuw, C. I., & Schonewille, M. (2011). Motor deficits in neurofibromatosis type 1 mice: The role of the cerebellum. *Genes, Brain and Behavior*, 10(4), 404–409. <http://doi.org/10.1111/j.1601-183X.2011.00685>
- Vinueza Veloz, M. F., Buijsen, R. A. M., Willemsen, R., Cupido, A., Bosman, L. W. J., Koekkoek, S. K. E., ... De Zeeuw, C. I. (2012). The effect of an mGluR5 inhibitor on procedural memory and avoidance discrimination impairments in Fmr1 KO mice. *Genes, Brain and Behavior*, 11(3), 325–331. <http://doi.org/10.1111/j.1601-183X.2011.00763.x>
- Vinueza Veloz, M. F., Zhou, K., Bosman, L. W. J., Potters, J. W., Negrello, M., Seepers, R. M., ... De Zeeuw, C. I. (2014). Cerebellar control of gait and interlimb coordination. *Brain Structure and Function*, 220(6), 3513–3536. <http://doi.org/10.1007/s00429-014-0870-1>
- Vitali, C., Wellington, C. L., & Calabresi, L. (2014). HDL and cholesterol handling in the brain. *Cardiovascular Research*, 103(3), 405–413. <http://doi.org/10.1093/cvr/cvu148>
- Wakabayashi, T. (2002). Megamitochondria formation - physiology and pathology. *Journal of Cellular and Molecular Medicine*, 6(4), 497–538. <http://doi.org/006.004.05> [pii]
- Wang, B., Li, J., Fu, F. H., Chen, C., Zhu, X., Zhou, L., ... Xiao, X. (2008). Construction and analysis of compact muscle-specific promoters for AAV vectors. *Gene Therapy*, 15(22), 1489–1499. <http://doi.org/10.1038/gt.2008.104>
- Wang, Y., Wang, F., Wang, R., Zhao, P., & Xia, Q. (2015). 2A self-cleaving peptide-based multi-gene expression system in the silkworm *Bombyx mori*. *Scientific Reports*, 5(iii), 1–10. <http://doi.org/10.1038/srep16273>

- Wood, P. L. (2012). Lipidomics of Alzheimer ' s disease : current status, (Figure 1), 1–10.
- Wu, G., Sher, R. B., Cox, G. a., & Vance, D. E. (2010a). Differential expression of choline kinase isoforms in skeletal muscle explains the phenotypic variability in the rostrocaudal muscular dystrophy mouse. *Biochimica et Biophysica Acta - Molecular and Cell Biology of Lipids*, 1801(4), 446–454. <http://doi.org/10.1016/j.bbalip.2009.12.003>
- Wu, G., Sher, R. B., Cox, G. A., & Vance, D. E. (2009). Biochimica et Biophysica Acta Understanding the muscular dystrophy caused by deletion of choline kinase beta in mice. *BBA - Molecular and Cell Biology of Lipids*, 1791(5), 347–356. <http://doi.org/10.1016/j.bbalip.2009.02.006>
- Wu, G., Sher, R. B., Cox, G. a, & Vance, D. E. (2010b). Differential expression of choline kinase isoforms in skeletal muscle explains the phenotypic variability in the rostrocaudal muscular dystrophy mouse. *Biochimica et Biophysica Acta*, 1801(4), 446–54. <http://doi.org/10.1016/j.bbalip.2009.12.003>
- Wu, G., Zhang, L., Li, T., Lopaschuk, G., Vance, D. E., & Jacobs, R. L. (2012). Choline deficiency attenuates body weight gain and improves glucose tolerance in ob/ob mice. *Journal of Obesity*, 2012(Cd). <http://doi.org/10.1155/2012/319172>
- Wurtman, R. J., Regan, M., Ulus, I., & Yu, L. (2000). Effect of oral CDP-choline on plasma choline and uridine levels in humans. *Biochemical Pharmacology*, 60(7), 989–992. [http://doi.org/10.1016/S0006-2952\(00\)00436-6](http://doi.org/10.1016/S0006-2952(00)00436-6)
- Zeisel, S. H. (2006). Requirements in Adults, (26), 229–250.
- Zeisel SH. (1992). Choline: an important nutrient in brain development, liver function and carcinogenesis. *J Am Coll Nutr*, 11(5), 473–81.
- Zeng, Y., Blain, M., Bendjelloul, M., Hastings, K. E., Karpati, G., Gilbert, R., ... Tong, A. W. (2008). 528. Development of Strong Muscle-Specific Promoters for Gene Therapy of Duchenne Muscular Dystrophy. *Molecular Therapy*, 16(May), S198. [http://doi.org/10.1016/S1525-0016\(16\)39931-2](http://doi.org/10.1016/S1525-0016(16)39931-2)
- Zincarelli, C., Soltys, S., Rengo, G., & Rabinowitz, J. E. (2008). Analysis of AAV serotypes 1-9 mediated gene expression and tropism in mice after systemic injection. *Molecular Therapy : The Journal of the American Society of Gene Therapy*, 16(6), 1073–1080. <http://doi.org/10.1038/mt.2008.76>
- Zweigner, J., Jackowski, S., Smith, S. H., van der Merwe, M., Weber, J. R., & Tuomanen, E. I. (2004). Bacterial Inhibition of Phosphatidylcholine Synthesis Triggers Apoptosis in the Brain. *The Journal of Experimental Medicine*, 200(1), 99–106. <http://doi.org/10.1084/jem.20032100>

BIOGRAPHY OF THE AUTHOR

Ambreen A. Sayed was born to Ahmed and Hasina Sayed in Mumbai, India on March 12th, 1989. She was raised in Mumbai where she completed her schooling. She then graduated with a Bachelors in Biotechnology from Jai Hind College with the Principals prize for “Outstanding academic achievement” in 2010. During her Bachelors she pursued a research project at Biocon Ltd, India’s largest biotech company. After her bachelors she pursued her interest in science by earning her Master’s in science in Biotechnology from G. N. Khalsa College in 2012. She completed her Masters dissertation research at Jaslok Hospital, Mumbai with work based on the ‘Identification of osteoarthritic markers in blood’. Her passion for science led her to complete various research projects in multiple hospitals and research laboratories and to the University of Maine in Orono. After rotating in the laboratories of Dr. Kevin Mills, Dr. Roger Sher and Dr. Jennifer Trowbridge she joined the laboratory of Dr. Gregory Cox in November 2013. She is a candidate for the Doctor of Philosophy degree in Biomedical Science from the University of Maine in December 2018.